Aus dem Institut für Physiologie
der Universitätsmedizin der Johannes Gutenberg-Universität Mainz

The Role of the $GABA_A$ Receptor-Stabilizing Protein Ubiquilin-1 in a Mouse Model of *in vitro* Epilepsy

Die Rolle des $GABA_A$ Rezeptor-stabilisierenden Proteins Ubiquilin-1 in einem Mausmodell der *in vitro* Epilepsie

Inauguraldissertation
zur Erlangung des Doktorgrades der
Medizin
der Universitätsmedizin
der Johannes Gutenberg-Universität Mainz

Vorgelegt von

Tabea Kürten
aus Bremen

Mainz, 2024

Wissenschaftlicher Vorstand: Univ.-Prof. Dr. H. Schild

1. Gutachter: [redacted]
2. Gutachter: [redacted]
3. Gutachter: [redacted]

Tag der Promotion: 08. Mai 2025

Table of Contents

Index of Figures

Index of Tables

Abbreviations

1. Introduction **1**

1.1 Epilepsy - (not) a *Sacred Disease* 1

1.2. Epilepsy Summarized 1

1.3. Epidemiology 2

1.3.1. Prevalence 2

1.3.2. Incidence 4

1.3.3. Mortality 4

1.4. Definition and Classification of Epilepsies 5

1.5. Symptoms of Epileptic Seizures 7

1.6. Pathophysiology and Epileptogenesis 8

1.6.1. The Critical Balance between Excitation and Inhibition 10

1.6.2. The GABAergic System 12

1.6.3. GABA in Epileptogenesis 14

1.6.4. Molecular Changes during Epileptogenesis 14

1.7. Traumatic Brain Injuries (TBI) and Posttraumatic Epilepsies (PTE) 17

1.8. Molecular Target Ubiquilin-1 19

1.8.1. The Ubiquitin-Proteasome System (UPS) 20

1.8.2. The Role of Ubiquilin-1 in Neurological Diseases 22

1.8.3. The Role of Nialamide (NM) and other MAO-Inhibitors (MAOIs) 23

1.9. Treatment 23

1.9.1. Seizure Recurrence 25

1.9.2. Drug-resistant Epilepsy (DRE) and Outcome 25

1.10. Prevention and Future Directions 26

2. Materials and Methods **28**

2.1. List of Materials for the Present Study 28

2.2. Animals and Ethical Statement 31

2.3. Preparation of Acute Brain Slices 31

2.4. Controlled Cortical Impact (CCI) 32

2.4.1. Method Description 32

2.4.2. Controlled Cortical Impact (CCI) in our Lab 34

2.5. Experimental Epilepsy 35

2.5.1. Animal Epilepsy Models 35

2.5.2. *In Vitro* Epilepsy in our Lab 36

2.6. Electrophysiology and Multielectrode Array (MEA) Recordings *in Vitro* 38
2.6.1. Experimental Setup..... 38
2.6.2. Positioning of the Slice..... 39
2.6.3. Data Acquisition..... 40
2.6.4. Experimental Conditions and Designs..... 40
2.6.5. Data Analysis..... 41
2.7. Western Blots..... 41
2.7.1. Method Description..... 41
2.7.2. Preparation of Western Blot Lysates..... 45
2.7.3. Electrophoretic Protein Separation and Transfer..... 47
2.7.4. Immunostaining 49
2.7.5. Densitometric Quantification with Image Studio Lite..... 50
2.8. Immunohistochemistry..... 50
2.9. Statistical Evaluation 52
3. Results **53**
3.1. Results from Experimental Setup and Data Analysis 53
3.1.1. Multielectrode Array Experiments 53
3.1.2. Western Blot Experiments..... 55
3.2. Preliminary Work for this Project 56
3.2.1. Fluorescence Activated Cell Sorting and Label-free Quantification 56
3.2.2. Western Blots from Cortex and Hippocampus 24 hours post-TBI..... 58
3.3. Results from the Present Study..... 59
3.3.1. *In Vitro* Epilepsy Model and its Properties in Hippocampal Horizontal Brain Slices during Extracellular Multielectrode (MEA) Recordings.... 59
3.3.2. Epileptiform Activity Causes a Reduction of Ubiquilin-1 Expression in Hippocampal and Cortical Slices 1-7 hours after Seizure Induction. 61
3.3.3. The Non-selective MAO-Inhibitor Nialamide Upregulates and Rescues Ubiquilin-1 Expression in Acute Slices 64
3.3.4. Immunofluorescence Staining of Ubiquilin-1 Reveals Cell-type Specific Expression in the Cortex but no Regulation of Protein Expression 67
3.3.5. Nialamide Mitigates the Number of Epileptiform Discharges and the Mean Peak Amplitude in Dose-Response Relationships of Increasing Picrotoxin Concentrations in Extracellular Multielectrode Arrays..... 69
4. Discussion..... **73**
4.1. Discussion of the Methods 73
4.2. Discussion of Previous Studies and Thesis Aims 75
4.3. Discussion of the Results..... 76

4.4. Discussion of the Limitations of the Present Study Design 80
4.5. Conclusions and Outlook 81
5. Summary **82**
5.1. Zusammenfassung (Deutsch) 83
6. Bibliography **85**
6.1. Figure References 85
6.2. Literature References 87
7. Acknowledgements **109**
8.Curriculum Vitae **111**

Index of Figures

Figure 1: Global map of the age-standardized epilepsy prevalence from the Global Burden of Disease Study 2016 (2016 GBD Collaborators, 2019)

Figure 2: Multi-level epilepsy classification by the International League Against Epilepsy (ILAE) (Scheffer et al., 2017)

Figure 3: Different interictal oscillatory patterns recorded in vivo by depth EEG in pilocarpine induced epilepsy in rats (modified from Lévesque et al., 2018)

Figure 4: Incidence of acquired epilepsy following various types of brain insults (Pitkänen et al., 2015)

Figure 5: Schematic representation of the GABA-glutamine cycle in neurons (Bak et al., 2006)

Figure 6: Structure of the $GABA_A$ receptor in the mammalian brain (Gong et al., 2015)

Figure 7: Changes in the mRNA expression of the $GABA_A$ receptor subunits early after TBI (Le Prieult et al., 2017)

Figure 8: Schematic representation of glutamate-mediated excitotoxicity (Mattson, 2003)

Figure 9: Pathomechanisms of posttraumatic epileptogenesis (Sharma et al., 2021)

Figure 10: Timeline of TBI-induced epileptogenesis (adapted from Timofeev et al., 2013)

Figure 11: The ubiquitin-proteasome system (UPS) simplified (Jansen et al., 2014)

Figure 12: Vibratome setup for the preparation of acute brain slices

Figure 13: PFA-fixed brain from GAD67-GFP mouse 24 hours after CCI-injury induction (modified from Kürten et al., 2022)

Figure 14: Milestones in the development of animal models in epilepsy research (modified from Löscher et al., 2017)

Figure 15: Chemical structure of picrotoxinin (modified from Olsen et al., 2006)

Figure 16: Chemical structure of kainic acid (modified from Tian et al., 2019)

Figure 17: Loop structure of the hippocampus (modified from Goldberg et al., 2013)

Figure 18: Multielectrode Array (MEA) chip layout

Figure 19: Standard curve of the Bicinchoninic acid assay (BCA)

Figure 20: Western blot signal detection methods (Oh, K., 2021)

Figure 21: Steps of the Bicinchoninic acid assay (BCA)

Figure 22: Transfer stack arrangement

Figure 23: Coronal brain section (modified from Allen Brain Atlas, [brain-map.org/])

Figure 24: Multielectrode Array setup with hippocampal slice and epileptiform activity

Figure 25: Epileptiform activity in the neocortex

Figure 26: Data analysis with Clampfit 11.1 software

Figure 27: Testing of primary antibody concentration for Western blots

Figure 28: Densitometric Western blot analysis with Image Studio Lite 5.2 software

Figure 29: Label-free quantification analysis of FACS-isolated GFP-positive interneurons of the contralateral cortex from GAD67-GFP mice 24 hours after CCI (modified from Kürten et al., 2022)

Figure 30: Western blot quantification of ubiquilin-1 expression of the whole cortex and hippocampus 24 hours after TBI (modified from Kürten et al., 2022)

Figure 31: Properties of epileptiform activity during MEA recordings (modified from Kürten et al., 2022)

Figure 32: Properties of epileptiform activity during MEA recordings with and without picrotoxin (PTX) (modified from Kürten et al., 2022)

Figure 33: Western blot quantification of ubiquilin-1 expression in the cortex after seizure-induction in acute brain slices (modified from Kürten et al., 2022)

Figure 34: Western blot quantification of ubiquilin-1 expression in the hippocampus after seizure-induction in acute brain slices (modified from Kürten et al., 2022)

Figure 35: Western blot quantification of ubiquilin-1 expression in the cortex after treatment of brain slices with monoamine oxidase (MAO) inhibitor nialamide (NM) (modified from Kürten et al., 2022)

Figure 36: Western blot quantification of ubiquilin-1 expression in the hippocampus after treatment of brain slices with monoamine oxidase (MAO) inhibitor nialamide (NM) (modified from Kürten et al., 2022)

Figure 37: Immunofluorescence staining of the somatosensory cortex (modified from Kürten et al., 2022)

Figure 38: Epileptiform activity with *in vitro* epilepsy, NM-treatment and NM-washout (modified from Kürten et al., 2022)

Figure 39: Picrotoxin-dependent dose-response relationships and Mann-Whitney-test of epileptiform activity at a PTX concentration of 10 µM (modified from Kürten et al., 2022)

Figure 40: Mann-Whitney-test of epileptiform activity at a PTX concentration of 50 µM

Index of Tables

Table 1: Animals

Table 2: Chemicals, Buffers, Assays and Kits

Table 3: Instruments and Consumables

Table 4: Antibodies

Table 5: Software

Table 6: Artificial cerebrospinal fluid (aCSF)

Table 7: Lysis buffer

Table 8: Western blot gels

Table 9: Buffers for 1 L

Abbreviations

aCSF	Artificial cerebrospinal fluid
AED	Antiepileptic drug
AMPA	α-Amino-3-hydroxy-5-methyl-4-isoxazolepropionic acid
ASD	Antiseizure drug
AsS	Acute symptomatic seizure
ATP	Adenosine triphosphate
BCA	Bicinchoninic Acid Assay
Bcl-2	B-cell lymphoma 2
BDNF	Brain-derived neurotrophic factor
Ca	Calcium
CA1-4	Cornu Ammonis subfield 1-4
CCI	Controlled cortical impact
CCD	Charge coupled device
Ctr.	Control
D	Dopamine
DALY	Disability-adjusted life years
DG	Dentate gyrus
DGN	German Neurological Society
DNA	Desoxyribonucleic acid
DRE	Drug-resistant epilepsy
DTT	Dithiothreitol
EC	Entorhinal cortex
ECL	Enhanced chemiluminescence
EEG	Electroencephalography
E/I	Excitatory-/inhibitory
ELISA	Enzyme-Linked Immunosorbent Assay
ER	Endoplasmic reticulum
FACS	Fluorescence-activated cell sorting
FPI	Fluid percussion injury
FR	Fast ripple
GABA	Gamma-Aminobutyric acid
GAD67	Glutamic acid decarboxylase 67 Kd
GAPDH	Glyceraldehyde 3-phosphate dehydrogenase
GAT-1	GABA transporter type 1
GDP	Giant depolarizing potential
GFP	Green fluorescent protein

HCN	Hyperpolarization-activated cyclic nucleotide-gated
HFO	High-frequency oscillations
HIC	High-income countries
HRP	Horseradish peroxidase
IGF-1	Insulin-like growth factor 1
iGluR	Ionotropic glutamate receptor
IHC	Immunohistochemistry
ILAE	International League Against Epilepsy
IL-1ß	Interleukin 1 beta
IL-6	Interleukin 6
IPSC	Inhibitory postsynaptic current
IP3	Inositol triphosphate
I/R	Ischemia-/reperfusion
JNK	C-Jun N-terminal kinase
K	Potassium
KA	Kainic acid
KAR	Kainic acid receptor
LCMS	Liquid chromatography-mass spectrometry
LDS	Lithium dodecyl sulfate
LLOQ	Lower level of quantification
LMIC	Low/middle-income countries
LTP	Long-term potentiation
mAChR	Muscarinic acetylcholine receptor
MAO	Monoamine oxidase
MAOI	Monoamine oxidase inhibitor
MEA	Multielectrode Array
MetR	Metabotropic glutamate receptor
MF	Mossy fibers
mPTP	Mitochondrial permeability transition pore
mRNA	Messenger ribonucleic acid
mTOR	Mammalian target of rapamycin
ß-ME	Beta mercaptoethanol
n	Number
Na	Sodium
NeuN	Hexaribonucleotide binding protein-3
NFL	Neurofilament light chain
NF-κB	Nuclear factor kappa B

NGS	Next Generation Sequencing
NIH	National Institute of Health
NM	Nialamide
NMDA	N-methyl D-aspartate
NPY	Neuropeptide Y
PVDF	Polyvinylidene difluoride
PP	Perforant path
PTE	Posttraumatic epilepsy
PTX	Picrotoxin
p53	Cellular tumor antigen p53
PTZ	Pentylenetetrazole
RC	Recurrent collaterals
RNA	Ribonucleic acid
RNS	Reactive nitrogen species
ROS	Reactive oxygen species
rt-PCR	Reverse transcription polymerase chain reaction
SCN1A	Sodium voltage-gated channel alpha subunit 1
SDS-PAGE	Sodium dodecyl sulfate polyacrylamide gel electrophoresis
SE	Status epilepticus
SEM	Standard error of mean
SLE	Seizure-like event
SSRI	Selective serotonin reuptake inhibitor
SST	Somatostatin
SUDEP	Sudden unexpected death in epilepsy
TA	Temporoammonic
TBI	Traumatic brain injury
TCA	Tricarboxylic acid cycle
TLE	Temporal lobe epilepsy
TNFα	Tumor necrosis factor alpha
Ub	Ubiquitin
UPS	Ubiquitin-proteasome system
VDCC	Voltage-dependent calcium channel
WHO	World Health Organization
YLD	Years lived with disability
YLL	Years of life lost
5-HT	Serotonin

1. Introduction

1.1. Epilepsy - (not) a *Sacred Disease*

“People think that epilepsy is divine simply because they don't have any idea what causes epilepsy. But I believe that someday we will understand what causes epilepsy, and at that moment, we will cease to believe that it's divine. And so it is with everything in the universe”(1).
—Hippocrates (c. 460-370 BC), On the Sacred Disease, Corpus Hippocraticum

The first documentation of an epileptic seizure appeared in an Akkadian text and dates back 4000 years (2). The term *epilepsy* derives from ancient Greek, meaning *to possess* or *to seize upon* (2, 3). For centuries, it had been postulated that the medical condition was of a divine origin (2). It had been attributed to a demonic possession or a punishment inflicted on the soul by the gods (2, 4). Therefore, epilepsy was given the names *Herculian disease* (the demigod Heracles was believed to suffer from it) or *sacred disease* (2, 4). Ever since, the term epilepsy has had a negative connotation and been surrounded by superstition and mysticism, a stigma which has been perpetuated in the post-Hippocratic era (2). Throughout the centuries and Middle Ages, the beliefs were supported by the Catholic Church and Greek philosophers such as Galen and Aristotle (2). To this day, people suffering from epilepsy experience stigmatization with far-reaching consequences in their individual lives (5).

Hippocrates on the other hand, scrutinized the popular belief of a divine origin (2). Instead, he was the first to study the condition from a scientific point of view and associate epilepsy with an underlying brain dysfunction (2). He went even further to postulate that the condition might be curable (2). His treatise *On the Sacred Disease* incorporates formal disease descriptions, delineations of a possible therapy and even assumptions about a hereditary etiology (2). Furthermore, he discovered an association of head injuries with seizures and first brought up the notion of posttraumatic epilepsy in *Injuries of the Head* (2). To this day, Hippocrates is hereinafter not only referred to as the father of medicine, but more specifically, the father of neurology as well (6).

1.2. Epilepsy Summarized

Epilepsy constitutes a major public health concern and cause in worldwide morbidity, disability, and mental health disorders (5). The growing socioeconomic health concern is not restricted by geographical or social boundaries, as people of all ages, genders, and nations are affected by it (5, 7). The common neurological disorder inflicts an immense burden upon individuals, their families, and health care systems (5, 8, 9). Epilepsy is defined as the chronic predisposition towards recurrent epileptic seizures (10-12). The characteristic symptoms of the disease range from nearly undetectable periods of unconsciousness to episodes of

uncontrollable convulsive shaking (13). Epileptic seizures are often accompanied by a loss of consciousness, severe physical injury, and automatisms (13). Long-term sequelae such as cognitive impairment, psychological comorbidities, a reduced life expectancy, and the experience of social rejection and stigmatization indicate the magnitude of this common neurological disorder (5). Affected individuals often experience denial of employment, banning from school, insurance issues, driving restrictions, and further discriminations (5, 9, 13). Along with the constant unpredictability of seizures and resulting physical injuries, these psychosocial disadvantages in everyday life contribute to the increasing rates and comorbidity of epilepsy with psychological disorders, depression, and anxiety (5).

Additionally, epileptic activity itself can cause and exacerbate cognitive or behavioral impairments (14). Uncontrolled seizures can interrupt the consolidation of short-term information, which in turn can lead to learning disabilities (5). The extent of cognitive impairment ranges from poor concentration to severe amnesia and disorientation (5). Neurological deficits that cannot be ascribed to the pathophysiological cause of epilepsy alone are referred to as epileptic encephalopathies (14, 15). They are often associated with a genetic etiology and result in early developmental slowing or regression (16). Even the adverse effects of antiepileptic therapy can severely affect the well-being of epilepsy patients (7, 17). Therefore, in addition to the immediate effects of the disorder on health, the quality of life can be substantially impaired. Epilepsy constitutes the second most burdensome global neurological disorder measured by disability-adjusted life years (18, 19). Disability-adjusted life years (DALY) is a measure introduced by the Global Burden Studies that takes demographic factors, life expectancy, disability etc. into account, whereby years of life lost (YLL) to premature death and years lived with disability (YLD) are the main determinants of DALY (20). In a systematic review for the Global Burden Disease Study from 1990-2016, the age-adjusted DALY was estimated at 182.6 per 100,000 population (21). Interestingly, between 1990 and 2016, the disease burden decreased significantly, likely reflecting improved access to health care and new effective treatment strategies (21). In addition to the individual burden, the direct and indirect economic costs are high due to premature mortality, loss of work productivity, and costs for health care systems (5).

1.3. Epidemiology

1.3.1. Prevalence

Epidemiological studies estimate that approximately 50 million people worldwide have been diagnosed with epilepsy (11, 22). About 80% of them reside in low/middle-income countries (LMIC) (5, 11, 23). The prevalence describes the number of diseased people in a population at a defined time point (24). According to a systematic review by Fiest et. al from 2016, the

mean active point prevalence amounts to 6.38 cases per 1,000 persons worldwide (18). The pooled lifetime prevalence, which includes cases in remission, accounts for about 7.60 per 1,000 people (18, 25). Prevalence rates are estimated to be higher in LMIC countries (24, 26, 27). This variation among epidemiological data is related to population-based factors such as access to health care systems, demographic structures, case ascertainment, environmental risk factors, and socioeconomic status (7, 8). In LMIC countries and rural areas where the disorder is still strongly stigmatized according to cultural beliefs, this can lead to discrimination and the concealing of symptoms (5, 7). Moreover, the unavailability of anti-seizure drugs (ASD) in developing nations aggravates the existing “treatment gap” (28). According to the World Health Organization (WHO), approximately 75% of all epilepsy cases in low-income countries remain untreated (11, 13). It is hypothesized that the prevailing CNS infections and parasite infestations, familial accumulation, and perinatal damage are partly responsible for the discrepancy in prevalence rates between high-income countries (HIC) and LMIC (5, 18, 26, 28). Deficient hygiene, lack of professional medical care, and poor nutrition contribute to this public health issue (8). Furthermore, socioeconomic status plays a role since unemployment and lower educational levels adversely influence the health care seeking behavior of individuals (8).

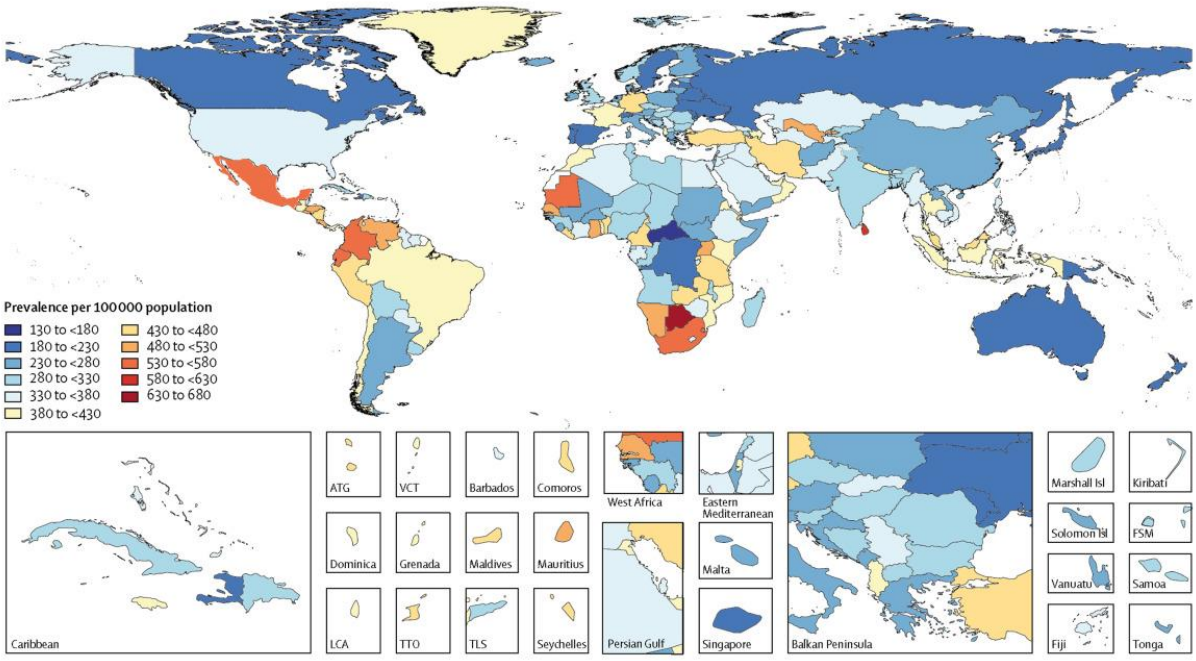

Figure 1. From the 2016 GBD collaborators, 2019 (1).

Global Burden of Disease Study 2016. Global map of the age-standardized prevalence per 100,000 of idiopathic epilepsies in both sexes for the year 2016.

1.3.2. Incidence

The incidence measure describes the frequency of a medical condition or disease in a population in a defined time window, often within a year. In the recent systematic review by Fiest et al., an overall worldwide epilepsy incidence rate of 61.44 per 100,000 persons annually was estimated (18). Again, industrialized high-income countries (HIC) report lower incidence rates than low/middle-income countries (LMIC) (7, 28). The age-related incidence of epilepsy peaks in the youngest and elderly age groups (25, 29, 30). An increasing incidence rate of epilepsy in people above 60 years has been reported (24). This correlates with the increasing risk of stroke, head trauma due to falls, metabolic disorders, neurodegenerative diseases, or brain cancer in this age group, all of them representing potential elicitors of epileptogenesis or acute symptomatic seizures (7, 25). However, the age-related incidence of epilepsy in the young has declined over the last decades due to an improvement in perinatal care, sanitation, and preventive steps, whereas the incidence in the elderly has increased with a rising life expectancy worldwide (7, 25, 28). Although the disorder affects both sexes, both incidence and prevalence rates minimally prevail in men (7, 18). Among other factors, that might partially be due to the higher rates of traumatic brain injuries in men (31). Another aspect being discussed is that in some parts of the world women are more likely to conceal their condition in order to avoid social marginalization (18, 32).

1.3.3. Mortality

Mortality rates are significantly increased in individuals diagnosed with epilepsy due to the risk of self-injury and *sudden unexpected death in epilepsy* (SUDEP) (33-35). Status epilepticus, SUDEP, sudden fatal injuries, and suicide represent frequent and immediate causes of death in epilepsy patients (35). The WHO estimates a three times elevated risk of premature death in people suffering from epileptic disorders as compared to the general population (11). Regarding the increased standardized mortality ratio (SMR) of 1.6-3.0 in HIC and 1.3-7.2 in LMIC, the overall risk of premature death is significantly elevated among people with epilepsy (23, 35). The incidence rate of SUDEP amounts to 1.2/1,000 patient-years in adults (36). Major risk factors for SUDEP comprise a frequent occurrence of nocturnal seizures and a preponderance of generalized tonic-clonic seizures (36, 37). The underlying pathophysiology of SUDEP remains elusive, but autonomic, cardiovascular, and respiratory dysfunctions have been hypothesized (38, 39). Early seizure control and compliance diminish the risk of SUDEP (10, 39).

The great variation of mortality rates and reported prevalence and incidence among the different countries is partly due to disparate epidemiological data acquisition and reporting (18). Furthermore, standardized epidemiological case ascertainment remains challenging due to

heterogenous epilepsy and seizure definitions and an inconsistency of inclusion criteria. Epidemiological data can be based on in-hospital registry and hence, pre-clinical fatalities or epileptic seizures are not necessarily registered in the statistics.

1.4. Definition and Classification of Epilepsies

Having seizures is not equivalent to sustaining epilepsy. Acute symptomatic seizures occur more frequently and are provoked by a precipitating elicitor in an otherwise physiologically functioning brain (7, 12). It is a transient secondary condition deriving from a cause such as brain insult, trauma, substance withdrawal, infection and metabolic changes (12, 17). In the majority of the events, complete remission can be accomplished by treatment and abolishment of the underlying cause (7). Other than provoked seizures, unprovoked seizures occur in the absence of common risk factors. First unprovoked seizures may also occur in the form of status epilepticus (SE), a dangerous condition of prolonged seizure activity or repetitive seizures emerging at brief intervals (40). SE can arise when endogenous mechanisms of seizure termination are malfunctioning (40). Depending on duration and seizure type, ongoing seizure attacks are associated with severe loss of neurons and neuronal injury (40).

Epilepsy, by contrast, constitutes the chronic predisposition towards recurrent and unprovoked seizures (7, 10, 41). In clinical settings this typically applies to having two unprovoked seizures with at least 24 hours in between (12). Officially, epilepsy is defined by several clinical conditions: at least two unprovoked seizures occurring more than 24 hours apart OR one unprovoked (or reflex) seizure with a high probability of recurrence, equivalent to the general recurrence risk of at least 60% in the next ten years after two unprovoked seizures, OR diagnosis of an epilepsy syndrome (12). Although reflex seizures (e.g. photosensitive seizures) constitute provoked seizures in a strict sense, the enduring susceptibility to recurrent seizures is pivotal to rank them among epilepsies (12). This also accounts for brain tumors and other diseases relating thereto. Therefore, the ‘new’ epilepsy definition of 2014 was adapted to this (12).

The refined ILAE Seizure Classification of the Epilepsies from 2017 comprises a multi-level guideline for diagnosis and categorization. If diagnostic resources and capabilities are sufficient, the central aim is to fulfill diagnostic assessment on all three levels (14). At the starting point of classification, all potential differential diagnoses and non-epileptic conditions such as convulsive syncope must be dismissed (12). A clinical examination includes electroencephalography (EEG), neuroimaging, physical examination, and further diagnostic tools and confirmatory tests. On the first diagnostic level of epilepsies, the seizure type is assessed. It is subdivided into the three categories of focal, generalized and unknown seizure

onset (14). In individual cases, multiple seizure types are present (14). Seizures with focal onset are more frequent than generalized seizures in all age groups (7, 42). Focal seizures have their origin in neuronal networks of one brain hemisphere, while generalized seizures originate bilaterally and involve both hemispheres (17). Synchronous firing activity can propagate, and seizures with focal onset can progress to secondarily generalized seizures (17), more recently referred to as *focal to bilateral tonic-clonic seizure* (14). The second level of diagnosis represents the epilepsy type. Various epilepsy types can be distinguished, including focal or generalized epilepsy, combined generalized and focal epilepsy, and unknown epilepsy type (14). Both epilepsy types can co-exist, therefore the new category of combined generalized and focal epilepsies was introduced (14). Generalized epilepsy covers absence, myoclonic, atonic, tonic, and tonic-clonic seizures (14). Focal epilepsies, on the other hand, are either of unifocal or multifocal origin. The final diagnosis is often based on an extensive clinical examination and typical interictal EEG abnormalities (14). If diagnostic resources are poor and the information is insufficient, the term “unknown epilepsy type” may be applied (14). In a final step on the third diagnostic level, the possibility of an epilepsy syndrome is assessed, characterized by related electroclinical clusters of symptoms and even prognostic and therapeutic implications (30). EEG and imaging features and seizure types that commonly appear together are often age-specific, for example in childhood absence epilepsy (14, 30). The etiology is either unknown or related to specific predispositions (8), and should be identified during every step of classification, as the critical choice of treatment might depend on it. However, according to recent epidemiological studies, even in HIC thorough documentation of the etiology is lacking in almost 50% of cases (7). The ILAE classification names six groups of potential etiologies: structural, genetic, metabolic, infectious, immune, and unknown etiology, all of which can co-exist (11, 14). Structural causes for epilepsies can be detected via neuroimaging. Therefore, the German Neurological Society (DGN) suggests diagnostic Magnetic Resonance Imaging for every new epilepsy case (10). Structural causes can be congenital or acquired by head trauma, stroke, or brain tumors etc. (14). Treatment options are versatile and may consist of surgery, classic antiepileptic drugs (AED), or novel targeted therapies like mTOR inhibitors (14, 43).

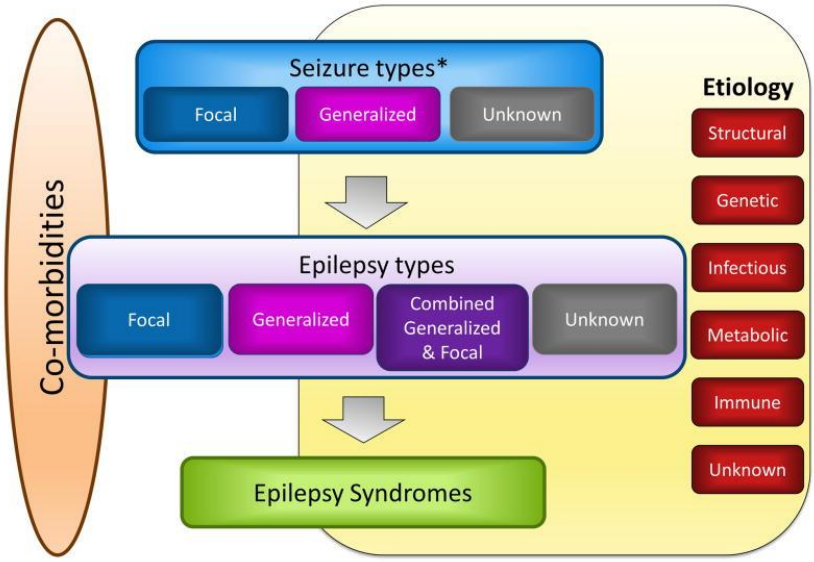

Figure 2. From the Scheffer et al., International League Against Epilepsy (ILAE), 2017 (2).

Multi-level epilepsy classification introduced by the ILAE. This guideline takes the seizure types, the epilepsy types, and the epilepsy syndromes into account, whereas related etiology and comorbidities are being assessed on all three diagnostic levels.

1.5. Symptoms of Epileptic Seizures

Seizure derives from the ancient Greek, for *to take hold* (44), which hints at its prominent behavioral manifestation. The term *seizure* applies to paroxysmal neurological dysfunctions induced by hypersynchronous discharges of neurons in the brain (17). Symptoms during active seizures appear heterogeneously, depending on etiology and seizure type (7). The stereotypical behavior usually emerges transiently and reflects abnormal excessive neuronal network activity in the brain (12). Recurrent hypersynchronous neuronal activity evokes a wide variety of clinical manifestations, ranging from almost undetectable symptoms (e.g. absence seizures) to vigorous motor actions (e.g. generalized tonic-clonic seizures) (17). Along with an impairment of consciousness, sensory, psychic, motor, cognitive, and autonomic functions can be affected (44). The time point of seizure onset is often easier to define than its termination, as it can be confused with the postictal state (44). Generalized tonic-clonic seizures, formerly called grand mal, typically manifest with a loss of consciousness, strong contractions, and stiffening of limbs and back followed by a clonic phase of bilateral symmetric convulsive shaking (17). Myoclonic seizures often present with involuntary muscle spasms that involve either parts or the entire body, while vigilance usually remains unaffected (17). Atonic seizures, on the other hand, are characterized by total loss of body tone and may result in falls and injuries (17). Generalized absence seizures, still known as petit mal, manifest with a brief

impairment and return of consciousness (17). In this case, the sudden interruption of ongoing activity, unresponsiveness, staring, or eye blinking are usually not followed by a postictal phase (17). Focal seizures can be preceded by an aura associated with the localization of the focus (17). For example, temporal lobe epilepsy can be accompanied by déjà-vu, while occipital origin evokes visual phenomena, and a seizure focus in the postcentral gyrus can cause sensory perceptions (17).

The postictal state, the clinical manifestation of an aftermath following seizures, can arise involving a variety of neurological deficits and EEG changes lasting minutes to days (45). During the postictal phase, it is generally assumed that recovery processes are taking place (45). This transient brain condition characteristically involves EEG-suppression and slowing of brain rhythms (45). Patients often remain unresponsive, while others report fatigue, headaches, or migraine (45). The postictal state is often accompanied by short-term retrospective amnesia, as only a minority of affected patients is able to remember the preceding seizure (46). Todd's paresis is a common postictal phenomenon typically manifesting as a focal weakness or full paresis involving one side of the body, contralateral to the affected brain hemisphere (46, 47). Due to its resemblance to hemiplegia, it is easily mistaken as a transient ischemic attack or stroke (45, 46). Moreover, postictal psychosis occurs in at least 4% of cases (45, 48).

1.6. Pathophysiology and Epileptogenesis

In the chronic condition of epilepsy, the pathologic lowering of the seizure threshold is responsible for an enduring susceptibility towards recurrent and unprovoked seizures (12). Epileptic seizures originate from cortical areas or subcortical structures, which involve thalamocortical circuits or the brainstem (44). The epileptiform activity that derives from large neuronal populations can be described as excessive, hypersynchronous high-amplitude discharges or bursts (49). The level of neuronal participation in epileptic network activity is determined by the inhibitory conductance and the surround inhibition (49), which modulates focal seizure propagation (50). Surround inhibition is a phenomenon of strong inhibitory conductance in adjacent but also remote brain areas that is able to suppress the spread of ictal activity from the seizure focus (50). The complex interplay of different types of neurons determines the ever-changing level of synchrony and takes place on multiple spatiotemporal scales (41). The underlying oscillations range from rhythmic spike patterns and spike-wave discharges, over high-frequency oscillations (HFO, 80-200 Hz) to fast ripples (FR, 250-600 Hz) (51-54). Especially in the hippocampus, HFO and FRs are regarded as the pathologic electrophysiological correlate underlying epileptic activity and thus, as potential biomarkers (15, 51, 54). The interictal spikes comprise a high amplitude, up to 100 ms lasting rapid spike

followed by a slow wave-component of 200-500 ms (52). Interestingly, interictal oscillatory patterns are being routinely detected in clinical settings during surgical interventions in order to localize the seizure origin in focal epilepsies (52). Here, the use of high-frequency oscillations as a biomarker can help to identify the core of seizure origin and to differentiate it from the surrounding penumbra by high-sampling rate- and intracranial EEG recordings (41).

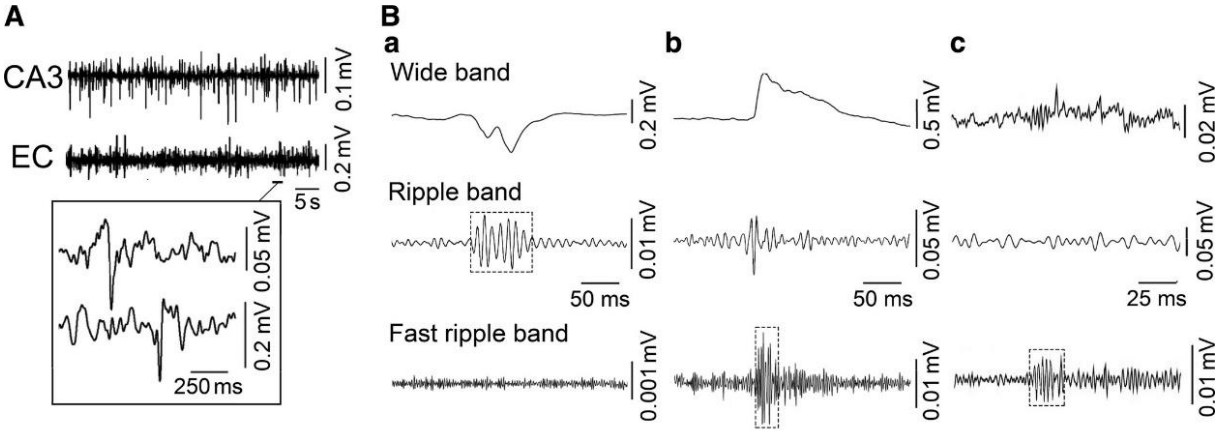

Figure 3. Modified from Lévesque et al., 2018 (3).

Different interictal oscillatory patterns recorded in vivo by depth EEG in pilocarpine-induced epilepsy in rats.

(A) Properties of interictal spikes in CA3 area and entorhinal cortex (EC) of the hippocampus.

(B) a-c indicate various forms of high frequency oscillations (HFOs) and fast ripples (FRs) with **(a,b)** or without **(c)** interictal spikes in CA3.

The term *epileptogenesis* is used to summarize the underlying mechanisms that enable brain tissue to generate spontaneous seizures (55, 56). It describes processes that eventually induce an onset or progression of an epileptic disorder, thus resulting in enhanced seizure susceptibility (55). The term is often attributed to the latent time period following an acquired brain insult, such as SE, stroke, or TBI, prior to spontaneous seizure onset (55, 57). Importantly, however, due to recent experimental and clinical assessments, epileptogenesis must be considered a dynamic phenomenon persisting also after the diagnosis of epilepsy (55).

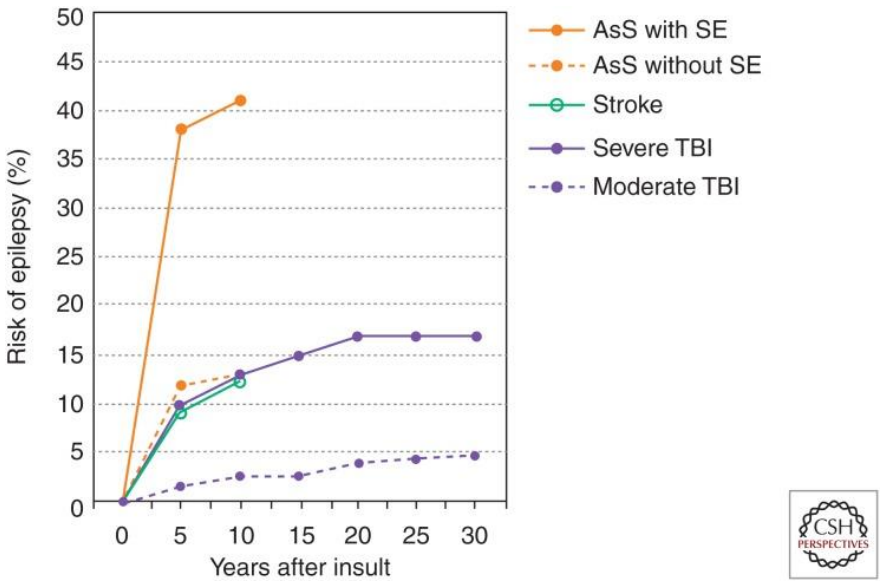

Figure 4. From Pitkänen et al., 2015 (4).

The authors summarized epidemiological data from studies that analyzed the incidence of acquired epilepsy following various types of brain insults: acute symptomatic seizure (AsS) with and without status epilepticus (SE), stroke, severe, and moderate TBI. The rates of epilepsy are comparable after stroke, AsS without SE, and severe TBI. Note the elevated risk of epilepsy for decades following the insult compared to the general population.

1.6.1. The Critical Balance of Excitation and Inhibition

Under physiological conditions in the brain, homeostatic mechanisms on the scale of neural circuits achieve a steady-state balance between the opposing effects of inhibition vs. excitation (41). Contrary to general assumptions, the underlying synchronic firing activity of neurons involves enhanced inhibition as well as excitation, meaning that an excess of excitation over inhibition is not necessarily given in epilepsy (44, 58). It is a frequent matter of discussion that excessive inhibitory action facilitates synchronization of neuronal populations or disinhibits epileptogenic circuits (59, 60). An important animal research model of temporal lobe epilepsy (TLE), the so-called *kindling*, is known to induce an increased $GABA_A$ receptor-mediated inhibition in hippocampal circuits but paradoxically leads to increased seizure susceptibility (61).

On the other hand, an imbalanced ratio of excess excitation over inhibition (E/I-imbalance) is assumed to play a major role in the pathogenesis of epilepsy and can be either of acquired or genetic origin (17, 41, 59, 62). For the latter, the technical milestone of next generation

sequencing (NGS) yielded large-scale studies of the genome in patients with epileptic disorder syndromes in global collaborations and the creation of databases incorporating >1000 genes (41, 63). Approximately 50% of all epilepsy cases are associated with a genetic origin (62). The Angelman syndrome is an example of predisposed E/I-imbalance due to a pathological deletion of the chromosomal 15q11-13 locus that encodes three $GABA_A$ receptor subunits (59, 64). Many mono- and polygenic mutations in genes encoding ion channels, enzymes, G-protein coupled receptors etc. are associated with altered neuronal excitability and a predisposition for seizures (17). Therefore, along with improved diagnostic tools, the role of the genetic predisposition has become more evident during the last decades and creates prerequisites for the development of novel targeted treatment options (62, 65, 66).

Another example for the importance of an E/I-balance is the young brain, in which a physiologically immature inhibitory system predisposes to seizures in neonates and children (59). At an early life-stage, GABAergic synapses are formed earlier than glutamatergic ones and mediate excitation instead of inhibition (67). This can be explained by a high intracellular chloride concentration and a reverse potential that leads to depolarization upon $GABA_A$ receptor-mediated chloride influx (59, 67). The excitatory actions of GABA are involved in generating giant depolarizing potentials (GDP) that promote synapse formation and neuronal growth during brain development (67). Later on, activity-driven molecular changes fulfill the necessary shift from GABAergic excitation to inhibition, protecting the developing brain from excess excitation (67). Not only in the course of brain development but also during adulthood, neural networks and patterns of connectivity are being dynamically modified in dependence of neuronal activity (61). Neural circuits mediate information processing and are functional clusters of neurons formed by synaptic connectivity (41). These clusters are subdivided into microcircuits of feedforward and backward connectivity between various types of neurons (41). In response to hypersynchronous firing, neurons and their synapses undergo complex molecular alterations to form aberrant functional connections (61, 68). This synaptic circuit plasticity during epileptogenesis involves immediate short-term plasticity, long-term potentiation, long-term depression, and further persistent and progressive cellular dysfunctions (61, 68-70). Acquired hyperexcitability of the brain develops following a stroke or a brain injury that initiates a reorganization of neural circuits and their synaptic connectivity (17). However, the underlying mechanisms are manifold and not confined to an impaired GABAergic signaling (59).

1.6.2. The GABAergic System

Although inhibitory interneurons amount to only approximately 10-20% of the neuronal population, their synapses, diverse firing properties, and recruitment provide a highly effective

inhibition in the brain (71). The primary inhibitory neurotransmitter in the brain is gamma-Aminobutyric acid (GABA), which is directly produced by decarboxylation of glutamate in interneurons where it accumulates in presynaptic vesicles (72). Glutamine is released from astrocytes and metabolized to glutamate, which is subsequently decarboxylated to GABA in interneurons (72). Both glutamate and thus also GABA derive from intermediates of the citric acid cycle (73). Hence, their production and availability depends on the cellular energy metabolism (73). There are two distinct types of GABA receptors: the ionotropic $GABA_A$ (and formerly $GABA_C$) receptor representing a ligand-gated chloride (and bicarbonate) channel and the metabotropic G-protein coupled $GABA_B$ receptor that operates with potassium and calcium currents through second messenger cascades (59, 72). The structure of the $GABA_A$ receptor has been extensively investigated: $GABA_A$ receptors are heteropentamers composed of two α and two β subunits in combination with a δ or γ subunit (59). In sum, there are about 16 $GABA_A$ receptor subunits in mammalians, which are differently expressed depending on affinity properties and function (59). Each subunit encompasses four hydrophobic transmembrane motifs, an intracellular domain between the transmembrane domains three and four, and an extracellular N-terminus (74).

The expression of the receptor subunits alters physiologically throughout the life-stages and pathologically as a result of TBI or seizures (59, 72, 75). The subunit composition also determines the kinetics of inhibitory neurotransmission. Phasic inhibition is characterized by fast presynaptic GABA release that acts predominantly on synaptic α1/γ2-containing $GABA_A$ receptors, while tonic inhibition has slower kinetics and activates $GABA_A$ receptors with α4/δ subunits located extrasynaptically (72, 75). Inhibitory neurotransmission is influenced by the number of available $GABA_A$ receptors at synaptic sites and can be altered by neuronal activity, growth factors, and clustering processes (74). Newly synthetized synaptic $GABA_A$ receptors are assembled in intracellular compartments, then follow the secretory pathway to be transported to the cell surface (64, 74). After taking effect on GABA receptors, reuptake of the released GABA is conducted through GAT-1 transporters into the pre-synapses, where the transmitter is recycled and re-assembles in vesicles (72). GABA plays an essential part in regulating and controlling neuronal development and maintaining a physiological E/I-balance by modulating excitatory synaptic transmission (59, 72).

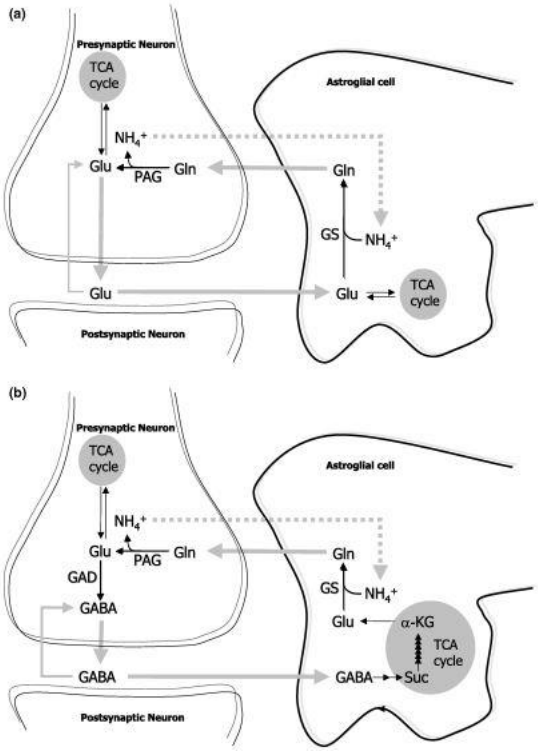

Figure 5. From Bak et al., 2006 (5).

Simplified illustration of the GABA-glutamine cycle taking place in presynaptic neurons, postsynaptic neurons, and astrocytes. The tricarboxylic acid (TCA) cycle provides the intermediates needed for the production of both neurotransmitters, glutamate (Glu), and GABA.

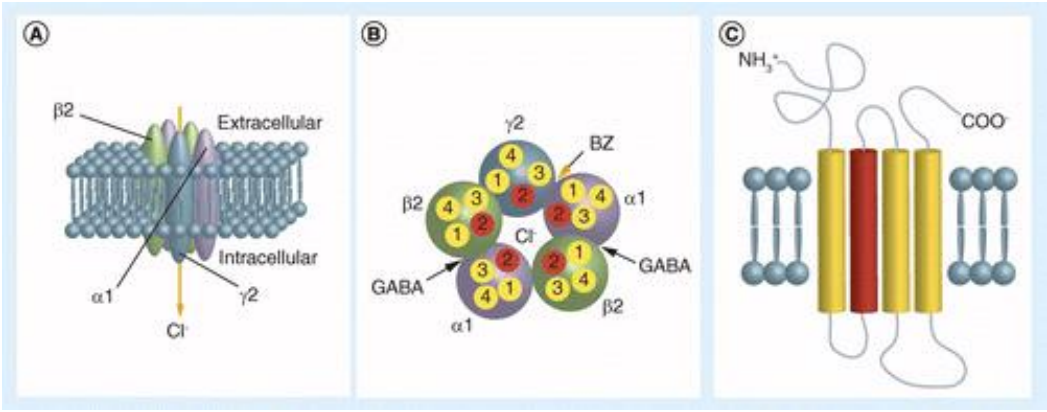

Figure 6. From Gong et al., 2015 (6).

Structure of the ionotropic $GABA_A$ receptor composed of α1β2γ2-subunits in the mammalian brain.

(A) Assembly of the five protein subunits in a heteropentamer forming a chloride-permeable pore that is opened upon ligand-binding.

(B) Indicated binding sites of GABA and benzodiazepines (BZ).

(C) Transmembrane domains TM1-4, extra-and intracellular domains and N- and C-terminal domains of a receptor subunit.

1.6.3. GABA in Epileptogenesis

In vivo and *in vitro* experiments have shown that diminished GABAergic signaling may uncover runaway excitation in the appearance of epileptiform discharges (58, 59). In epileptogenesis, an impaired GABAergic inhibition is caused by severe loss of interneurons (76) and GABA-producing cells (72), a reduced postsynaptic current (IPSC) frequency, changes in presynaptic GABA release probability, and an altered subunit composition of $GABA_A$ receptors (56). Pathological alterations in the molecular assembly of $GABA_A$ receptor subunits have been observed in animal models following TBI with a reduction and down-regulation of α1/γ2-subunits and elevation of α4/δ-subunit levels (Figure 7), reflecting a switch from phasic to tonic inhibition (72, 77). Furthermore, a decrease of functional postsynaptic $GABA_A$ receptors might be responsible for pharmacoresistance to AEDs such as benzodiazepines in SE (78). Additionally, as observed in TLE, enhanced glutamatergic excitation and increased pools of releasable glutamate disrupt the critical E/I-balance (56). In contrast, a gain of inhibitory neurotransmission can likewise evoke abnormal synchronization or disinhibit excitatory circuits (58, 59, 79). Rebound excitation, for example, is a phenomenon observed in T-type-calcium channels, where mostly chloride-dependent hyperpolarizing inputs trigger enhanced firing rates and bursts that propagate to surrounding neurons (58, 80). It is assumed that rebound excitation in thalamocortical circuits underlies human absence seizures, which can be effectively treated with ethosuximide, an inhibitor of the T-type calcium channel and its low-threshold calcium current (58). In addition, specific populations of GABAergic interneurons, especially hilar somatostatin (SST)- and neuropeptide Y (NPY)- immunoreactive interneurons, are severely affected by cell death (81-83).

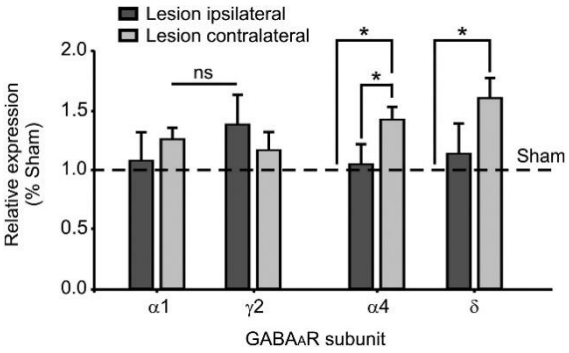

Figure 7. From Le Prieult et al., J Neurotrauma, 2017 (7).

TBI changes the $GABA_A$ receptor subunit composition 1-2 days after the injury, measured by mRNA expression. The increase in $GABA_A$ receptor α4- and δ-subunit expression indicates a shift from phasic to tonic inhibition post-TBI.

1.6.4. Molecular Changes during Epileptogenesis

In addition to an impaired GABAergic inhibition, molecular signaling pathways on a cellular level play a central role in epileptogenesis. Oxidative stress, free radical formation, and mitochondrial damage are implicated in neurodegenerative diseases and epilepsy (25, 84), ischemic stroke (85), or traumatic brain injuries (72). To date, a critical imbalance between

production and enzymatic removal of reactive oxygen- (ROS) or nitrogen species (RNS) has been discussed as the primary source of oxidative stress (84). Altered signaling pathways in epilepsy lead to reduced levels of available nitric oxide (NO) and, in contrast thereto, an increased generation of RNS and ROS, resulting in an imbalanced ratio (84). Oxidative stress per se is known for causing damage to mitochondria, cell structures, DNA, RNA, and proteins (25, 84).

Furthermore, glutamate-induced excitotoxicity is associated with numerous acute and chronic neurological diseases, including epilepsy (25). In traumatic brain injuries, studies often attribute a key role to excitotoxicity in TBI-inflicted secondary damage (86, 87). Here, the mechanical impact of TBI generates an immediate transmitter and ion release into extracellular space, including glutamate (72). Subsequently, an increased binding to AMPA or KA receptors causes an influx of sodium ions, and partly calcium ions (88). The resulting membrane depolarization opens more voltage-dependent calcium channels (VDCC) (88). Upon strong membrane depolarization, the extracellular magnesium ions blocking the NMDA receptors are lifted, leading to a large calcium influx into the cell (88, 89). In addition, the activation of G-coupled metabotropic glutamate receptors (MetR) initiates a release of calcium from the intracellular ER, further increasing the cytoplasmic calcium level (88). Subsequently, high intracellular calcium concentrations set off multiple cascades and activate catabolic enzymes, such as phospholipases and endonucleases, and initiate pathways leading to dysfunctions in cell metabolism (87). Cytoskeletal structures are damaged, mitochondrial membrane potentials are disrupted, and the DNA is fragmented (86). The high calcium concentration alters the mitochondrial permeability by opening the calcium-dependent mPTP pore, releasing cytochrome c and uncoupling the electron transport chain (86). The released cytochrome c promotes caspase-mediated apoptosis (86). The cellular supply of ATP declines and the synthesis of new ATP molecules is compromised, leading to the failure of the Na^+/K^+-ATPase (72, 86). The deficit of ATP elicits necrotic processes which cause cell swelling, and eventually, the rupture of the cell membrane (86). A dysfunction of the Na^+/K^+ pump correlates with neurological diseases such as depression, brain injury, Alzheimer's disease, hyperexcitability, and epilepsy (25, 90).

Other mediators in the pathogenesis of epileptic disorders involve neuroinflammation, reactive astrogliosis, synaptic reorganization, mossy fiber sprouting, all of which have been observed in animal models and human TLE (76, 81, 83, 91). Aside from a rarefication of neurons in hippocampal subfields, astrogliosis and microgliosis were found in resected tissue of TLE patients (56). All of these molecular alterations might contribute to the age-related incidence peak of epilepsy in the elderly (25).

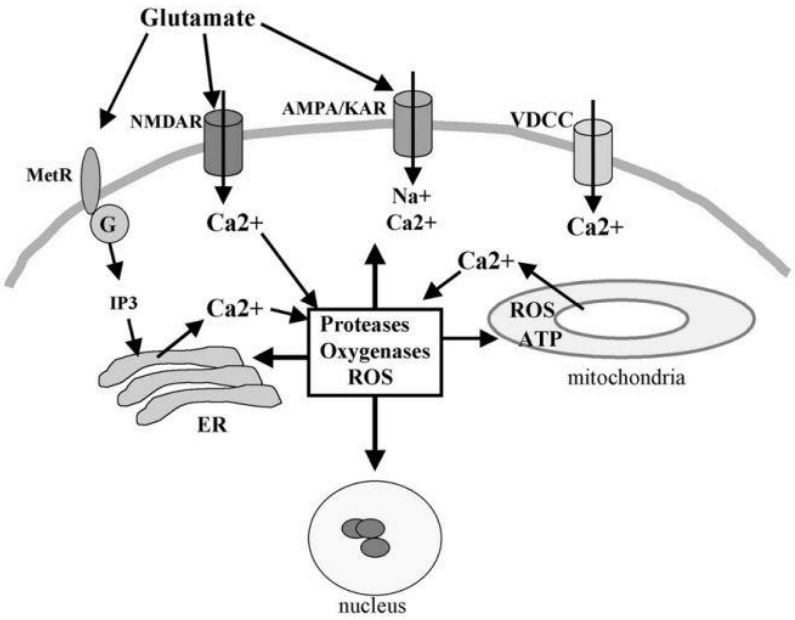

Figure 8. From Mattson, 2003 (8).

Simplified scheme of glutamate-driven excitotoxicity.

Glutamate binds to AMPA receptors and kainic acid receptors (KAR), which leads to Na^+ influx and membrane depolarization, upon which voltage-dependent Ca^{2+} channels (VDCC) open. Subforms of AMPA receptors are also permeable to Ca^{2+}. Upon strong depolarization, the external Mg^{2+} blockade of NMDA receptors is lifted, causing a large Ca^{2+} influx into the cell soma. Additionally, the activation of the G-coupled metabotropic glutamate receptors (MetR) sets off the phospholipase C- and IP3-cascade that results in further Ca^{2+} release from the endoplasmic reticulum (ER). The high intracellular Ca^{2+} concentration causes manifold disturbances, such as the activation of proteases and other catabolic enzymes, or Ca^{2+} uptake into the mitochondria. Subsequently, reactive oxygen species (ROS) are produced, ATP-production is impaired, DNA is fragmented, ending in apoptotic or necrotic cell death.

1.7. Traumatic Brain Injuries (TBI) and Posttraumatic Epilepsies (PTE)

According to recent epidemiologic reviews, 69 million people worldwide are estimated to experience TBI annually (92). It can be predicted that about half the earth's population will sustain at least one TBI in their lifetime (93). Epidemiological studies state that approximately 7.7 million individuals suffer from TBI-associated long-term disabilities in Europe (94), and about 5.3 million in the US (95). In young adults, the primary cause of death and disability worldwide are traumatic brain injuries (93, 96). Furthermore, TBI represents a major cause of acquired epilepsy in young adults (72, 97). Posttraumatic epilepsy (PTE) is a vast public health concern, since approximately 10-20% of all symptomatic epilepsy cases in the general population occur posttraumatic (97-99). Here, the rates of PTE and the risk of seizure recurrence are the highest related to severe brain injuries and multiple contusions (98). Severe TBI results in a 30-times increased incidence of epilepsy in comparison to the general population (97).

Primary brain damage is the immediate result of mechanical stress (100). Rotational forces can cause diffuse axonal injury through axonal shearing, impacting axonal transport (100). Physical impact also damages the cytoskeleton, mechanoactivates sodium and calcium channels and increases the permeability of the plasma membrane (100). In addition to the primary brain damage, the subsequent secondary brain injury is characterized by neuroinflammation, mossy fiber sprouting , disruption of the blood brain barrier and loss of dentate hilar neurons, which have been reported in various animal models of TBI and discussed as important mediators of epileptogenesis (57, 81, 101, 102). In focal TBI, the pathological alterations propagate to remote and intact parts of the brain as well and do not remain confined to the adjacency of the lesion site, a phenomenon termed *diaschisis* (103). In a previous study in our lab of unilateral TBI in mice conducted by Le Prieult et al., cortical hyperactivity was discovered particularly in the uninjured contralateral hemisphere 24-48 hours post-TBI (75). Concomitantly, phasic GABA-mediated neurotransmission was reduced, whereas $GABA_A$ receptor subunits associated with tonic inhibition were upregulated (**Figure 7**) (75). It is hypothesized that TBI-induced loss of GABAergic control results in increased glutamatergic transmission and a critical E/I-imbalance, which facilitates the process of epileptogenesis (100, 101).

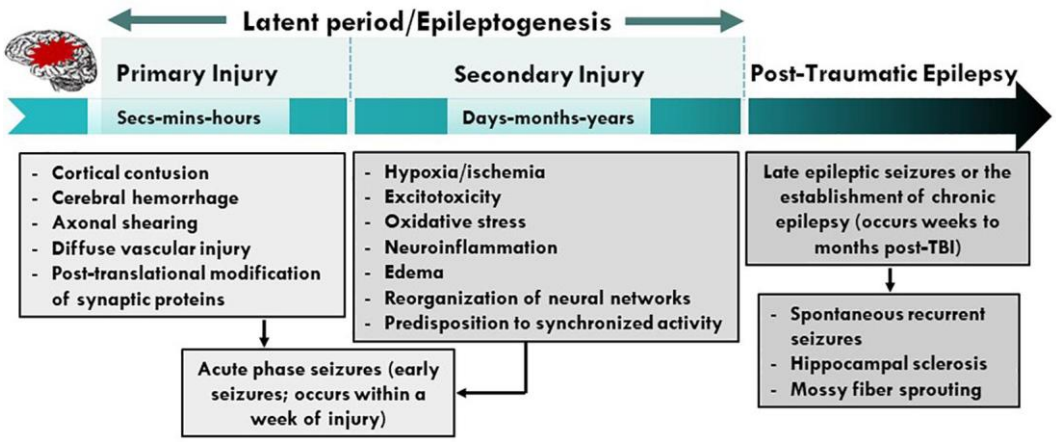

Figure 9. From Sharma et al., 2021 (9).

Mechanisms and pathophysiology of posttraumatic epileptogenesis from the time of the immediate injury beyond the diagnosis of posttraumatic epilepsy (PTE).

The latent epileptogenic period following the brain injury can last several years until the onset of symptoms (101). For more than ten years after TBI, the risk of PTE is significantly elevated (104). That latent time window could be of great importance for an effective antiepileptogenic treatment (43). Until today, PTE in particular remains difficult to target and treat, both pharmacologically and surgically (97). To date, no effective therapy preventing late-onset seizures has been discovered and options are limited to a mainly symptomatic treatment aimed at seizure control (98). Studies suggest that specific molecular targets prove promising for devising novel treatment strategies (43, 91, 98). Examples for such targets are brain-derived neurotrophic factor (BDNF), insulin-like growth factor 1 (IGF-1), interleukin 1 beta (IL-1ß), HCN channels, the JNK, and the mTOR pathways (43, 55, 81, 98). Modulating gene expression through epigenetic regulation or transcription factors acting as activators or repressors might become useful antiepileptogenic strategies (55). Rapamycin, an mTOR-inhibitor, was able to suppress axon sprouting, cell death, and seizure activity in animal epilepsy models and hippocampal cell cultures (105-108). In a mouse model of TBI, one month of rapamycin-treatment was able to mitigate epileptogenesis in a 16-week EEG-recording period (109). In another recent study, increased cytokine of IL-1ß, IL-6 and tumor necrosis factor alpha (TNFα) as well as reactive microglia and astrocyte activation were measured in a model of posttraumatic epileptogenesis, displaying evident neuroinflammation (110). Then, the authors deployed a polyclonal TNFα-antibody that was able to decrease ictal discharges during MEA recordings in organotypic hippocampal slice cultures after TBI (110). Not only the therapeutic strategies are of importance, but there is also a great necessity for potential biomarkers that quantify the severity and identify the patients at risk of developing PTE that could profit from

antiepileptogenic treatment (97). Gene array data acquired after TBI and status epilepticus (SE) have been compared in a meta-analysis by Pitkänen et al. in 2011 to disclose common gene regulations on the level of the transcriptome (111). Interestingly, only 17 proteins out of 46 regulated proteins were regulated in common after both TBI and SE and could represent potential treatment targets, e.g. IL6R (111). Pre-clinical *in vivo* and *in vitro* studies of TBI-related epileptogenesis remain of great importance to discover novel effective treatments and biomarkers (91, 98).

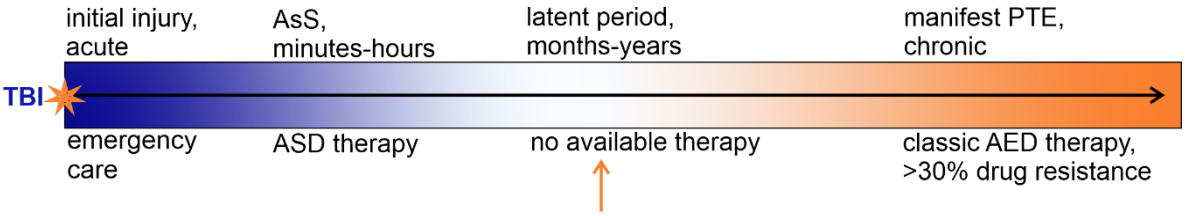

Figure 10. Adapted from Timofeev et al., 2013 (10).
Timeline of a possible course of TBI-induced epileptogenesis resulting in PTE. The orange arrowhead highlights the time point for a possible antiepileptogenic intervention. TBI = Traumatic brain injury, AsS = acute symptomatic seizure, ASD = anti-seizure drug, AED = antiepileptic drug, PTE = posttraumatic epilepsy.

1.8. Molecular Target Ubiquilin-1

In search of further molecular targets involved in posttraumatic epileptogenesis, we came across the $GABA_A$ receptor-stabilizing protein ubiquilin-1, also referred to as plic-1 (64, 74, 112, 113). It interacts with the ubiquitin-proteasome system (UPS) (113-116), which is responsible for protein homeostasis (*proteostasis*) and the elimination of accumulated or misfolded proteins (117). A pathological downregulation of ubiquilin-1 expression has been reported in neurodegenerative diseases (118-120), epileptic disorders (64), and stroke-caused brain injuries (121).

The 63 kD protein concentrates at synaptic sites and forms a functional link between the ubiquitination machinery and poly-Ub-tagged substrates with specific subunits of the proteasome (64, 114, 115). Within the cellular domains of $GABA_A$ receptor α- and β- subunits, several ubiquitin-like proteins recognize a conserved amino acid sequence (74, 112). The C-terminal domain of ubiquilin-1 directly interacts with poly-Ub $GABA_A$ receptors (64, 115, 116). The N-terminal has a proteasome-binding motif, which is homologous to ubiquitin and facilitates protein degradation *in vivo* (64, 114). At inhibitory synapses, ubiquilin-1 co-localizes with $GABA_A$ receptor β2-/3-subunits, prolongates their half-life, and protects from early ER-associated degradation (64, 74, 112, 113). Along with α- and γ2- subunits, a large proportion

of benzodiazepine- and barbiturate-sensitive $GABA_A$ receptors in the central nervous system is composed of these subunits (59, 74, 122). The negative modulation of the proteasome augments the amount of available receptors for membrane insertion and is mediated through ubiquitin-like proteins such as ubiquilin-1(74, 112, 114). $GABA_A$ receptors are assembled intracellular within the ER and subsequently inserted into the neuronal plasma membrane, whereby ubiquilin-1 is regarded as a regulatory element of membrane trafficking (112). Studies suggest that ubiquilin-1 promotes the insertion of recycled and newly synthetized $GABA_A$ receptors into the neuronal plasma membrane (64, 74, 112, 113). Thus, it might influence the insertion rate that determines the receptor cell surface expression (112) and ensure efficient inhibition through stable receptor numbers on the cell surface (74). As demonstrated by Bedford et al., whole-cell ELISAs of A239 cells that overexpress ubiquilin-1 and co-express α1β3γ2 $GABA_A$ receptors revealed a significantly augmented total number of cell surface receptors (74). Furthermore, the stability of the GABA receptor β3- subunit was increased when ubiquilin-1 was co-expressed (74, 112). Ubiquilin-1 controls the $GABA_A$ receptor cell surface expression by steadying intracellular receptor pools within the secretory pathway, without changing receptor internalization rates, ion channel function, or endocytic anchoring and sorting (74, 112).

1.8.1 The Ubiquitin-Proteasome System (UPS)

Protein homeostasis is the essential ability of cells to survive and adapt to changing external conditions and thus, an evolutionary conserved process in eukaryotes (123, 124). The maintenance of proteostasis in a steady state requires not only correct protein synthesis but also functioning protein degradation. The ubiquitin-proteasome system is one of the two major biological pathways orchestrating protein degradation (117, 125). For its discovery, Aaron Ciechanover, Avram Hershko and Irwin Rose were awarded with the Nobel Prize for Chemistry in 2004 (125). Autophagy, on the other hand, represents the other important key player in protein degradation by the formation of intracellular autophagosomes for lysosomal digestion (117). It is categorized into three underlying pathways: micro- and macroautophagy, and the chaperone-mediated autophagy (117). The complex machinery of autophagy will not be discussed here, however it is worth mentioning that both systems, the UPS and autophagy, are closely interconnected through a complex interplay of ligand molecules and linking proteins (126).

Ubiquitination is a main determinant of the levels, function, and translocation of proteins, and the cell fate through regulating signaling pathways (125). The UPS is responsible for the degradation of more than 80% of cellular proteins and the preservation of a protein quality control and dynamic equilibrium, which is optimal for cell and organ function (123). Its highly

selective capacity enables an elimination of misfolded or damaged proteins on the one hand, and proteins with specialized functions on the other (123). Regulatory proteins of cell death, for example Bcl-2- related proteins or caspases, are tagged and decomposed by the UPS (125). Even transcription factors, such as P53 or NF-κB that mediate the expression of proteins associated with the cell cycle and programmed cell death, are target substrates of the UPS (125). Moreover, inflammatory reaction, immune response, metabolic regulation, or antigen presentation are modulated by the ubiquitin-proteasome machinery (123, 127). The process of ubiquitin-dependent degradation is composed of multiple steps and requires energy in the form of ATP (123). First of all, substrates determined for degradation undergo tagging with a ubiquitin molecule chain made up of a polypeptide containing 76 amino acids (117, 123). Then, enzymatic cascades catalyzed by the three enzymes E1-E3 enact the ubiquitin conjugation usually at more than one lysine-containing binding site of the substrate (117, 123). As soon as at least four ubiquitin chains label the substrate, the trafficking to the proteasome is set off (123). The 26S proteasome itself is organized as a tubular organelle built up of two complexes: a catalytic 20S core subunit and two regulatory particles of gating, the 19S caps (123, 125, 126). The substrates first interact with the 19S subunits through shuttle proteins and are de-ubiquitinylated prior to reaching the 20S core containing six ATP-dependent serine-protease sites for protein hydrolysis (123, 125). Afterwards, the released peptides with a size of 3-25 amino acids are further processed into single amino acids by peptidases (126). The whole process of ubiquitin-dependent degradation is controlled by various possibilities of mono-ubiquitination, multiple mono-ubiquitination, poly-ubiquitination, the modification of Ub-chains on tagged substrates, or the inter-linkage of ubiquitin polymers (126, 127). Furthermore, at different stages of the UPS, so-called ubiquitin-like proteins are intertwined, refining the whole degradation process (127). Additionally, the continuous and dynamic assembly and deconstruction of ubiquitin polymers also affect the fate of protein substrates (127). The manifold modifications and interactions with the UPS remain elusive to a large part, which only hints at the complexity and the scope of its importance in cellular regulation (127). An impaired UPS function and protein homeostasis, however, is known to be implicated in various neurological diseases and to disrupt cellular homeostasis (117). The accumulation of ubiquitinylated proteins is considered a hallmark of neurodegenerative diseases such as Alzheimer’s or Parkinson’s disease (117, 125).

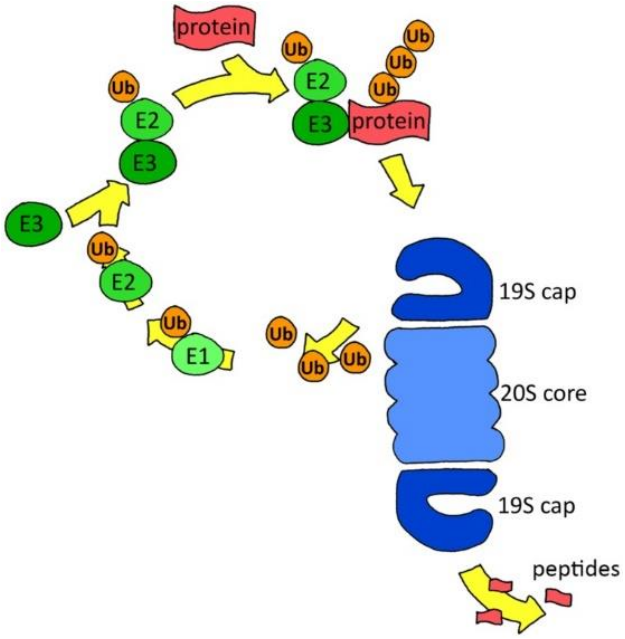

Figure 11. From Jansen et al., 2014 (11).

Simplified representation of the ubiquitin-proteasome system (UPS). Substrates are labeled with ubiquitin for proteasome-mediated degradation via E1, E2 and E3 enzymes. The 26S proteasome is composed of two 19S caps, which de-ubiquitinate the labeled proteins and unfold them in order to reach the 20S core complex. The end product of protein hydrolysis are small peptides, which are further degraded into single amino acids through peptidases.

1.8.2. The Role of Ubiquilin-1 in Neurological Diseases

Bearing in mind these essential functions, it is not very surprising that the ubiquilin-1 expression is strongly affected by epileptic activity or brain injuries. In a study by Zhang et al., a reduced ubiquilin-1 expression was observed in neocortical samples from TLE-patients who had at least four years of clinical history (64). Additionally, the downregulation of ubiquilin-1 was consistent in rat models of PTZ- or pilocarpine-induced epilepsy (64). In the PTZ-treated rats, lentivirus-mediated ubiquilin-1 overexpression elevated the mIPSC amplitude and frequency in *in vitro* whole-cell clamp recordings of CA1 pyramidal neurons, exclusively affecting phasic GABAergic currents (64). Moreover, mitigated seizure severity and duration were observed *in vivo* (64). Additionally, an intrahippocampal injection of PePα peptide disrupted the protein interacting with $GABA_A$ receptors, which revealed a shortened latency of seizure onset, increased seizure severity and duration in behavioral and EEG multichannel monitoring (64). In the pathophysiology of ischemic brain injuries, ubiquilin-1 also plays a role. In a study by Lou et al. in neonatal mice, exposure to hypoxic ischemia significantly reduced

ubiquilin-1 levels one to three days following the injury (121). In another study of stroke-induced brain injuries, transgenic mice that overexpressed ubiquilin-1 exhibited signs of improved motor function and recovery as well as reduced infarct volumes following brain injury (128). In knockout mice, on the other hand, the authors found an increase of neuronal injury and accumulated ubiquitylated proteins in the brain (128). Moreover, an improvement of functional post-ischemic recovery and *proteostasis* in models of ubiquilin-1 overexpression by LV-transfection underline these findings (129). In a proteomics approach in our lab, we observed a severe reduction of ubiquilin-1 expression in the somatosensory cortex contralateral to the lesion site after 24 hours following experimentally induced traumatic brain injury in mice (130).

1.8.3. The Role of Nialamide (NM) and other MAO-Inhibitors (MAOIs)

The research group of Liu et. al were the first to pharmacologically increase the expression of ubiquilin-1 by use of the non-selective monoamine oxidase (MAO) inhibitor nialamide (NM) (85). In their study, striatal cell cultures were treated with NM, which significantly upregulated ubiquilin-1 expression in Western blot and semiquantitative rt-PCR analyses (85). Strikingly, following ischemia/reperfusion (I/R)-injury in mice, the authors reported diminished ubiquilin-1 levels, which could be rescued by application of NM (85). Even an injection of NM at one to three hours post-lesion ameliorated functional recovery, whereas measured infarct volumes significantly decreased (85). Furthermore, the authors observed an alleviation of I/R-caused neuroinflammation through NM-administration, reflected by reduced TNFα-levels and number of microglia and astrocytes in immunostainings (85). Under knockout conditions, the authors verified that neuroprotective effects of NM can be ascribed to MAO- and ubiquilin-1 (85). In the present study, NM was deployed in order to restore ubiquilin-1 expression and investigate its potential antiepileptic effects.

Taken together, ubiquilin-1 plays a vital role for protein homeostasis and GABAergic inhibition in the brain, whereas its regulation is implicated in various neurological diseases. Hence, we considered the protein an interesting molecular target to investigate *in vitro* after experimental TBI-induction and onset of epileptiform activity. The present study's aim was to determine alterations of ubiquilin-1 expression using Western blots. Furthermore, electrophysiological recordings were conducted in the hippocampal CA1 region and used to investigate the potential neuroprotective role of the MAO inhibitor NM.

1.9. Treatment

The treatment of epileptic disorders predominantly addresses clinically manifest epilepsy through interrupting acute seizures and preventing seizure recurrence after disease onset (91). Therefore, pharmacological anticonvulsive therapy is not a curative but mainly a symptomatic

treatment approach. There are more than 20 antiepileptic drugs (AED) available that diminish electrical activity in the brain and augment the seizure threshold through distinct mechanisms (10). Classic AEDs such as valproate, carbamazepine and phenytoin suppress neuronal depolarization by blocking sodium or calcium channels (98). As mentioned earlier, generalized absence seizures can be effectively suppressed by ethosuximide, which blocks low-threshold calcium currents in the thalamus (58). Further medical options strengthen the inhibitory GABA receptor-mediated hyperpolarization, either by indirectly elevating the levels of available neurotransmitter or activating and modulating the corresponding $GABA_A$ receptors (17). Common preparations of that mechanism are benzodiazepines, barbiturates, and tiagabine (17).

Another pharmacological strategy is to suppress the glutamate-driven NMDA and AMPA receptor-mediated excitation, e.g. with felbamate (17). The choice of AED therapy is made with respect to individual features, epilepsy type, and underlying etiology (10). An in house-protocol for seizures or SE is usually adhered to and provides a high standard of acute therapy (131). Usually, prolonged acute seizures or status epilepticus are first treated with rapidly effective drugs, such as benzodiazepines (10, 131). If seizures remain refractory, further non-anesthetizing AEDs or even anesthetizing drugs are used (131). The vital parameters are assessed continuously, while the underlying cause of status epilepticus or seizure should be identified and treated as quickly as possible (131). As a long-term prophylaxis to prevent seizure recurrence, AEDs are commonly prescribed in the form of monotherapies at a low dosage, which can be increased, if necessary (10). In isolated cases and after preclusion of potential drug interactions, combination therapies can emerge as more effective after failure of a monotherapy (17). Unfortunately, adverse drug reactions are common in AED therapy and can cause serious side-effects (98), as most anticonvulsant drugs have a narrow therapeutic range. A major fraction of them is metabolized by isoforms of the cytochrome P450 enzymes, and hence, often causes drug interactions (10). Sedation, allergic reactions, psychiatric side effects, hepatotoxicity and decreases in bone mineral density, inter alia, have been reported (10, 132, 133). In order to monitor and prevent toxicity, therapeutic drug levels in the blood should be controlled at regular intervals (10).

In pharmaco-refractory cases after several failed treatment attempts, resective surgery (“lesionectomy”) represents an alternative treatment option and sometimes a last but good chance to become seizure-free (10, 134). In Germany, affected patients are invited to certified epilepsy centers to assess the eligibility for surgery (10). However, a surgical intervention also bears risks. Depending on the localization of the epileptic focus, access to it and the surgery itself can be complex (134, 135). Nowadays, the callosotomy, a surgical transection of the

corpus callosum, remains only a palliative procedure that aims to reduce repetitive falling (10). Vagus nerve- and deep brain stimulation of the anterior nuclei of thalamus are further treatment alternatives (10, 136). Complementary approaches such as ketogenic diet or biofeedback are assumed to be supportive measures yet not based on strong evidence (10). At the current state of research, an effective prevention of epileptogenesis has not been implemented in clinical practice (81, 91). There are several therapeutic approaches involving specific molecular targets and cell signaling pathways that affect neuronal network activity (81).

1.9.1. Seizure Recurrence

Following a first unprovoked seizure, the average risk of recurrence consistently decreases over time according to population-based studies (12, 25). The seizure recurrence rate ranges from 17-50% in the first 20 months, depending on seizure type and EEG characteristics (137, 138). The risk of seizure recurrence is assumed to be highest in focal and nocturnal seizures, while a history of brain injury or -insult is known to increase the risk (7, 137, 139). Individuals suffering head trauma prior to seizure carry an increased risk of recurrence, amounting to 46% in 20 months (137). The two most reliable predictors of seizure relapse are a known documented etiology and EEG abnormality, including slow and epileptiform activity or spike-wave discharges (7, 137, 138). The question of whether or not to initiate long-term antiepileptic treatment after a first unprovoked seizure, is based on clinical findings, EEG and neuroimaging, the individual treatment benefit, and preferences of the patient (12). Provided the risk of recurrence is high after a single seizure, the importance of an early treatment can outweigh adverse drug effects (12).

1.9.2. Drug-resistant Epilepsy (DRE) and Outcome

With regard to seizure freedom, the overall outcome for treated epilepsy patients is positive, as approximately 60-70% newly diagnosed cases achieve prolonged seizure remission after about five years (22, 140, 141). However, considering that most affected people in LMICs do not receive effective treatment, the reported numbers have to be interpreted with caution. Despite many cases being self-limited or pharmacoresponsive to AED therapy, a fraction of affected patients continues to suffer from recurrent seizures (140). In children diagnosed with epilepsy, 7-20% exhibit drug-resistant epilepsy, whereas 30-40% of cases in adults remain intractable (140-142). Epilepsy can be considered ‘resolved’, if an individual has been seizure-free for the last ten years, of which at least five years were off antiepileptic medication (12). By contrast, a failure of at least two pharmacological treatment attempts with AEDs, either as monotherapies or in combination, defines drug-resistance (135).

There are several risk factors for developing a drug-resistant, intractable form of epilepsy, which were identified in a recent systematic review by Xue-Ping et. al. The most important and consistent risk factors for DRE are abnormal electroencephalography (EEG showing slow wave and epileptiform activity), status epilepticus (SE), a symptomatic etiology, focus onset seizure, and the presence of multiple seizure types (140). Some of them correspond to the risk factors of recurrence after a first unprovoked seizure. Interestingly, in head trauma or brain insults that damage the blood brain barrier, the effectiveness of AEDs can be negatively affected by an overexpression of efflux transporters (140). An early ascertainment of these risk factors in clinical practice could help to predict the patient's outcome and to consider alternative treatment possibilities (140). Early seizure control is essential to prevent long-term sequelae, e.g. cognitive impairment that can exacerbate when the condition is left untreated (109). On the other hand, there are also epilepsy syndromes that are self-remitting or can be outgrown, such as the benign epilepsy with centrotemporal spikes and childhood onset (14).

1.10. Prevention and Future Directions

The burden of epilepsy is steadily rising with a growing world population and higher life-expectancy (25). Therefore, preventive measures will play an increasingly important role in the future (25). Primary prevention evades the development and onset of a disease through an abolishment of underlying risk factors and epileptogenic causes (143). A large fraction of causes leading to seizure onset in children and adults are partly preventable, including perinatal stroke, CNS infections, TBI, and stroke (35). Taken together, most of these avoidable causes prevail in LMIC compared to HIC (143). Disparities in the access to health care among regions and countries are major obstacles that have to be overcome in the future. The gradual facilitation of access to emergency and professional medical care can save many lives (143).

Broadening the health care infrastructure, improving hygiene, sanitation, and perinatal care, reducing exposure, and supporting immunization programs are useful improvement strategies (32, 143). Immunizations significantly reduce the number of CNS infections such as meningitis in LMIC (143). Additionally, public health and education aid programs are trying to eradicate parasite infestations, this accounts especially for neurocysticercosis caused by *Taenia solium* (143). Next to head injuries acquired during war and military service in veterans and soldiers, road traffic accidents can be ascribed to the high proportion of traumatic brain injuries (31, 96-98). As the incidence of traffic injuries and TBI is higher in LMIC (92, 144), the risk of developing PTE is proportionally elevated (92, 143). To reduce the number of road traffic accidents, programs and initiatives aimed at improving vehicle and road safety might accomplish good results, e.g. by public education on safety measures (143, 144). Stroke-caused epilepsies, on the other hand, constitute a greater burden in HIC (143). Therefore, primary prevention

predominantly addresses the corresponding risk factors associated with stroke. Even in LMIC, preventive measures in this field become more relevant on account of an increasingly aging population (143).

The ILAE, the International Bureau for Epilepsy (IBE), and the WHO formed a corporate initiative in over 90 countries, the Global Campaign Against Epilepsy, with the purpose of improving epilepsy care, raising awareness, and reducing the burden of epilepsy worldwide (32). The Global Campaign Against Epilepsy launched an action plan that promotes collaborative work and interchange between industrialized and developing countries, in particular for epidemiological data or clinical trials (32). By supporting national governments with public health work and by estimating regional resources and needs, the campaign contributes to improved conditions and epilepsy control (32). Educational programs for the general population raise awareness for the disease and encourage safety measures and health-seeking behavior (8). Furthermore, training for health-care providers in epileptology raises the global standard in professional epilepsy care (32). Meanwhile, huge advances have been accomplished in research over the last decades thanks to an increasing knowledge on epileptogenic mechanisms and the deployment of new technologies (145). In the field of basic research, novel techniques such as calcium imaging, voltage-sensitive dye, or optogenetic interventions enable data acquisition on single cell and network levels (81). On this basis, a multidisciplinary approach would promote the development of effective treatment strategies by implementing research into clinical trials, for the benefit of millions of affected individuals.

2. Materials and Methods

2.1. List of Materials for the Present Study

Table 1. Animals	
C57BL/6N mice (Charles River Laboratories)	Translational Animal Research Center (TARC), Mainz

Table 2. Chemicals, Buffers, Assays and Kits		
NaCl	Carl Roth GmbH + Co. KG	Karlsruhe, Germany
$NaHCO_3$	Carl Roth GmbH + Co. KG	Karlsruhe, Germany
$NaH_2PO_4H_2O$	Carl Roth GmbH + Co. KG	Karlsruhe, Germany
$CaCl_2H_2O$	Carl Roth GmbH + Co. KG	Karlsruhe, Germany
$MgSO_47H_2O$	Carl Roth GmbH + Co. KG	Karlsruhe, Germany
KCl	Carl Roth GmbH + Co. KG	Karlsruhe, Germany
Glucose	Carl Roth GmbH + Co. KG	Karlsruhe, Germany
DMSO	Sigma-Aldrich® (Merck KGaA)	St. Louis, MO, USA (Darmstadt, Germany)
Tween-20	Sigma-Aldrich® (Merck KGaA)	St. Louis, MO, USA (Darmstadt, Germany)
2-Propanol 99.8%	Carl Roth GmbH + Co. KG	Karlsruhe, Germany
Ethanol ≥99.8%, p.a.	Carl Roth GmbH + Co. KG	Karlsruhe, Germany
Ethanol ≥70%, denatured	Carl Roth GmbH + Co. KG	Karlsruhe, Germany
ImmunoSelect® Antifading Mounting Medium	Dianova	Hamburg, Germany
Immobilon™ Western Chemiluminescent HRP Substrate	Millipore Corporation	Burlington, VT, USA
Isoflurane 4%	AbbVie	Wiesbaden, Germany
X100, Triton® X-100	Sigma-Aldrich® (Merck KGaA)	St. Louis, MO, USA (Darmstadt, Germany)
Phosphate buffered saline (PBS 10x), pH 7.4	Gibco™ (Thermo Fisher Scientific)	Grand Island, NY, USA (Waltham, MA, USA)
Phosphate buffered saline (PBS 1x), pH 7.4	Gibco™ (Thermo Fisher Scientific)	Grand Island, NY, USA (Waltham, MA, USA)
Methanol ROTISOLV®	Carl Roth GmbH + Co. KG	Karlsruhe, Germany
ROTIPHORESE® Gel 30 Acrylamide, Bisacrylamide (37.5:1)	Carl Roth GmbH + Co. KG	Karlsruhe, Germany
TEMED 99%	Carl Roth GmbH + Co. KG	Karlsruhe, Germany
ROTI® PVDF pore size 0.45 µm	Carl Roth GmbH + Co. KG	Karlsruhe, Germany
NuPAGE™ LDS Sample Buffer (4x)	Invitrogen™ (Thermo Fisher Scientific)	Waltham, MA, USA
Halt™ Protease and Phosphatase Inhibitor, Cocktail (100x), 0.5 M EDTA	Thermo Fisher Scientific	Waltham, MA, USA
N-PER™ Neuronal Protein Extraction Reagent	Thermo Fisher Scientific	Waltham, MA, USA
Pierce BCA Protein Assay Kit (Reagent A + B), Albumine	Thermo Fisher Scientific	Waltham, MA, USA
Ammmonium persulfate (APS) 5%	Carl Roth GmbH + Co. KG	Karlsruhe, Germany
Lidocaine + Prilocaine salve	Aspen Germany GmbH	Munich, Germany

SDS solution 10%	Sigma-Aldrich® (Merck KGaA)	St. Louis, MO, USA (Darmstadt, Germany)
ROTIPHORESE® 10x SDS-PAGE	Carl Roth GmbH + Co. KG	Karlsruhe, Germany
CELLSTAR® 96 Well Plate	Greiner Bio-One International GmbH	Frickenhausen, Germany
ROTI® Histofix 4%	Carl Roth GmbH + Co. KG	Karlsruhe, Germany
Powdered milk, low-fat, Blotting Grade	Carl Roth GmbH + Co. KG	Karlsruhe, Germany
ROTI® Fair 1M Tris 7.4	Carl Roth GmbH + Co. KG	Karlsruhe, Germany
Picrotoxin, 1128	Tocris Bioscience	Bristol, EN, UK
Kainic acid, 0222	Tocris Bioscience	Bristol, EN, UK
Nialamide, 252999	Sigma-Aldrich® (Merck KGaA)	St. Louis, MO, USA (Darmstadt, Germany)
TRIS PUFFERAN® 99.3%, Buffer Grade	Carl Roth GmbH + Co. KG	Karlsruhe, Germany
Glycin PUFFERAN® 99%, p.a.	Carl Roth GmbH + Co. KG	Karlsruhe, Germany
Goat serum 10%	Vector Laboratories	Burlingame, CA, USA
Avidin/Biotin Blocking Kit	Vector Laboratories	Burlingame, CA, USA
Permabond® Glue	Permabond USA	Somerset, NJ, USA
3M Animal Care Vetbond Tissue Adhesive	3M Animal care products	St. Paul, MN, USA

Table 3. Instruments and Consumables		
Blotting apparatus: PowerPac HC Power Supply	Bio-Rad Laboratories Inc.	Hercules, CA, USA
Western Blot chamber	Bio-Rad Laboratories Inc.	Hercules, CA, USA
Electrophoresis apparatus	Bio-Rad Laboratories Inc.	Hercules, CA, USA
Vibratome VT 1200S	Leica Microsystems	Wetzlar, Germany
Microtome CM1325	Leica Microsystems	Wetzlar, Germany
CCI-impactor Impact One™	Leica Microsystems	Wetzlar, Germany
Pump System Minipuls 3	Gilson	Middleton, WI, USA
MEA chip	Multi Channel Systems	Reutlingen, Germany
MEA2100 headstage	Multi Channel Systems	Reutlingen, Germany
MEA2100 interface board	Multi Channel Systems	Reutlingen, Germany
Temperature Controller	Multi Channel Systems	Reutlingen, Germany
Vibratome VT 1200S	Leica Microsystems	Wetzlar, Germany
ChemiDoc XRS+	Bio-Rad Laboratories	Hercules, CA, USA
Microscope IX81	Olympus	Shinjuku, Japan
Grant Bio™ Platform Rocker PMR-30	Grant Instruments™	Cambridge, EN, UK
Centrifuge 5424 R	Eppendorf Research	Hamburg, Germany
SB3 rotator wheel	Cole-Parmer Stuart	Staffordshire, EN, UK
Orbital incubator S1500	Cole-Parmer Stuart	Staffordshire, EN, UK
Plate Reader Infinite M1000	Tecan Group Ltd.	Männedorf, ZH, Switzerland
Pipettes	Eppendorf Research	Hamburg, Germany
Menzel SuperFrost® slides	Thermo Fisher Scientific	Waltham, MA, USA
Lab dancer vario	IKA®Werke GmbH & Co. KG	Staufen, Germany
Deckgläser	Carl Roth GmbH + Co. KG	Karlsruhe, Germany
Fine-haired brush	Leonhardy	Nuremberg, Germany
Polypropylene sutures	Ethicon	Somerville, NJ, USA

Sterile Surgical Blades, Bayha 15	Carl Roth GmbH + Co. KG	Karlsruhe, Germany
Blades, double-edge PTFE coated stainless steel	Ted Pella, Inc.	Redding, CA, USA
Filter paper Mini Trans-Blot	Bio-Rad Laboratories Inc.	Hercules, CA, USA
Parafilm 4IN.x125 ft roll	Sigma-Aldrich® (Merck KGaA)	St. Louis, MO, USA (Darmstadt, Germany)

Table 4. Antibodies

Antibody	Species	Dilution	Company	Headquarter
Ubiquilin 1 (63 kD) Polyclonal Antibody, PA1-759	Rabbit	1:1000	Thermo Fisher Scientific	Waltham, MA, USA
Anti-GAPDH (36 kD) Antibody, A303-878A	Goat	1:1000	Bethyl Laboratories	Montgomery, TX, USA
Anti-NeuN, clone A60, MAB377	Mouse	1:250	Sigma-Aldrich® (Merck KGaA)	St. Louis, MO, USA (Darmstadt, Germany)
HRP-conjugated IgG anti-Rabbit, Secondary Antibody, AB_2307391	Goat	1:10000	Jackson ImmunoResearch Labs	West Grove, PA, USA
HRP-conjugated anti-Goat IgG, Secondary Antibody, 705-035-003	Donkey	1:10000	Dianova	Hamburg, Germany
Anti-Mouse IgG Secondary Antibody, Alexa Fluor™ 647, A-31571	Donkey	1:500	Thermo Fisher Scientific	Waltham, MA, USA
Anti-Rabbit IgG Secondary Antibody, Alexa Fluor™405, A-31556	Goat	1:500	Thermo Fisher Scientific	Waltham, MA, USA

Table 5. Software

Clampfit 11.1	Molecular Devices	Sunnyvale, CA, USA
Microsoft® Excel® for Microsoft 365	Microsoft® Corporation	Redmond, WA, USA
Microsoft® Word for Microsoft 365	Microsoft® Corporation	Redmond, WA, USA
Multi Channel Experimenter	Multi Channel Systems	Reutlingen, Germany
Multi Channel Analyzer	Multi Channel Systems	Reutlingen, Germany
Multi Channel Data Manager	Multi Channel Systems	Reutlingen, Germany
MEA Monitor	Multi Channel Systems	Reutlingen, Germany
Image Lab 2.0 Software	Bio-Rad	Hercules, CA, USA

ImageJ	Rasband, W.S., ImageJ, U.S. National Institutes of Health	Bethesda, MD, USA
CorelDRAW Graphics Suite	Corel Corporation	Ottawa, ON, Canada
Image Studio Lite 5.2	LI-COR Biosciences	Lincoln, NE, USA
EndNote X8.2	PDF Tron™ Systems Inc.	Vancouver, BC, Canada
GraphPad Prism 9	GraphPad Software Inc.	San Diego, CA, USA

2.2. Animals and Ethical Statement

All experiments in the present study were performed in strict accordance with European standards for the use of animals in research and guidelines of the Johannes Gutenberg University Mainz, Germany. Permission of the TBI-protocol was provided by the Animal Ethics Committee of the Landesuntersuchungsamt Rheinland-Pfalz (permission numbers 23 177-07/G20-1-112 and 23 177-07/G15-1-039). C57BL/6n wild type mice (n_{total}=58) of either sex aged 17-26 days had free access to food and water and were housed at a constant room temperature of 23 ± 2 °C with a standard 12-hour light/dark cycle. All possible efforts were made to minimize suffering of the animals.

2.3. Preparation of Acute Brain Slices

The animals for this study were black wildtype C57BL/6N mice and sacrificed at an age of 17-26 days. Deep anesthesia was induced by use of 4 vol% isoflurane (Abbvie, Wiesbaden, Germany). We observed the breathing pattern and checked nociception before the mice were quickly decapitated. After an immediate removal of the brain, it was placed in ice-cold standard oxygenated artificial cerebrospinal fluid (aCSF), which resembles the physiological liquor composition. Its contents are listed below in **Table 6**. Subsequently, several sections were made with razor blades to receive the ideal alignment to obtain horizontal brain slices from both brain hemispheres. Exceptionally for immunohistochemistry, coronal slices were prepared. The brain was transferred to the slicing platform of the vibratome and fixated with Permabond glue. Cooling and oxygen supply was ensured during the whole procedure. The vibratome (LEICA, VT-1200-S, Germany) was utilized to prepare acute horizontal brain slices with a thickness of 400 µm. Throughout the procedure, the slices were consecutively transferred onto a nylon net bathed aCSF and continuously supplied with carbogen (95% O_2, 5% CO_2). Afterwards, the brain sections were left in the incubation chamber to recover for approximately 60 minutes at room temperature.

Table 6. Artificial cerebrospinal fluid (aCSF) pH 7.4	
NaCl	125 mM
$NaHCO_3$	26 mM
KCl	3.0 mM
$MgSO_4 \times 7H_2O$	1.3 mM
$CaCl_2 \times H_2O$	2.5 mM
NaH_2PO_4	1.25 mM
D-glucose	13.0 mM

Figure 12. Picture of the Leica vibratome setup and the instruments in our lab arranged for the next brain slice preparation.

2.4. Controlled Cortical Impact (CCI)

2.4.1. Method Description

In order to study traumatic brain injury in mice, our lab has adapted the controlled cortical impact (CCI)-model. The CCI has been well-established as a model of focal injuries in pre-clinical TBI research since the 1980s (146). It was first introduced by Lighthall and colleagues in 1988 (147) and based on the previous work of Thomas Anderson, who designed a constrained stroke pneumatic impactor to optimize the reproducibility of experimental brain trauma some years earlier (146, 148). The device was first utilized in ferrets and was then transformed to serve different animal models (146, 147). In short, the procedure comprises a surgical exposure of the dura mater and a subsequent perpendicular impact through an accelerated stereotaxic rod (146, 149). The impactor device is either driven by a pneumatic piston or, more recently, an electromagnetic actuator (146, 149, 150). Mechanical parameters such as cortical depth, velocity, and dwell time can be adjusted precisely with the great advantage of controlling the severity of head trauma and low mortality rates (146). CCI-induced

focal injury mimics brain contusion, ballistic, or sports-related injuries and causes dysfunctions similar to human brain injury (146, 149). In addition to cerebrovascular injury caused by laceration of blood vessels and disruption of the blood brain barrier, CCI reproduces hemorrhage (subdural/ subarachnoid/ intraparenchymal), diffuse axonal injury, cortical tissue loss as well as hippocampal cell loss (146, 149, 150). Many of these acute dysfunctions persist chronically (for at least two weeks after lesion induction), which enables an investigation of impairments and secondary injury cascades (146). Due to its scalability and manifold application possibilities, CCI represents a highly accurate and reproducible laboratory method (146). The initial CCI concept of focal injury has recently been expanded to the examination of repetitive closed head injuries (149).

Another well-established brain injury model is the fluid percussion injury (FPI) that is used to study mixed brain injury (focal and diffuse), e.g. resulting from sports and falls (149). This method is widely established in the exploration of head injury without skull fracture, and is either located laterally or at midline (151). Histopathological disturbances that arise from a mixed injury type are characteristic vascular and axonal damage, necrotic and apoptotic cell death, petechial or confluent hemorrhage, and homeostatic imbalance (151). Trauma-induced acute intracranial pressure (ICP) represses the cerebral perfusion pressure (CPP) and, in response, the blood pressure rises (“Cushing reflex”) to ensure cerebral blood flow (151, 152). For FPI, a plastic cap called Luer-Lock is implanted into a small skull window and connected to a liquid-filled tube and pressure detector (149). The strike of a pendulum onto the piston at the end of the tube generates a fluid pressure impulse directly onto the exposed dura (149). However, FPI (especially in midline position) is related to a higher morbidity compared to other TBI models such as CCI (146, 151).

In addition to CCI and FPI, there are numerous laboratory TBI methods that reproduce different types of injury mechanisms. The gravity-driven weight drop model, the shock-tube model, or the penetrating ballistic-like brain injury for example, constitute further well-investigated animal models (149). Although preclinical studies with animal TBI models have been carried out for more than 50 years, the field of research is still evolving due to the complex and variegating trauma mechanics (149). Each available animal model reproduces certain histopathological and functional features of human TBI, but just as in every research animal model, none of the available methods is outright applicable to the clinical condition in humans (146). However, they give us the chance to understand the underlying mechanisms of different forms of TBI on cellular and molecular levels with newer and better techniques (149). Interestingly, in all of these TBI-models, an enduring lowering of the seizure threshold and increased susceptibility, e.g. to PTZ-induced or even spontaneous seizures, has been reported (99).

2.4.2. Controlled Cortical Impact (CCI) in our Lab

The TBI-model of CCI is an important method in our lab and was performed by [redacted] as part of the preliminary work for the ubiquilin-1 project, which is further described in the results section. For this purpose, GAD67-GFP mice generated by Tamamaki et al. (153) and wild-type C57BL6/N mice from the Translational Animal Research Center (TARC) in Mainz were deeply anesthetized using 4 vol% isoflurane (Abbvie, Wiesbaden, Germany). During the procedure, anesthesia was maintained through administration of 1-2% vol% isoflurane in a mixture of 40% O_2 and 60% N_2 via face mask. A heating pad ensured a constant body temperature of the mice of 37 °C and a stereotactic frame allowed the fixation of the head before the fur of the upper head was shaved. Next, the area was disinfected with ethanol and lidocaine-containing salve (EMLA cream, Aspen GmbH, Germany) was applied onto the scalp. Craniotomy comprised a median cut of 1 cm in length and the opening of a cranial window over the right parietal sensorimotor cortex of 4 mm^2 size starting from bregma 0. Bregma is located at the perpendicular intersection of the coronal and sagittal suture of the frontal and parietal cranial bones. The cranial window was drilled without damaging the dura mater underneath and extended towards caudal and lateral from bregma. Prior to CCI-induction, the surface of the dura mater was cleaned with Dulbecco's Phosphate Buffered Saline (DPBS, Lonza, Basel, Switzerland). The lesion was implemented perpendicular to the dura using an impactor device (Impact One™, Leica Mikrosysteme, Wetzlar, Germany) with a 1.5 mm diameter tip, a velocity of 6 m/s, a depth of 0.8 mm and dwell time of 200 ms. Following the impact, the removed cranial bone flap was repositioned and glued with tissue adhesive containing cyanoacrylate (3M Vetbond, 3M Animal Care Products, St. Paul, MN, USA). As a last step, the wound was sewed up using polypropylene sutures (Ethicon, Somerville, NJ, USA). After termination of the isoflurane influx, the animals were left to recover under an infrared lamp. All TBI-experiments were analyzed with respect to sham-operated littermates serving as controls. Sham-operated animals were treated similarly except for the craniotomy and CCI-impact.

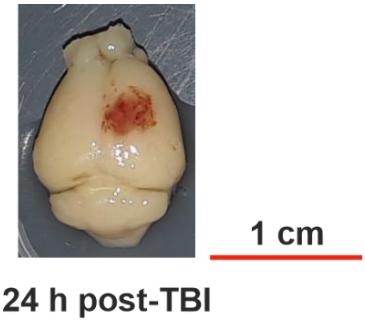

Figure 13. Modified from Kürten et al., 2022 (12).
PFA-fixed GAD67-GFP mouse brain after experimentally induced traumatic brain injury in the sensorimotor cortex of the right brain hemisphere. The visible coagulated blood left in the lesion area was caused by a disruption of the blood brain barrier. The CCI was performed by [redacted] in our lab and the photograph was taken 24 hours after TBI. Scale bar = 1 cm.

2.5. Experimental Epilepsy

2.5.1. Animal Epilepsy Models

Experimental studies of epileptogenesis in humans are accompanied by great obstacles, such as the acquisition of statistically valid amounts of resective hippocampal tissue (from patients with manifest epilepsy) or age-matched control specimens (56). Furthermore, a great heterogeneity of the tissue location and etiology, or the unavailability of control hippocampi at early stages of epileptogenesis complicate reproducible research strategies in humans (56). To overcome these obstacles and gain insight into the molecular mechanisms underlying the phenomenon of induced epileptogenesis, animal models provide valuable opportunities to do so (56). Preclinical epilepsy models also enable an interference with the process of epileptogenesis, forming a basis for future antiepileptogenic treatment options (56). To date, the number of animal models of epileptogenesis is monumental, since each animal model addresses different aspects of pathological features.

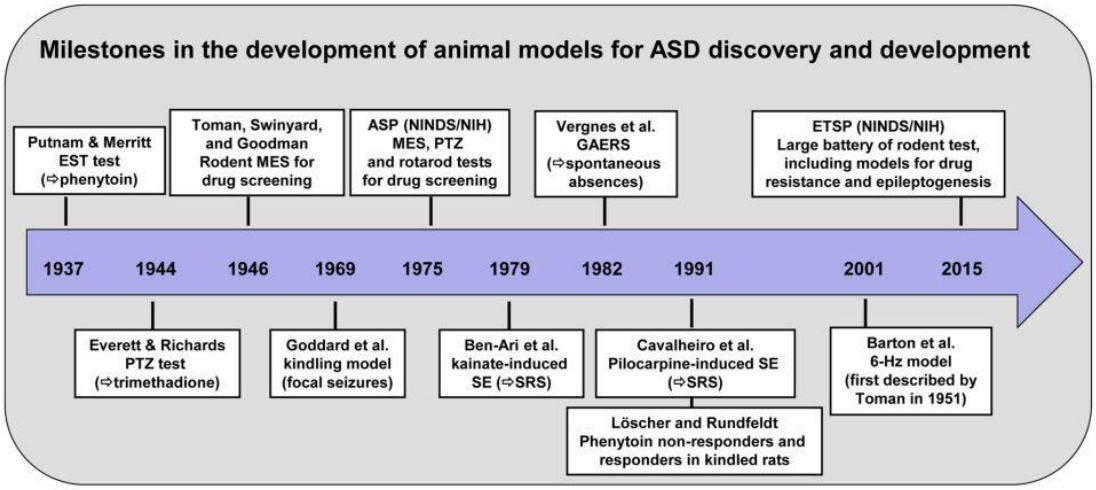

Figure 14. Modified from Löscher, 2017 (13).

The evolution of animal models in epilepsy research for the development of anti-seizure drug (ASD) therapies.

First of all, a well-studied model of epileptogenesis and temporal lobe epilepsy (TLE) is *kindling* (56, 61). Kindling was first coined by Goddard et al. in 1969 and operates with repetitive electrical stimuli at a low intensity in animals (154, 155). Eventually, this prolonged stimulation of limbic brain areas (e.g. basolateral nucleus of the amygdala) generates seizure-like after-discharges in the neuronal networks of the temporal lobe (56). The kindling protocol causes functional reorganizations with an abnormal circuit plasticity and loss of neurons that progresses towards an enduring vulnerability to recurrent seizures, as seen in chronic epilepsy (56, 61). However, the seizures commonly do not occur spontaneously after the classic kindling treatment in contrast to chemoconvulsant rodent models (156). Another disadvantage of the

kindling model might be the less pronounced and more regionally restricted neuropathological alterations as compared to chemoconvulsive or post-SE TLE-models (56, 156).

An *in vivo* application of chemoconvulsives in rodents generates repetitive seizures, up to status epilepticus for several hours (157). The local or systemic use of kainic acid (KA) has been widely established as an epileptic model, as it acts on ionotropic glutamate receptors (iGluR) and depolarizes neurons leading to seizures (56). The kainic acid model of status epilepticus (SE) was first introduced by Ben-Ari et al. in 1978 (158, 159). Especially neuropathological alterations upon KA-administration, such as severe and selective pyramidal neuronal loss in hippocampal subfields CA3-CA4, have been extensively investigated in the past (159, 160). In preclinical studies of temporal lobe epilepsy, KA has often been co-applied with pilocarpine, since the combination reproduces characteristic features of human TLE, e.g. mossy fiber sprouting (76, 157). Pilocarpine is a cholinergic agent that interacts with muscarinic acetylcholine receptors (mAChR) and causes recurrent convulsions in rats lasting for months and in turn structural brain lesions, which might underlie the development of epileptic foci (161). Antiepileptic drugs have been tested in TLE-models with the two substances to identify efficient medication at different disease stages: in the acute phase, in the latent period of epileptogenesis, and in the chronic epileptic phase (157). The GABA-interacting drug pentylenetetrazole (PTZ), the voltage-gated potassium channel (Kv1) blocker 4-aminopyridine, and $GABA_A$ receptor antagonists bicuculline and picrotoxin represent further established pharmacological compounds to induce epilepsy in animals (162-165). Different approaches are the 6 Hz-stimulation model, the post-SE model, TBI models, genetic animal models, or even encephalitis models based on viral transfection (164). Furthermore, animal models of therapy resistance play an emerging role in the current state of research (164).

2.5.2. In Vitro Epilepsy in our Lab

We chose a chemoconvulsive epilepsy model to evoke epileptiform activity *in vitro* that would mimic the disinhibition and impaired GABA-signaling as witnessed in TBI-pathophysiology and our injury model (72, 75, 166, 167). Therefore, we decided to use the non-competitive $GABA_A$ receptor antagonist and allosteric modulator picrotoxin (PTX, **Figure 15**) (168). As its binding site is located within the ion channel of $GABA_A$ receptors, it impedes chloride influx (168, 169). We adopted an established *in vitro* epilepsy model according to Ridler et al. by applying a combination of picrotoxin (50 µM) and kainic acid (500 nM) (170). Kainic acid (KA, **Figure 16**) (171) binds to tetrameric receptors with compositions similar to other ionotropic glutamate receptors (iGluRs) (172). Kainic acid receptors are ligand-gated cation channels that are characterized by fast activation and desensitization kinetics (172). Both picrotoxin (Cat. No. 1128) and kainic acid (Cat. No. 0222) were ordered from Tocris Biosciences, Bristol, UK. In

the present study, the *in vitro* epilepsy model was intended for extracellular multichannel recordings in hippocampal areas and for treating brain slices for Western blot lysates. As hippocampal regions are organized in a functional loop (**Figure17**) and considered to be susceptible to abnormal network oscillations (76, 173), horizontal brain sections were ideal to monitor local field potentials and seizure-like events (SLEs) extracellularly.

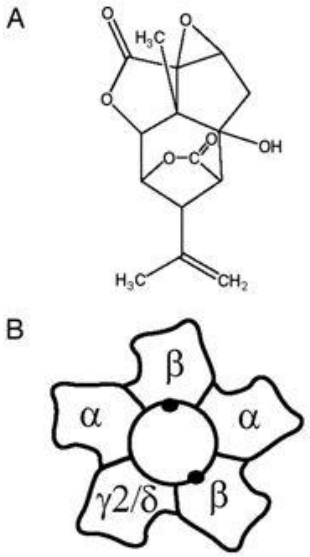

Figure 15.
Modified from Olsen, 2006 (14).
(A) Chemical structure of picrotoxinin **(B)** Binding site within the ion channel of a native GABA receptor heteropentamer (noncompetitive antagonism)

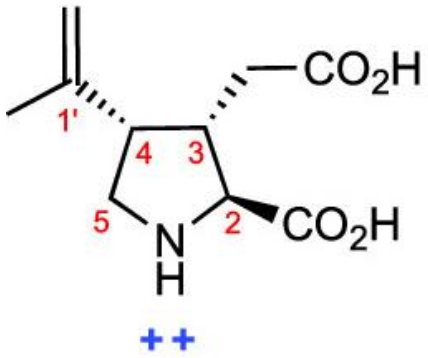

Figure 16.
Modified from Tian et. al, 2019 (15).
Chemical structure of kainic acid (KA)

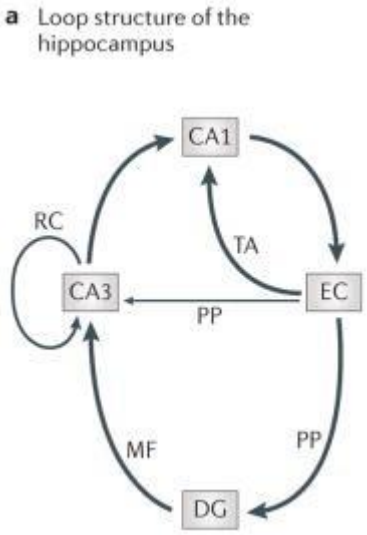

Figure 17. Modified from Goldberg et al., 2013 (16).

Simplified loop structure of the hippocampal network. There are two afferent inputs arriving at the hippocampus, the perforant path (PP) and the temporoammonic (TA) pathway. Firstly, the dentate gyrus (DG) and the neurons in the CA3 subunit receive input from the entorhinal cortex (EC) via the lateral and medial PP. Mossy fibers (MF) deriving from the DG in turn, form a connection with CA3 pyramidal neurons. From the CA3 neurons axons project to ipsilateral CA1 pyramidal neurons in the Schaffer collateral pathway and to contralateral CA1 neurons in the associational commissural pathway (not shown). Additionally, the CA3 pyramidal cells are interconnected through recurrent collaterals (RC). Afferent signals arrive at CA1 also directly from the EC in a short loop via the TA pathway. From there, the CA1 cells send axons carrying the major output information back to the EC or the subiculum (not shown), representing a functional loop.

2.6. Electrophysiology and Multielectrode Array (MEA) Recordings *in Vitro*

2.6.1. Experimental Setup

Extracellular recordings of neuronal activity in spatially defined hippocampal areas were monitored by the use of Multielectrode Array chips (60MEA200/30iR-Ti-gr), manufactured and provided by Multichannel Systems MCS GmbH, Reutlingen, Germany. The MEA chips are equipped with 59 planar titanium nitride (TiN) electrodes, plus one internal reference electrode. They are arranged in a square area with inter-electrode distances of 200 µm in between. Each electrode allows recording as well as stimulation and has a diameter of 30 µm respectively,

while the impedance lies below 100 kΩ. For multiple measurements, one MEA-chip was utilized repeatedly and carefully cleaned with ethanol and ddH_20 before and after each use. Slices from mice aged 17-24 days were used for the recordings. **Figure 18** shows a sketch of the MEA-chip and its layout of the electrode recording grid.

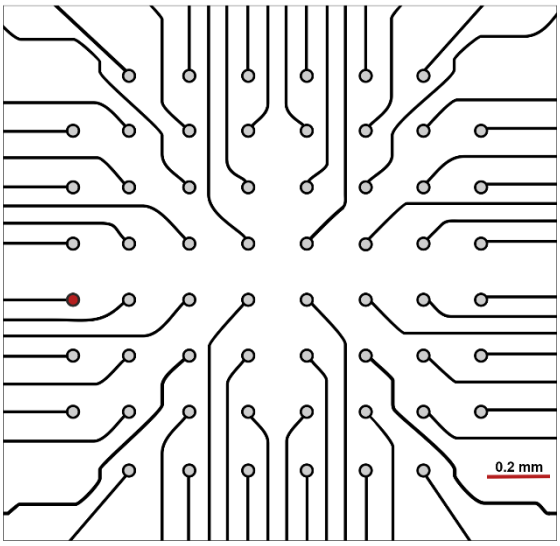

Figure 18. MEA chip layout.
Schematic representation of the layout of a multielectrode array chip (60 MEA 200/30iR-Ti-gr). The 59 electrodes are represented by the gray dots and the internal reference electrode is shown in red. The red scale bar indicates inter-electrode distances of 0.2 mm.

2.6.2. Positioning of the Slice

The chamber for the brain tissue is mounted on top of the MEA chip and was constantly perfused with oxygenated aCSF through an attached tube pump system (Minipuls 3, Gilson, Middleton, WI, USA) with perfusion cannulas. Prior to the recordings, the prepared slices were carefully transferred to the circular MEA-chamber with a glass pipette and supplied with oxygenated aCSF. Subsequently, the slice was positioned using the built-in high-resolution camera and the MEA Monitor program (Multichannel Systems MCS GmbH, Reutlingen, Germany). To secure the exact position of the slice and to improve contact between tissue and electrode, a platinum grid was laid on top. Pictures of the exact electrode arrangements in the hippocampus were captured and saved, allowing an electrode selection in a specific brain region at later time points. Recordings were performed in the CA1 region and Schaffer collaterals. A single channel was picked in order to assess epileptiform activity and local field potentials in the neuronal network surrounding the electrode. Prior to data acquisition, the slices incubated for 30 minutes in the chamber.

2.6.3. Data Acquisition

Electrophysiological multi-unit signals were acquired at constant 32°C, maintained by use of a temperature controller (TC02, Multichannel Systems MCS GmbH, Reutlingen, Germany) and water bath for the aCSF. By occupying both slots of the MEA2100-headstage, two recordings could be performed simultaneously. The acquired raw signals of the 60 or less selected electrodes per chip were transmitted to the MEA2100-headstage that was equipped with an integrated amplifier and analog-to-digital converter (Multichannel Systems MCS GmbH, Reutlingen, Germany). The MEA2100-interface board subsequently processed the data and transferred them to a personal computer. Data acquisition was accomplished using the Multichannel Experimenter Software (Multichannel Systems MCS GmbH, Reutlingen, Germany). The sampling rate was set to 50 kHz. No filters or stimulation were applied during the recordings of spontaneous and pharmacologically-induced epileptiform activity. Epileptiform events were monitored during recording periods of 10 minutes, respectively.

2.6.4. Experimental Conditions and Designs

The central aim of our study was to combine electrophysiological recordings and Western blots to investigate the role of ubiquilin-1 under pharmacological *in vitro* epilepsy conditions according to the protocol described above.

Dose-response relationships:

In presence of KA (500 nM) we applied increasing concentrations (0, 10, 25, 50, 100 µM) of PTX to assess dose-response relationships and to detect the minimal concentration needed for the induction of seizure-like events. The additional PTX doses were administered and washed in for 15 minutes in between the recordings (n = 9 slices from 5 mice aged p17-24).

Nialamide (NM):

In order to assess the antiepileptic effect of the non-selective MAO-inhibitor nialamide (252999, Sigma-Aldrich, St. Louis, MO, USA), we examined epileptiform activity in comparison to the control condition without NM-treatment. For this purpose, the same procedure for dose-response relationships was repeated by applying increasing doses of PTX, this time in presence of KA (500 nM) and NM (10 µM). Since we assumed an antiepileptic effect depending on an upregulation of ubiquilin-1 expression, we pre-incubated the brain slices for at least one hour with regard to our Western blots results after one hour (n = 15 slices from 5 mice aged p17-24).

Washout:

Additionally, we performed a washout-experiment to ensure that our findings were NM-dependent, partially reversible in the mean peak amplitude of the events, and that the vitality of the neural tissue was not impaired. For this experiment, brain slices were pre-incubated in aCSF containing NM (10 µM) for an hour before being placed in the MEA chamber that was perfused with aCSF containing PTX (50 µM) and KA (500nM). The acquired data of 7 slices from one mouse aged 20 days were compared to the results of the control and the NM-group at a PTX concentration of 50 µM. (*n* = 7 slices from 1 mouse aged p20).

2.6.5. Data Analysis

Using the Multichannel Analyzer program (Multichannel Systems MCS GmbH, Reutlingen, Germany), a single channel per slice from the hippocampal CA1 region or Schaffer collaterals was selected for the analysis. For offline analyses, the collected data were converted to ASCII files by use of the Multichannel Data Manager (Multichannel Systems MCS GmbH, Reutlingen, Germany). Seizure-like discharges were detected via threshold-based Clampfit analysis (pCLAMP 11.1, Molecular Devices, Sunnyvale, CA, USA) and analyzed with regard to the mean number of events and mean peak amplitude during 10 min. recording periods. The detection threshold was adjusted individually per slice. The amplitude was slightly variable due to influencing factors, such as age, electrode contact and position, preparation, viability etc. Per slice and dose-response curve, the same detection threshold was maintained. The threshold was kept relatively low at 30-50 % of the max. amplitude of events at a concentration of 100 µM PTX and ranged from a minimum of 0.015 mV to a maximum of 0.2 mV. The baseline was constantly maintained at 0. Note that the time ranges were not converted correctly between the Multichannel Experimenter and Clampfit software and, hence, had to be rectified with the factor 6×10^{-2}. The voltage scale was corrected with factor 10^{-9}. Statistical evaluation and graphics were conducted with GraphPad Prism 8 software (GraphPad Software, San Diego, CA, USA).

2.7. Western Blots

2.7.1. Method Description

Following the invention of Southern blotting for DNA and Northern blotting for RNA around 1977, the analogous term *Western blotting* for protein expression was first coined by Dr. Burnette and Towbin et al. around 1980 (174-176). Based on the principle of specific antibody to antigen-binding, a target protein of interest in a sample could be detected and quantified (174). This immunoassay has constituted a well-established and indispensable method in diagnostic and therapeutic testing as well as in basic research for more than 40 years (177). Initially, the method was intended only for qualitative analyses, but rapid scientific advance

paved the way for (semi-) quantitative Western blot evaluation (178, 179). In sum, Western blotting comprises many steps including total protein extraction and quantification, equal loading of samples, electrophoretic protein separation by molecular weight, electrophoretic transfer to a suitable membrane, immunostaining with primary and secondary antibodies and, finally, imaging and analyzing (174, 178, 180). First, diligent preparation of the samples and antibody selection are vital to achieve reproducible Western blot results. Proteins from the tissue of interest are extracted and solubilized in specific cell lysis buffers containing protease and phosphatase inhibitors (174). Protease and phosphatase inhibitors are required to protect the target protein from alterations and early degeneration during the lysis process (174). It is strongly recommended to maintain a consistent and standardized protocol throughout the whole test series (178). For an accurate quantitative data analysis, data should be collected within a linear range of detection to maintain proportionality between sample loading and band intensity (178). An endogenous reference housekeeping protein, such as actin, β-tubulin or GAPDH, functions as a so-called Internal Loading Control (ILC) (177, 181). The ubiquitous housekeeping gene and its product are contained in the test sample itself, expressed in all cells and most importantly, are biologically stable under all experimental conditions (174, 178, 181). The routine of normalization to the housekeeping protein is used to calculate the relative protein expression and minimizes small errors of unequal sample loading. However, equal concentrations of protein per sample and lane in the Western blot are of great importance for valid results (174). Therefore, the total protein concentration can be quantified beforehand by conducting colorimetric protein assays along with spectrophotometric detection (174). For this purpose, known protein standards are applied in addition to the study samples. Bicinchoninic acid assays (BCA), Lowry protein- or Bradford assays are utilized to generate standard curves (**Figure 19**), which are used to compute the unknown protein extract amounts (174). Subsequently, the samples can be adjusted to equivalent concentrations by altering the ratio of lysis buffer to protein extract, respectively. To complete the lysates, a Western blot sample buffer, sodium- or lithium dodecyl sulfate (SDS/ LDS), which serve as anionic detergents and provide a net negative charge on the proteins, is added (177). Additionally, the reducing agents dithiothreitol (DTT) or mercaptoethanol (β-ME) are able to break disulfide bonds (177).

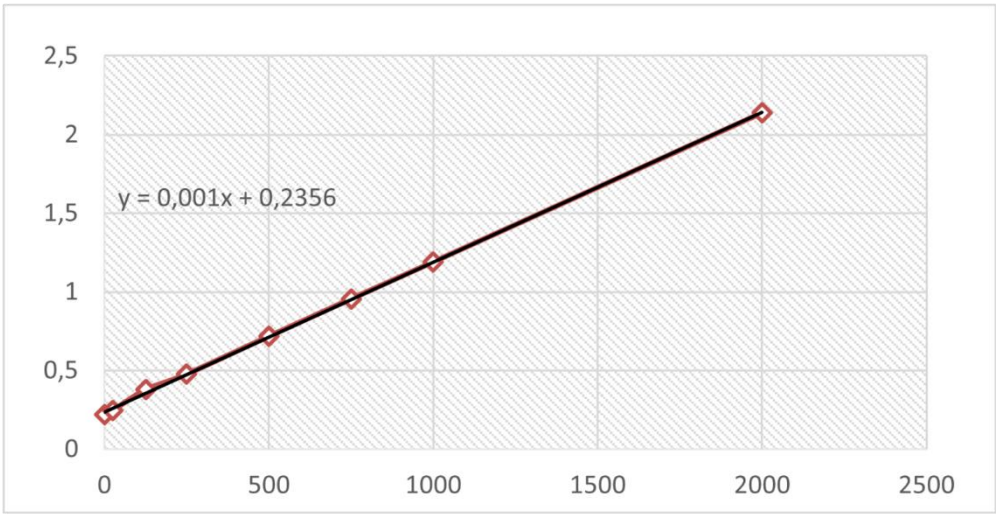

200901	Maus 200831_1							
Konz. [mg/m	0	25	125	250	500	750	1000	2000
Probe	0,2233	0,2434	0,3676	0,4988	0,7253	0,9702	1,1963	2,0946
Replikat	0,214	0,2488	0,3863	0,4553	0,7087	0,9399	1,1835	2,1809
Mittelwert	0,21865	0,2461	0,37695	0,47705	0,717	0,95505	1,1899	2,13775

Figure 19. Screenshot of one of the standard curves in Excel.
Exemplary standard curve for the Bicinchoninic acid assay (BCA). BCA tests were performed in order to determine the total protein concentrations in the lysates for the Western blots. Subsequently, equal protein amounts in the Western blot samples could be achieved.

The method of sodium dodecyl sulfate polyacrylamide gel electrophoresis, well-known under its acronym SDS-PAGE, enables a separation of proteins by molecular weight (174). The step of coating with SDS or LDS ensures an equal charge-to-mass-ratio, meaning that the migration rate is inversely proportional to the molecular weight (177). Smaller and lighter proteins migrate faster and further towards the positively charged anode, as they pass the narrow pores of the polyacrylamide gel matrix more easily than larger proteins. Furthermore, two distinct types of gels are deployed, the stacking and the resolving gel. The stacking gel is characterized by larger pore sizes and acidity so that the applied proteins form a line on the same level before entering the resolving gel simultaneously (174). The resolving gel, on the other hand, separates the proteins through more narrow pores and basicity (174). Into one of the lanes a weight marker is loaded, also referred to as ladder (174). Along with the test samples, it migrates towards the anode and generates standard bands of molecular weight (174).

After electrophoretic separation, the proteins in the gel are transferred onto a polyvinylidene difluoride (PVDF) or nitrocellulose membrane to become accessible for the subsequent

immunostaining. The PVDF membrane is usually dipped in methanol before use (180). In a wet transfer system, the transfer stack (**Figure 22**) consisting of sponges, filter papers, gel, and membrane, is arranged in a container filled with transfer buffer (174). The applied voltage induces protein migration in an orthogonal direction towards the anode again and onto the membrane (174).

The surface of the membrane has a strong affinity for proteins (177). Therefore, it is necessary to temporarily coat it with a blocking solution before the following immunodetection (177). Blocking reagents such as non-fat dry milk concentrated up to 5% protect the unoccupied sites of the membrane and, most importantly, prevent nonspecific antibody binding (177). Casein contained in skim milk is an inert protein that has a low affinity to the target protein and the antibody (174). After blocking, the immunodetection protocol is performed including repetitive steps of washing and incubation with the primary and secondary antibodies. The diligent washing procedures are required to dispose of excess antibody and background noise and to impede nonspecific antibody binding (177). For this purpose, Tris-buffered saline mixed with Tween 20 (TBS-T) is typically deployed (174). The variable F_{ab} (antigen-binding) fragment of the primary immunoglobulin has a specific affinity for the target of interest (177). As the appropriate dilution of the primary antibody depends on the source of the antibody and the experimental procedure, it should be tested and verified beforehand according to the manufacturer's instructions (**Figure 27**) (177). The secondary antibody, on the contrary, binds the F_c (constant) fragment of the primary antibody and carries a conjugated substrate, which enables the subsequent signal detection (174).

Finally, the detection methods of enhanced chemiluminescence (ECL), autoradiography, colorimetry or fluorescence are performed to visualize the protein bands. Colorimetric detection generates a colored precipitate upon substrate application, whereas no substrate is needed for fluorescence detection, as the secondary antibody is directly conjugated with a fluorophore (177). The most common way of signal detection is the indirect enzyme-catalyzed chemiluminescence, which works with chemical reactions that emit light as a secondary product upon substrate administration (177). The secondary antibodies are often linked to the reporter enzymes alkaline phosphatase (AP) or horseradish peroxidase (HRP) (177). The signal capture on X-ray films has been replaced by the faster charge coupled device (CCD) cameras for digital imaging (177).

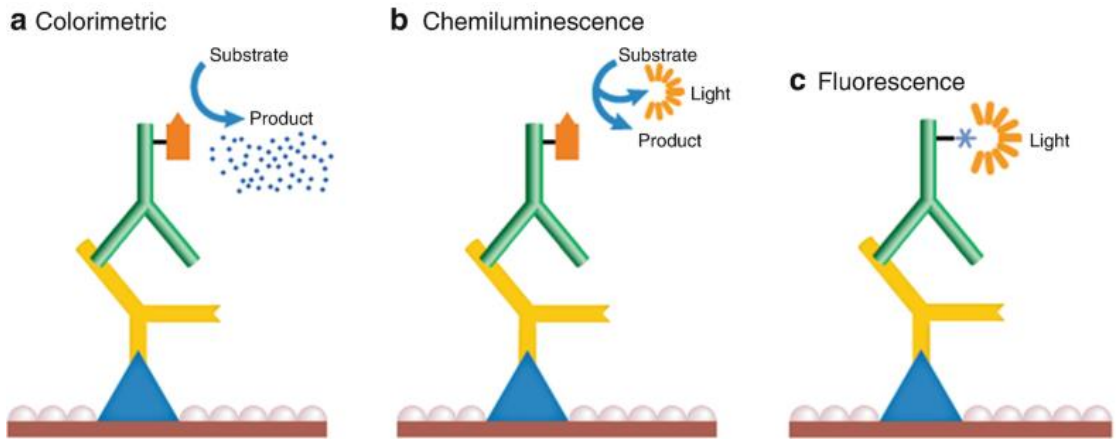

Figure 20. From Oh, K., 2021 (17).

Signal visualization methods to detect secondary antibody binding:

(a) Colorimetric detection, **(b)** Chemiluminescence, **(c)** Fluorescence

2.7.2. Preparation of Western Blot Lysates

After having established the model of epileptiform activity as mentioned above, we were interested in its impact upon cortical and hippocampal ubiquilin-1 expression. For this purpose, 400 µm thick horizontal brain slices were prepared as usual and left to incubate in aCSF containing 50 µM of picrotoxin and 500 nM of kainic acid for one to seven hours. Optionally, 10 µM of NM were added after one hour of incubation in the *in vitro* epilepsy model or in control standard aCSF. For each experimental condition lysates from eight mice were prepared, respectively. At defined time points of incubation, several slices were removed, and hippocampal and cortical regions were separated by use of sterile scalpel blades under a magnifying lamp. The separated tissue was immediately cooled down with liquid nitrogen and stored in Eppendorf cups at -80 °C. In the next step, the collected tissue was further processed and homogenized. Lysis buffer (**Table 7**) was added containing N-PER™ Neuronal Protein Extraction Reagent (87792, Thermo Fisher Scientific, Waltham, MA, USA) plus Halt™ Protease and Phosphatase Inhibitor Cocktail and 0.5 M EDTA solution (78440, Thermo Fisher Scientific, Waltham, MA, USA) in a 100:1:1 ratio (10 ml N-Per+ 100 µl Protease+ 100 µl EDTA solution). The probes were placed in a rotator wheel in the cooling room (4°C) for half an hour. Every 10 minutes the homogenizing process was accelerated mechanically by blending with a pipette. Subsequently, the epilepsy- and the TBI-samples were centrifuged for 15 minutes at 13 000 rpm at 4 °C. Afterwards, the supernatants were transferred to new Eppendorf cups, whereas the remaining pellet was discarded. The total protein concentration of each sample was disclosed via bicinchoninic acid assay (**Figure 21**) using the Pierce™ BCA Protein Assay Kit (23225, Thermo Fisher Scientific, Waltham, USA) and photometric measurement (Infinite M1000 multi-mode plate reader, Tecan, Crailsheim, Germany). The aliquots were finished by

adding DTT (43815, Sigma-Aldrich, St. Louis, MO, USA) and Nu®PAGE LDS (4x) (NP0007, Invitrogen™/ Thermo Fisher Scientific, Waltham, MA, USA) and adjusting the concentration of lysate and lysis buffer. Prior to storage at -20 °C, they were placed in a heating block at 70 °C for 10 minutes.

Table 7. Lysis buffer (100:1:1 ratio)	
N-PER™ Neuronal Protein Extraction Reagent	10 ml
0.5 M EDTA solution	100 µl
Halt™ Protease and Phosphatase Inhibitor Cocktail	100 µl

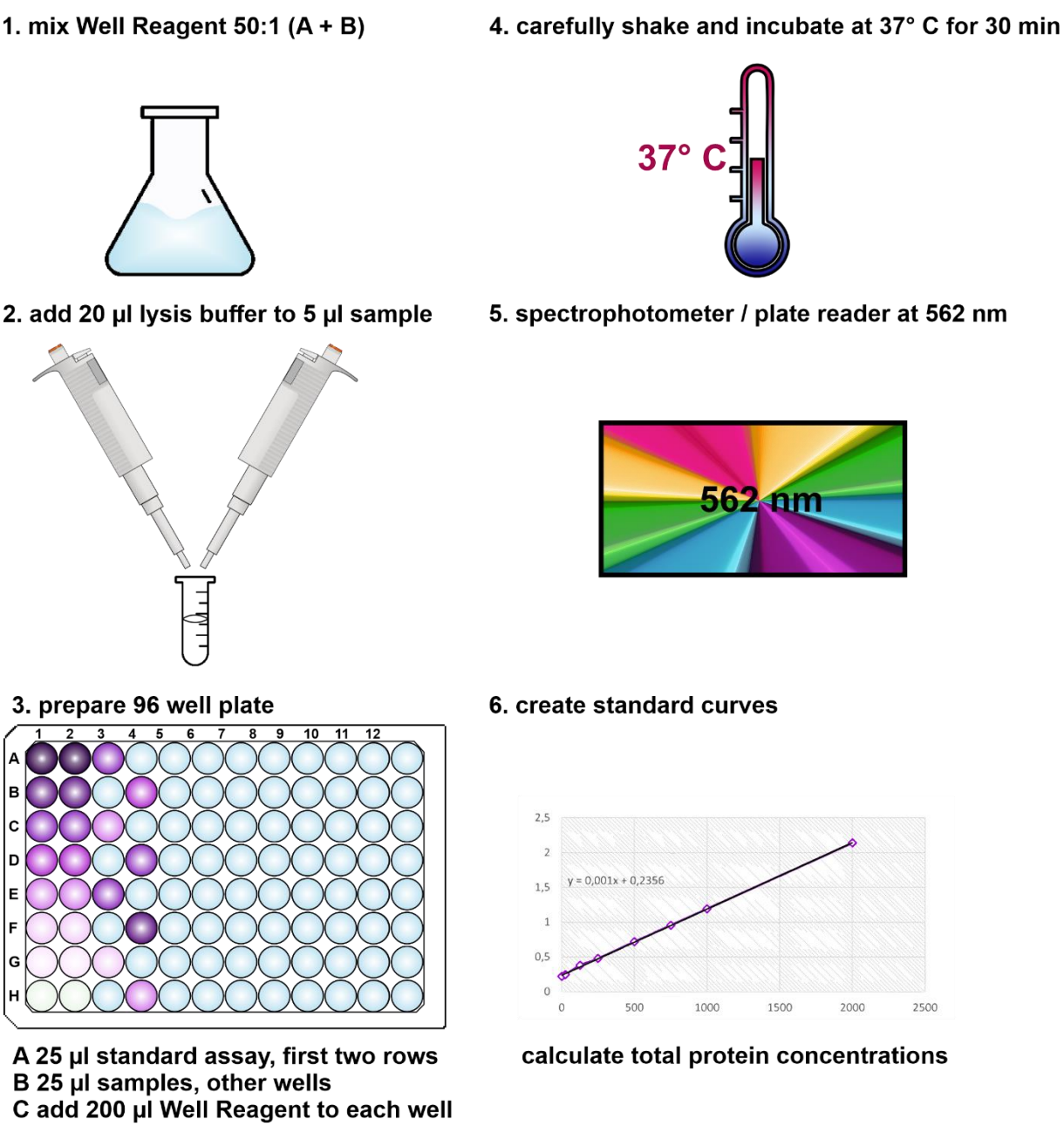

Figure 21. Schematic representation of the steps of the bicinchoninic acid assay (BCA) for the purpose of generating equal protein concentrations in the Western blot samples.

2.7.3. Electrophoretic Protein Separation and Transfer

The Western blot gels, resolving, and stacking gel, had to be prepared separately and then layered. First, the resolving gel was made according to **Table 8** below, then filled between two glass plates and left to dry for at least 30 minutes with isopropanol stacked on top. Meanwhile, the stacking gel was prepared. The isopropanol was discarded and the gel washed with ddH_2O before the stacking gel (**Table 8**) was loaded on top. During the drying process, a Bio-rad comb forming ten wells was placed between the glass plates.

Table 8. Western blot gels			
Resolving gel		**Stacking gel**	
H_20	4.1 ml	H_20	6.1 ml
30 % Acrylamide	3.3 ml	30% Acrylamide	1.3 ml
Resolving gel buffer (1.5M Tris-HCl pH 8.8)	2.5 ml	Stacking gel buffer (1M Tris-HCl pH 6.8)	2.5 ml
10% SDS	0.1 ml	10% SDS	0.1 ml
10% APS	50 µl	10% APS	50 µl
TEMED	5 µl	TEMED	5 µl

Prior to electrophoresis, the Western blot samples of interest were warmed up in a heating block at 70 °C for approximately 10 minutes. Equal amounts of protein (20 µg) were loaded per lane and separated by molecular weight in the 10% self-prepared separating gel. The blotting apparatus was filled with running buffer consisting of 10% SDS-PAGE diluted 1:10 in ddH_2O (**Table 9**). Bio-rad dual color marker was filled into one of the ten wells, while empty wells were loaded with LDS sample buffer. Gel electrophoresis ran at a voltage of 175 V and 3000 mA for 50 minutes.

The electrophoretic transfer of the migrated proteins onto a suitable membrane is required for the subsequent antibody staining. For this purpose, the polyvinylidene difluoride (PVDF) membrane (Carl Roth, Karlsruhe, Germany) was activated with methanol (Carl Roth, Karlsruhe, Germany).

After completion of the electrophoretic separation, the gel was taken out of the blotting chamber, the PVDF membrane was carefully laid on top and both were placed in a cassette between foam sponges and filter papers, forming a “sandwich” (**Figure 22**). The blotting chamber was arranged with transfer buffer (**Table 9**) and a cooling ice block. Electroblotting was conducted for 90 minutes at 120 V and 3000 mA.

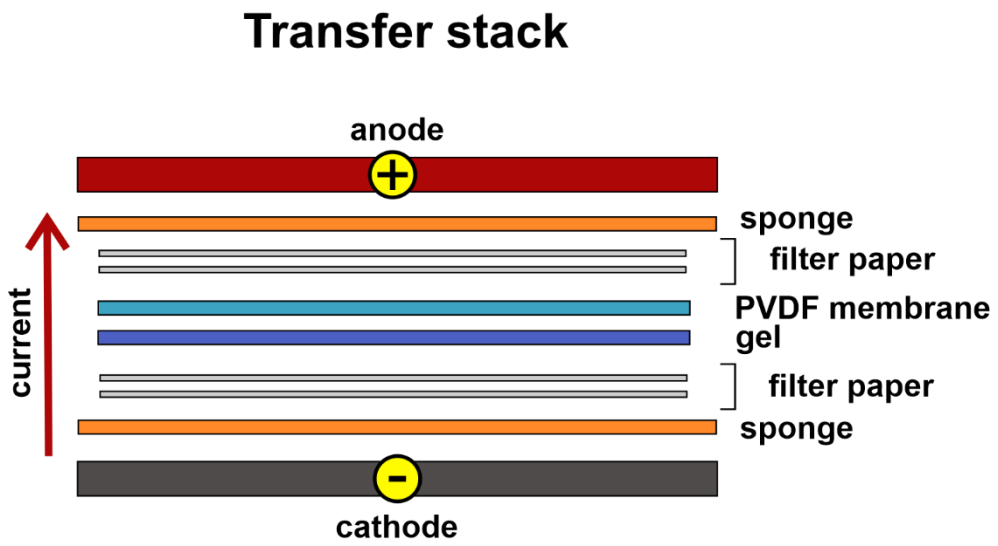

Figure 22. Illustration of the transfer stack with different layers between cathode and anode, resembling a 'sandwich'. The current flows from the positively charged cathode to the negatively charged anode. This process transfers the negatively charged proteins on the gel onto the membrane.

2.7.4. Immunostaining

Afterwards, the Western blot membrane was removed from the cassette, washed with ddH_2O and blocked in 4% non-fat dry milk (diluted in Tris-buffered saline+Tween-20 (TBS-T)) at room temperature. After 45 minutes, the milk was removed and the probing buffer containing the primary anti-ubiquilin polyclonal antibody (1:1000, PA1-759, Thermo Fisher Scientific, Waltham, MA, USA) was applied to incubate overnight at 4 °C. On the following day, the membrane was washed for 30 minutes with changes of TBS-T (**Table 9**) every 10 minutes prior to secondary antibody-administration. The secondary HRP-conjugated antibody (HRP anti-rabbit antibody, 1:10000, Jackson ImmunoResearch, West Grove, PA, USA) incubated for another 30 minutes. Then, the membrane was washed again three times with TBS-T and immersed in TBS (**Table 9**). Finally, enhanced chemiluminescent detection (ECL) was performed to display signal intensities using the Immobilon Western HRP Substrate (WBKLS0500, Millipore, Burlington, MA, USA). For the final step of image capture, the membrane was transferred to our CCD imaging system, the ChemiDoc XRS+ (Bio-Rad Laboratories, Hercules, CA, USA) and placed between two laminated films. ImageLab 2.0 software (Bio-Rad Laboratories, Hercules, CA, USA) was utilized with the following settings: no filter, program: Western blot/ ECL Marker Light, manually set exposure time (ca. 15 s for ubiquilin-1, 5 s for GAPDH, 0.1 s for marker detection). For normalization, the housekeeping protein glyceraldehyde 3-phosphatase dehydrogenase (GAPDH, 36 kD) was quantified. The primary goat-anti-GAPDH antibody (1:1000, A303-878A, Bethyl Laboratories, Montgomery, TX, USA) incubated at room temperature for 60 minutes. The secondary horseradish

peroxidase (HRP)-conjugated anti-goat antibody (1:10000) was obtained from Dianova, Hamburg, Germany. Washing procedures, secondary antibody administration and ECL detection were repeated according to the protocol described above.

<table>
<tr><th colspan="5">Table 9. Buffers for 1 L</th></tr>
<tr><th>Running buffer (1:10)</th><th>Transfer buffer</th><th colspan="3">Washing buffer (TBS-T)</th></tr>
<tr><td>10 x SDS-PAGE
100 ml</td><td>Tris
14 mM
2.91 g</td><td colspan="3">10 x TBS pH 7.2
100 ml</td></tr>
<tr><td rowspan="3">ddH_20
900 ml</td><td>Glycine
192 mM
14.41 g</td><td>Tris
500 mM
60.57 g</td><td>NaCl
1.5 M
87.66 g</td><td>ddH_20
→ 1 l</td></tr>
<tr><td>99% Ethanol
200 ml</td><td colspan="3">ddH_20
900 ml</td></tr>
<tr><td>ddH_20
→ 1 l</td><td colspan="3">Tween-20
1 ml</td></tr>
</table>

2.7.5. Densitometric Quantification with Image Studio Lite

Densitometric quantification of ubiquilin-1 expression was performed using Image Studio Lite 5.2 Software (LI-COR Biosciences, Lincoln, NE, USA). The program allows optimization of image properties such as contrast without changing the signal intensities, enabling a precise differentiation of the protein band borders. In the analysis section of the program, the function “draw rectangle” was used to frame the single protein bands on the membrane from left to right depending on the size of the signals (**Figure 28**). The same frame size was maintained for all signals per image, while the border width was set to 3; top/bottom (background → median). Raw signal intensities were automatically exported to an excel document. Calculations and normalization to control group and housekeeping protein were performed in additional self-created excel sheets. Raw data values of the control conditions were normalized to one, all other detected signals were set in relation. The resulting data values in turn, were set in relation to the results of GAPDH quantification. Statistical evaluation was accomplished with GraphPad Prism Software.

2.8. Immunohistochemistry

Cortical ubiquilin-1 distribution was investigated in coronal slices from three mice aged 26 days under three different experimental conditions: control, *in vitro* epilepsy (1 h incubation in aCSF containing PTX and KA) and rescue (NM-treatment of the *in vitro* epilepsy group for another 1h). After preparation and incubation, the 400 µm thick slices were quickly fixated by use of 4% formaldehyde solution (ROTI®Histofix 4%, P087.1, Carl Roth GmbH, Karlsruhe, Germany). 30% sucrose in 0.1 M phosphate buffer saline solution (pH=7.4) ensured cryoprotection overnight at 4 °C. On the following day, 20 µm thin subslices were prepared using the Leica microtome (CM1325, Leica Mikrosysteme, Wetzlar, Germany). Throughout the

procedure, the generated subslices were consecutively transferred to a well plate filled with PBS. The coronal subslices were washed three times with PBS before they were immersed in Block A buffer consisting of 10% goat serum, 20% Avidin (both Avidin/Biotin Blocking Kit, SP-1002, Vector Laboratories, Burlingame, CA, USA) and PBS/0.2 %Triton-X 100 (PBS: Gibco, Grand Island, NY, USA; Triton-X 100: Thermo Fisher Scientific, Waltham, MA, USA) for 90 minutes at room temperature. Primary antibodies were diluted in Block B buffer including 1% goat serum, 20% biotin (Avidin/Biotin Blocking Kit, SP-1002, Vector Laboratories, Burlingame, CA, USA) and PBS/0.2% Triton-X 100 to incubate overnight at 4 °C. The ubiquilin-1 distribution (primary antibody: Anti-Ubiquilin Polyclonal Antibody, PA1-759, Thermo Fisher Scientific, Waltham, MA, USA) was examined in relation to NeuN expression (primary antibody: mouse Anti-NeuN Antibody, clone A60, MAB377, Sigma-Aldrich, St. Louis, MO, USA). NeuN antibodies detect a specific DNA-binding protein in all types of neurons and are used to stain neuronal nuclei.

On the following day, the secondary antibodies (Alexa Fluor 647 donkey anti-mouse IgG, A-31571, Thermo Fisher Scientific, Waltham, MA, USA and Goat anti-rabbit IgG (H+L) Secondary Antibody, Dylight 405, 35551, Thermo Fisher Scientific, Waltham, MA, USA) which were diluted in 1% goat serum and PBS/0.1% Triton-X 100, were applied for two hours at room temperature. Finally, the slices were mounted on Menzel glass slides using ImmunoSelect Antifading Mounting Medium (Dianova, Hamburg, Germany). For imaging, an IX81 Olympus inverted microscope (Olympus, Shinjuku, Japan) was deployed. First, an overview of each slice was made (4x magnification). For the subject of analysis, layer 2/3 of the somatosensory cortex, images with 20x magnification were taken. The images were exported and analyzed with ImageJ software (Rasband, W.S., ImageJ, U.S. National Institutes of Health, Bethesda, MD, USA). Statistical analysis of the three groups was operated with GraphPad Prism Software.

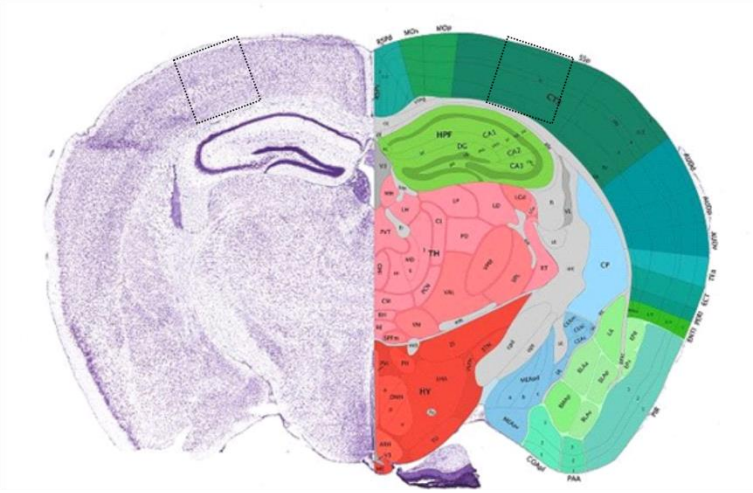

Figure 23. Modified from Allen Brain Atlas (18).

Adult mouse p56, coronal, midbrain, image 73/132. The atlas image shows a coronal section of an adult mouse brain, left half Nissl-stained. The added black dotted square indicates our area of interest for IHC in the somatosensory cortex.

2.9. Statistical Evaluation

Graph Pad Prism 8 software (GraphPad Software, San Diego, CA, USA) was deployed for statistical analyses. All results of the present work are represented as mean ± SEM. Kruskal-Wallis and pairwise Mann-Whitney tests were performed for non-parametric distributions. To statistically compare the dose-response relationships and curve progression, Two-Way ANOVA analysis was performed. Significantly different values are indicated as asterisks in the figures (*:P<0.05; **:P<0.01; ***:P<0.001).

3. Results

3.1. Results from Experimental Setup and Data Analysis

3.1.1. Multielectrode Array Experiments

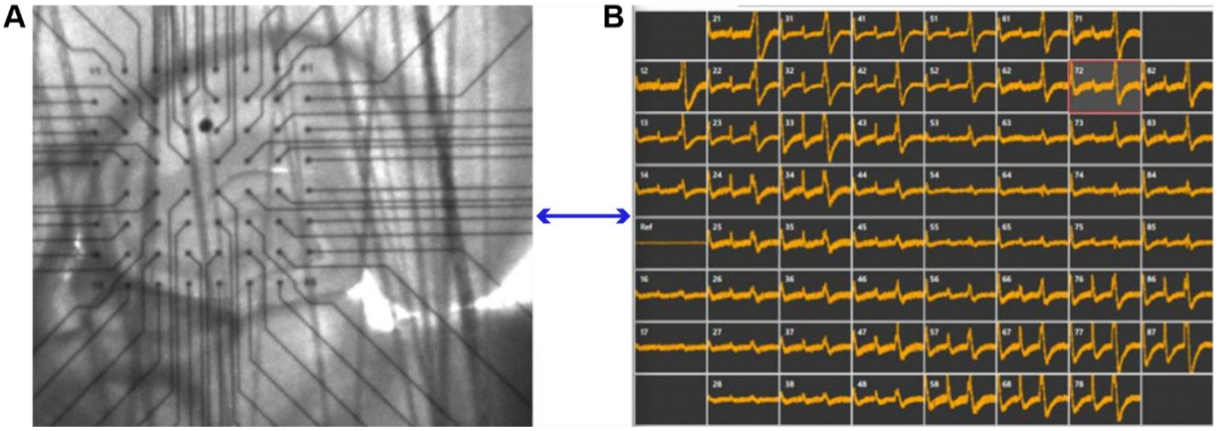

Figure 24. MEA setup.
Left: position of a horizontal brain slice in the MEA recording chamber taken by the built-in high-resolution camera.
Right: screenshot of the Multichannel Experimenter software during *in vitro* epilepsy recordings. Note the anatomical correlation of the SLE-amplitudes with the position of the electrodes in the histological regions of the hippocampus CA1 to CA4.

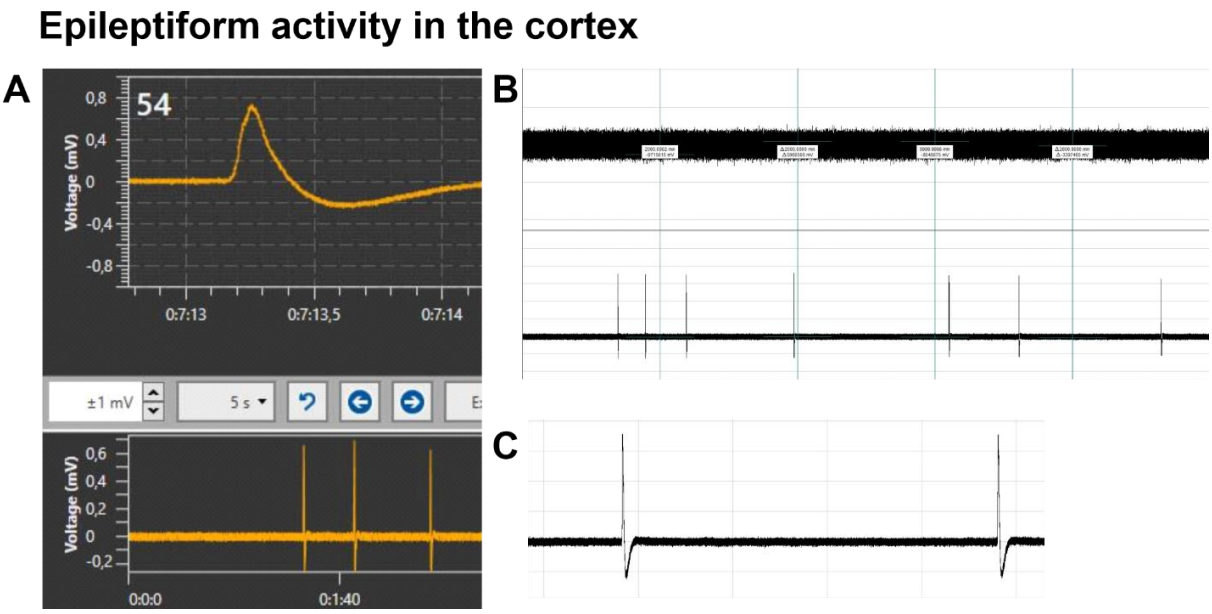

Figure 25. Screenshots from Multi Channel Experimenter and Clampfit 11.1 software. Since we measured ubiquilin-1 expression under *in vitro* epilepsy

conditions with Western blots in the cortex too, we had to verify the appearance of epileptiform activity in the cortex.

(A) Representative single cortical SLE recorded in layer 2/3 using 50 µM PTX and 500 nM KA. Note the high event amplitude of >0.6 mV.

(B) Whole 10 min voltage trace in Clampfit (upper trace: internal reference, lower trace: single channel in cortical layer 2/3). The number of events is substantially smaller than in the hippocampus, whereas the detected event amplitudes were higher.

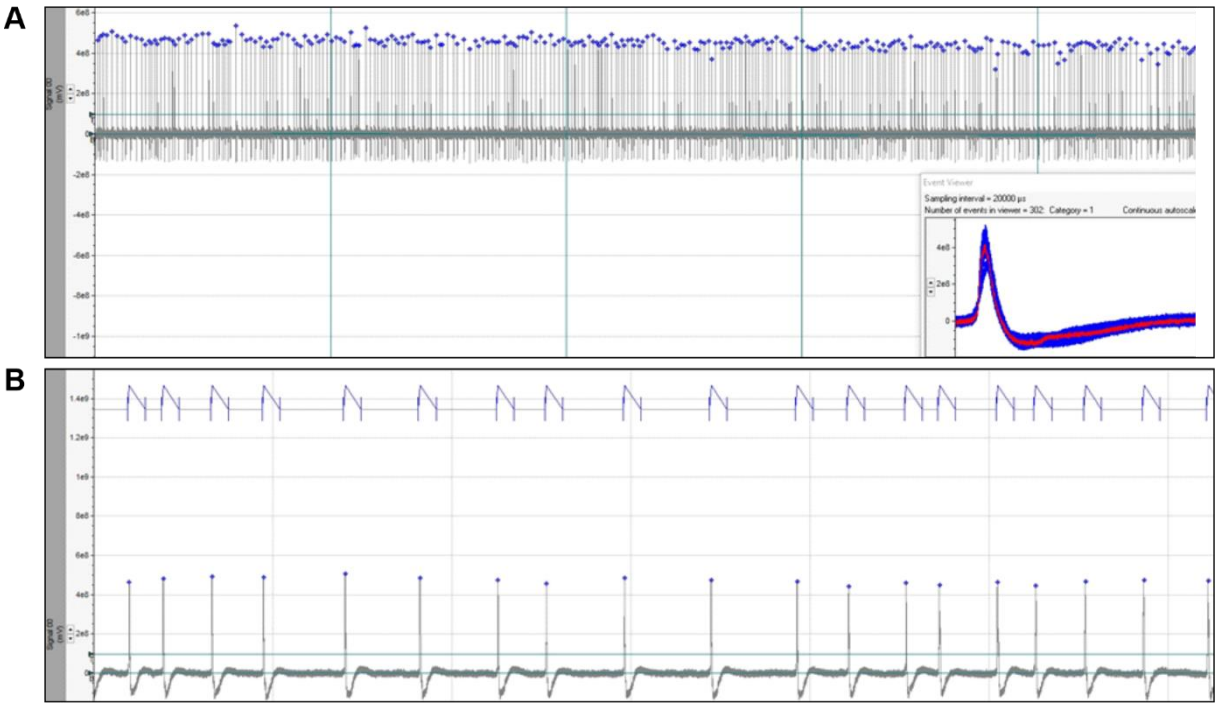

Figure 26. Screenshots from Clampfit 11.1 software.

Threshold-based event detection using Clampfit 11.1 software. The blue dots above the signals indicate detected events, respectively.

(A) Representative voltage trace of 10 min single-channel recording in the hippocampus. The window in the lower right corner displays an overlay of 302 detected SLEs.

(B) Excerpt from the upper trace at a higher resolution for better display of the single SLEs.

3.1.2. Western Blot Experiments

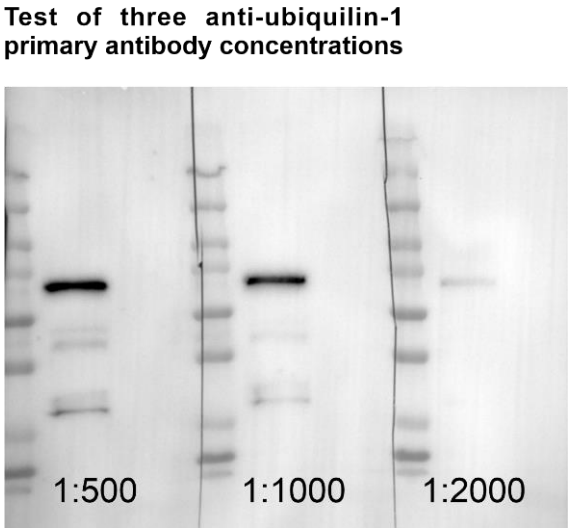

Figure 27. First Western blot membrane cut into three parts to test various anti-ubiquilin-1 antibody (PA1-759, Thermo Fisher Scientific, Waltham, MA, USA) concentrations. Optimal signal detection could be accomplished with a dilution of 1:1000, which was also recommended by the manufacturer.

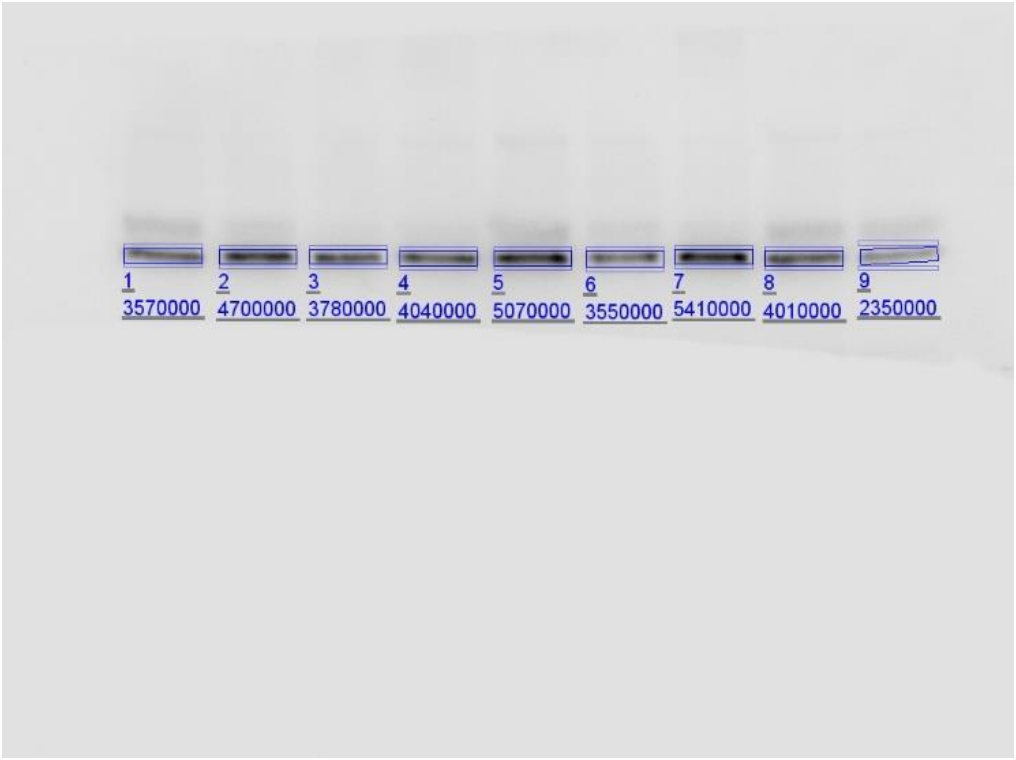

Figure 28. Densitometric Western blot analysis with Image Studio Lite 5.2 software. Representative Western blot membrane with weight bands for ubiquilin-1 and blue detection rectangles framing each signal.

3.2. Preliminary Work for this Project

These experiments were part of our publication and the starting point for this project. Detailed descriptions of results and methods of the following two experiments performed by [redacted] and [redacted] can be found in our publication (130).

3.2.1. Fluorescence Activated Cell Sorting (FACS) and Label-free Quantification

Previously, a posttraumatic hyperexcitability and transhemispheric diaschisis was demonstrated in our lab by Le Prieult et al. early after controlled cortical impact in mice (75). Furthermore, impaired GABAergic control and a shift in the $GABA_A$ receptor subunit composition with a loss of phasic and an increase of tonic inhibition have been observed (75). These early alterations led us to a proteomics approach in order to identify target proteins involved in the development of cortical hyperexcitability in GABAergic interneurons. For this purpose, a label-free quantification analysis was performed by [redacted] on isolated GABAergic interneurons in GAD67-GFP mice, as described in Kürten et al. (130) and Ihbe et al. (182). 24 hours post-TBI, the contralateral cortices of six CCI-treated and six sham-treated GAD67-GFP mice (n_{total} = 12) were collected for a single cell suspension. Subsequently, GFP-positive interneurons and cells were isolated from the suspension via fluorescence activated cell sorting (FACS), detailed in Ihbe et al. (182). In GFP-positive interneurons a total number of 15 proteins were identified that showed an altered expression in the contralateral cortex 24 hours post-TBI compared to sham animals (**Figure 29**). Those encompassed mainly structural proteins such as Neurofilament light chain (NFL) or other proteins associated with tight junctions. Furthermore, we also identified ubiquilin-1, which was strongly regulated and particularly interesting with regard to its interactions with $GABA_A$ receptors and its pathophysiological role.

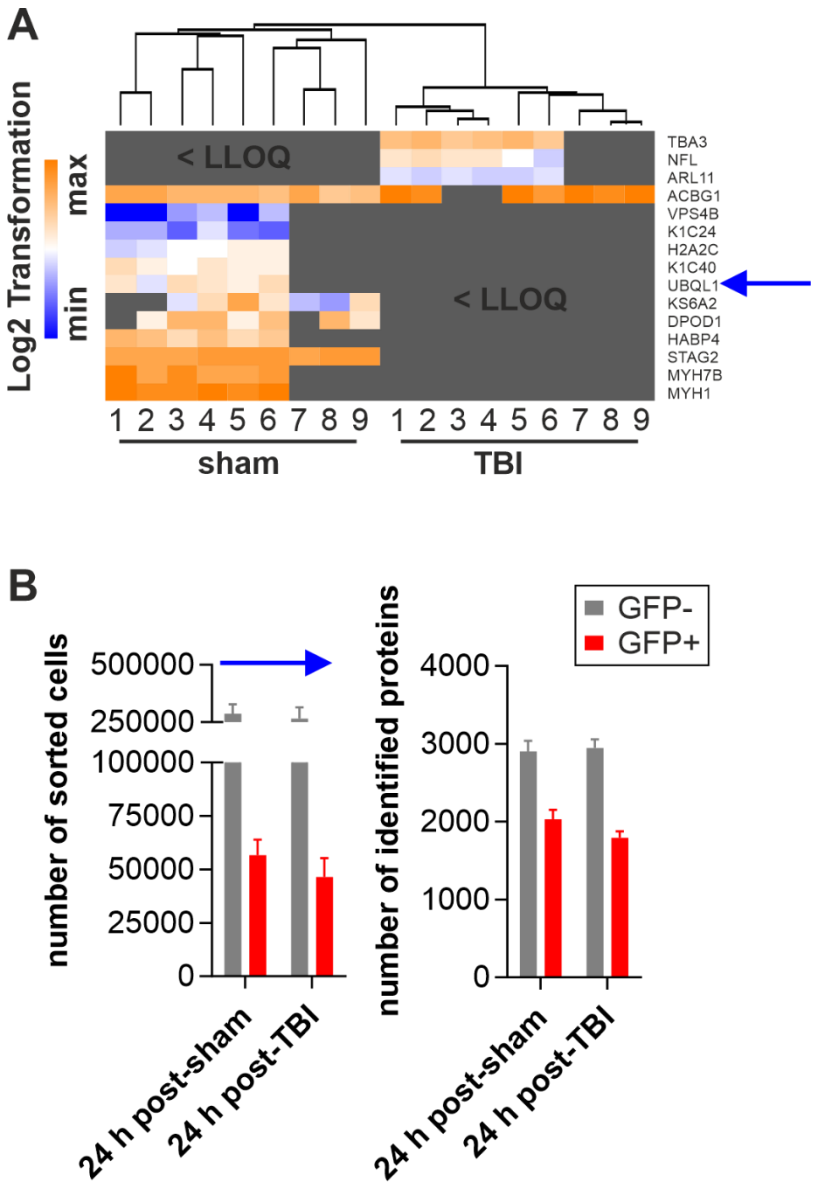

Figure 29. Modified from Kürten et al., 2022 (12).

Log2 transformed heat map (orange = high abundance, blue = low abundance, gray = below lower level of quantification, LLOQ) of relative protein abundance by use of liquid chromatography-mass spectrometry (LCMS), performed by [redacted] The heat map shows the label-free quantification of FACS-isolated GFP-positive interneurons of the contralateral cortex obtained from GAD67-GFP mice 24 hours after controlled cortical impact. The expression of ubiquilin-1 (see arrowhead) is strongly reduced in GFP-positive interneurons of TBI-treated mice compared to sham conditions.

3.2.2. Western Blots from Cortex and Hippocampus 24 hours post-TBI

In order to validate the observed downregulation of ubiquilin-1 in GABAergic interneurons, we generated Western blot lysates from whole cortices and hippocampi 24 hours post-lesion. To do so, we compared eight TBI-treated and eight sham-treated animals (n_{total} = 16) and performed a quantitative analysis of hippocampal and cortical ubiquilin-1 expression using Kruskal-Wallis tests. We could confirm a decreased expression of ubiquilin-1 in the contralateral cortex (**Figure 30, A.i.;** *n* = 8; p vs sham: *0.0401) in relation to cortical lysates from sham animals. However, this reduction was not evident in the ipsilateral cortical hemisphere (*n* = 8; p vs sham: ns; p vs contralateral: *0.0174). Strikingly, regarding the hippocampal expression of ubiquilin-1 from the same animals, the cortical lesion caused a loss of ubiquilin-1 expression in the contralateral (*n* = 8; p vs sham: *0.0233) as well as the ipsilateral (**Figure 30, B.i**.; *n* = 8; p vs sham: *0.0401) hippocampus compared to sham-treated animals. These findings clearly indicate that the decreased ubiquilin-1 expression revealed by label-free quantification of isolated GABAergic interneurons was not masked in the whole and unsorted cortex. These Western blot data 24 hours after TBI on whole brains were acquired by [redacted] in our lab.

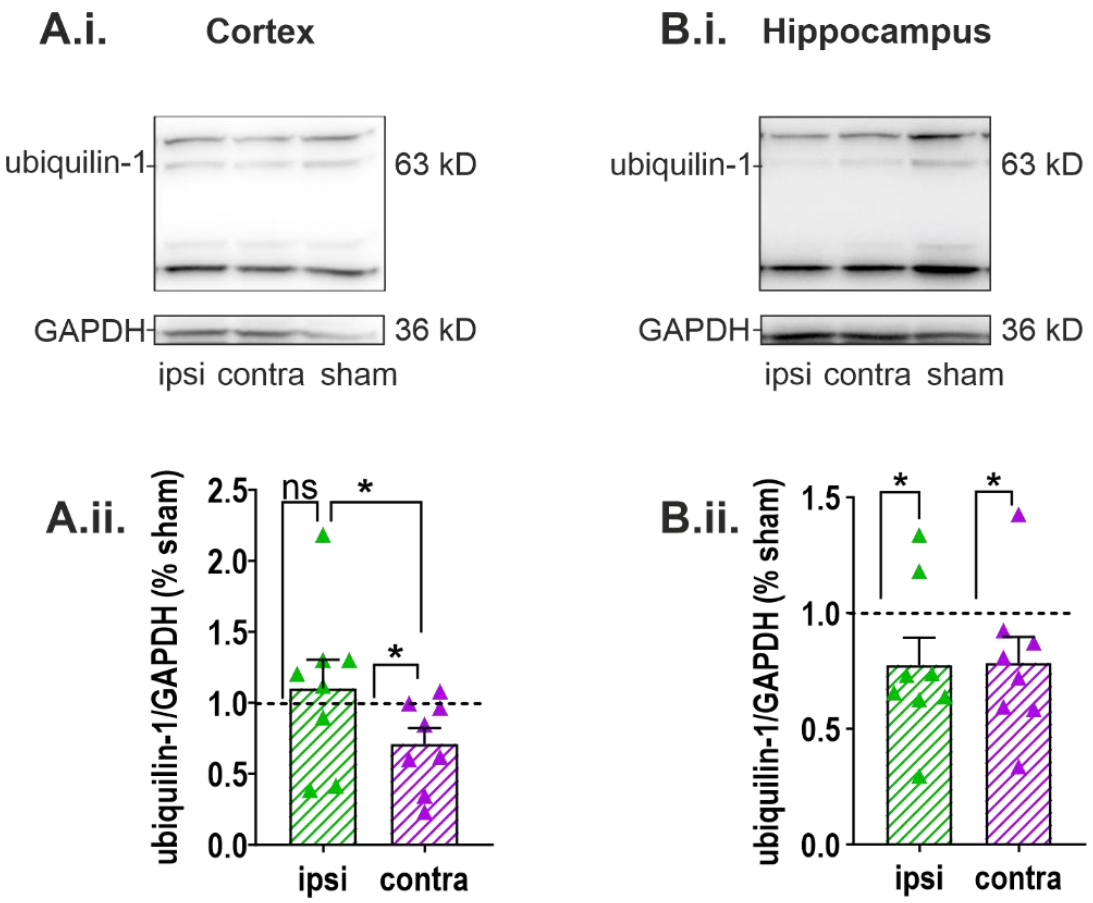

Figure 30. Modified from Kürten et al., 2022 (12).

Quantitative Western blots of TBI- and sham-treated C57BL/6n mice 24 hours after the induced cortical lesion demonstrate a regulation of ubiquilin-1 expression in the whole hippocampus and cortex. **(A.i.)** and **(B.i.)** show molecular weight bands for ubiquilin-1 (63kD) and GAPDH (36 kD) from ipsilateral-, contralateral-, and sham-lysates of the cortex and the hippocampus, respectively. The scatter plots in **(A.ii.)** and **(B.ii.)** illustrate the downregulation of ubiquilin-1 in the contralateral cortex as well as in the ipsilateral and contralateral hippocampus 24 hours post-TBI in comparison to sham-treated mice.

3.3. Results from the Present Study

3.3.1. In Vitro Epilepsy Model and its Properties in Hippocampal Horizontal Brain Slices during Extracellular Multielectrode (MEA) Recordings

In order to detect alterations in excitability of neuronal populations, we induced epileptiform activity pharmacologically in acute brain slices according to an established *in vitro* epilepsy model by Ridler et al. (170). Continuous epileptiform discharges were reliably evoked by bath-application of picrotoxin (PTX, 50 µM) and kainic acid (KA, 500 nM) containing aCSF. Over the whole recording period, the seizure-like events (SLEs) appeared continuously instead of in bursts (**Figure 31, B**). The reproducible induction and highly repetitive occurrence of epileptiform discharges allowed an investigation of alterations and a modulation of epileptiform activity in the neuronal network of the hippocampus.

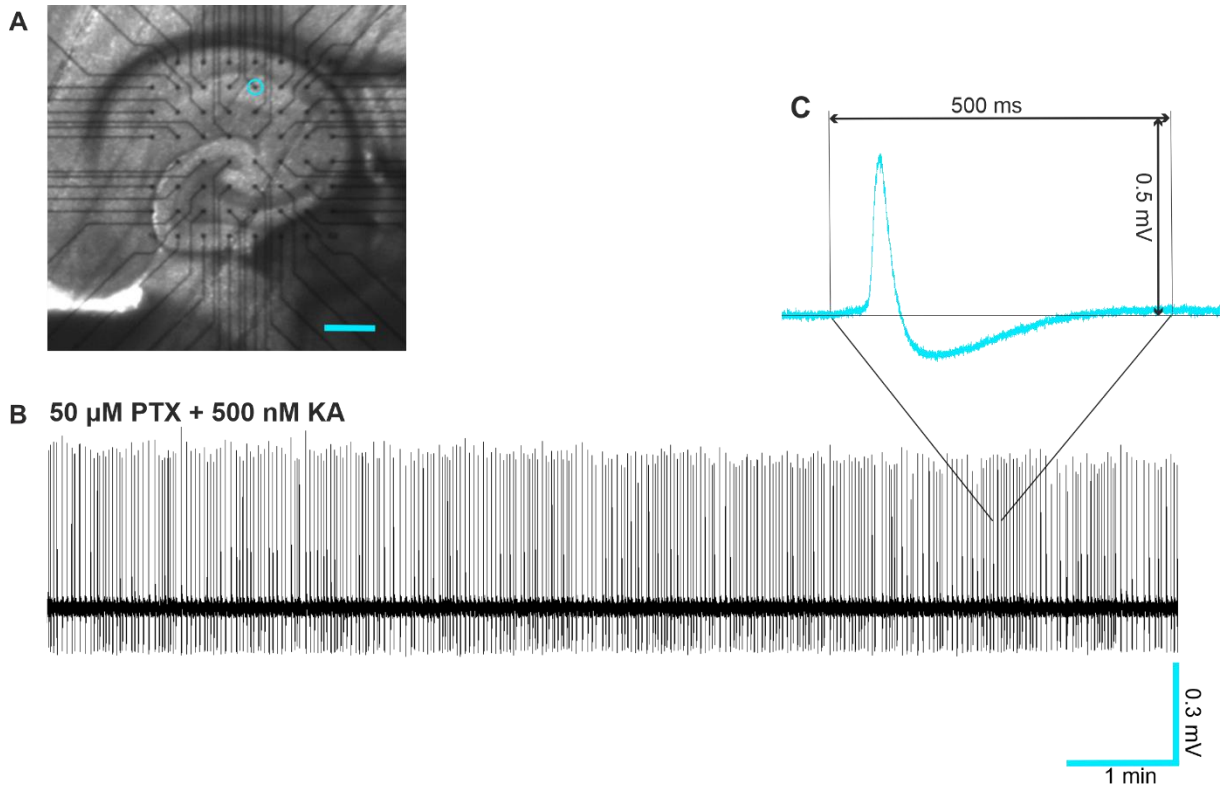

Figure 31. Modified from Kürten et al., 2022 (12).

Electrophysiological multielectrode array recordings in the hippocampal CA1 region *in vitro*. The Figure displays the properties of pharmacologically induced epileptiform activity. The seizure-like events (SLEs) were evoked via bath-application of 50 µM picrotoxin (PTX) and 500 nM kainic acid (KA).

(A) Position of a horizontal brain slice with a thickness of 400 µm in the MEA recording chamber. Scale bar = 400 µm. The location of 59 TiN-recording electrodes plus one internal reference electrode are indicated by the black dots. Each electrode has a diameter of 30 µm. The inter-electrode distance amounts to 200 µm. One single channel (blue circle) located in CA1 or the Schaffer collaterals was selected for data acquisition and analysis.

(B) Representative voltage trace of 10 minutes demonstrating the repetitive and continuous occurrence of SLEs over the whole recording period.

(C) Higher temporal resolution of a single epileptiform discharge.

Figure 32. Modified from Kürten et al., 2022 (12).

Electrophysiological multielectrode array recordings in the hippocampal CA1 region *in vitro*.

(A) Segment of 10 SLEs lasting 18 seconds from the representative trace in **Figure 31, B**.

(B) Representative voltage trace with experimental conditions devoid of PTX but with 500 nM KA. No epileptiform events occurred in the absence of PTX. Please note the higher resolution of the voltage signal for better display of the noise resolution.

3.3.2. Epileptiform Activity Causes a Reduction of Ubiquilin-1 Expression in Hippocampal and Cortical Slices 1-7 hours after Seizure Induction

After having established an *in vitro* epilepsy model, we initially focused on its impact on hippocampal and cortical expression of the $GABA_A$ receptor stabilizing protein ubiquilin-1 in acute brain slices. Subsequently, we quantified protein expression at defined time points of incubation following the induction of SLEs as described above. For this purpose, lysates from hippocampal and cortex were analyzed separately. Strikingly, ubiquilin-1 expression levels were reduced at all time points of incubation as compared to the control that was kept in standard aCSF. Significant values were identified using a Kruskal-Wallis-test. In cortical tissue, protein expression (**Figure 33, B**) was diminished after one hour (n = 8; p vs control: **0.0056), five hours (n = 8; p vs control: **0.0053), and seven hours (n = 8; p vs control: **0.0035), whereas in hippocampal lysates (**Figure 34, B**) we disclosed significant declines of protein expression after one hour (n = 8; p vs control: **0.0025) and seven hours (n = 8; p vs control: *0.0466) of incubation compared to control levels (n = 8). To sum up, these Western blot data indicate that the expression levels of ubiquilin-1 are severely affected in this acute time window up to seven hours after the onset of epileptiform activity.

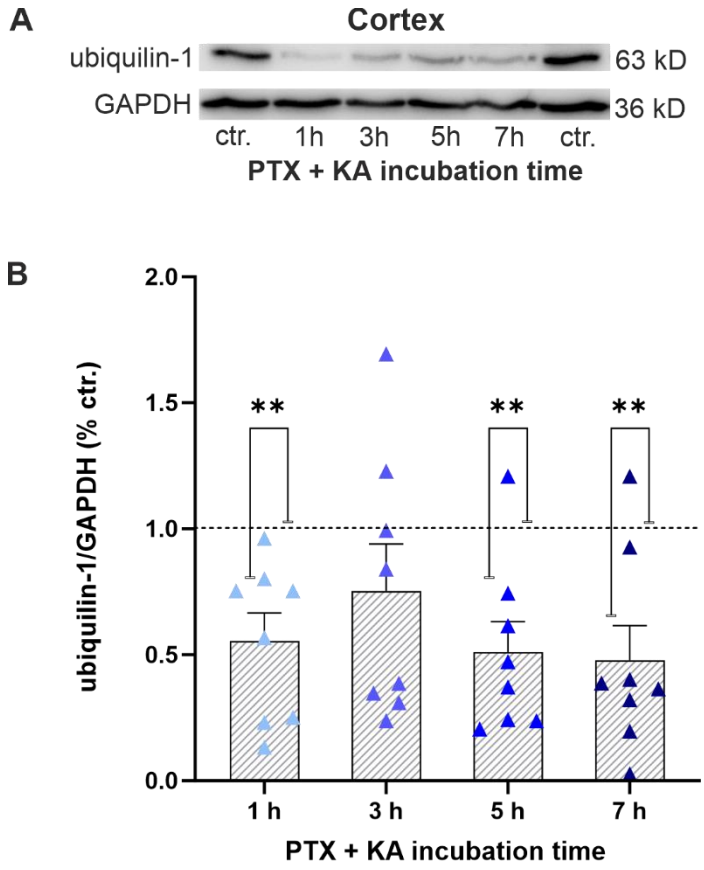

Figure 33. Modified from Kürten et al., 2022 (12).

Ubiquilin-1 expression levels in cortical slices at defined time points of incubation following the induction of *in vitro* epileptiform activity with PTX and KA.

(A) Exemplary Western blot weight bands of lysates from cortical slices acquired after one to seven hours of incubation. Quantification of ubiquilin-1 (63 kD) expression was performed after normalization to the housekeeping protein GAPDH (36 kD). **(B)** In the lower segment, the scatter plot displays the ubiquilin-1 levels in the cortex (n = 8) of eight animals each in relation to the control condition kept in standard aCSF. Protein levels of the control are indicated by the dashed line and normalized to one. The data in the scatter plots constitute relative values for protein expression at defined incubation times per animal, mean ± SEM are represented by bars and errors bars. Kruskal-Wallis test was performed for statistical analysis, significantly different values are indicated as **p<0.01. Analysis of the cortical protein expression level disclosed a significant reduction after one hour, after five hours, and seven hours of incubation.

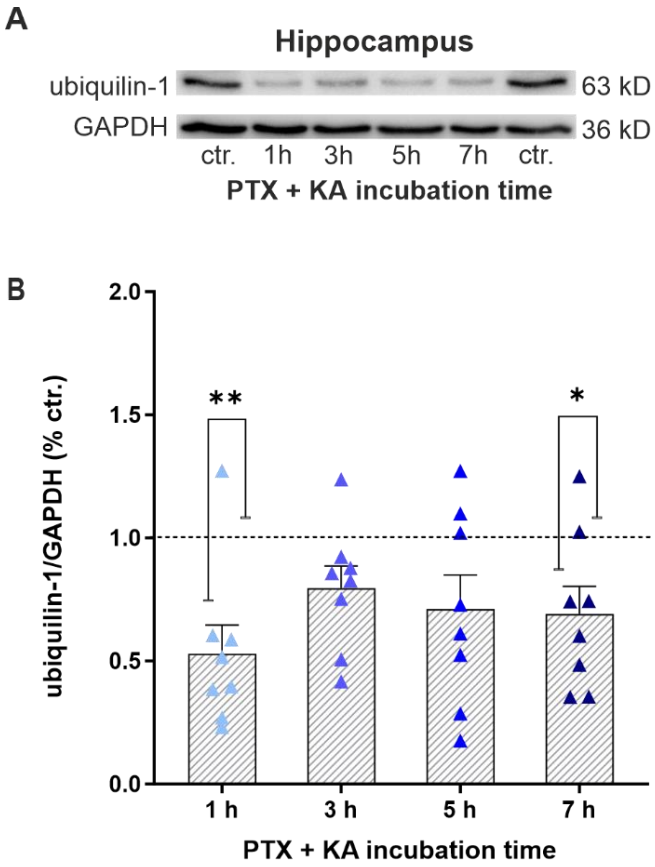

Figure 34. Modified from Kürten et al., 2022 (12).

Ubiquilin-1 expression levels in hippocampal slices at defined time points of incubation following the induction of *in vitro* epileptiform activity with PTX and KA. **(A)** Exemplary Western blot weight bands of lysates from hippocampal slices acquired after one to seven hours of incubation. Quantification of ubiquilin-1 (63 kD) expression was performed after normalization to the housekeeping protein GAPDH (36 kD). **(B)** In the lower segment, the scatter plot displays the ubiquilin-1 levels in the hippocampus ($n = 8$) of eight animals each in relation to the control condition kept in standard aCSF. Protein levels of the control are indicated by the dashed line and normalized to one. The data in the scatter plots constitute relative values for protein expression at defined incubation times per animal, mean ± SEM are represented by bars and errors bars. Kruskal-Wallis test was performed for statistical analysis, significantly different values are indicated as **$p<0.01$, p*<0.05. Note that the protein expression level is significantly decreased after one hour and after seven hours in the hippocampus.

3.3.3. The Non-selective MAO-Inhibitor Nialamide Upregulates and Rescues Ubiquilin-1 Expression in Acute Slices

In search of potential ways to modify ubiquilin-1 expression levels, we included the non-selective MAO inhibitor nialamide (NM) in our study. In previous studies the drug NM increased ubiquilin-1 expression and reduced neuronal injury in cell culture experiments (85). We investigated whether these effects could also be applied to our epilepsy model in mice to achieve a potential rescue of ubiquilin-1 expression. Therefore, we quantified protein levels at different time points of incubation with NM under two experimental conditions: first, under control conditions and secondly, in our *in vitro* epilepsy model. In order to detect a potential rescue in our Western blots, the epilepsy group (1h of incubation in aCSF with PTX and KA) without any NM-treatment was included in our analysis. Interestingly, NM-treatment of the epileptic brain slices increased cortical (**Figure 35, B**) and hippocampal (**Figure 36, B**) ubiquilin-1 expression, reaching an ubiquilin-1 expression close to the level of untreated controls (normalized to one). The observed recovery was predominant after one hour of incubation and subsided slightly after three and five hours. There was no significant difference between these groups and the control condition that was kept in standard aCSF. In the hippocampus (**Figure 36, B)**, Western blot quantification revealed significantly different values after one hour between the epilepsy slices and the NM-treated controls (n = 8; p vs control + 1h NM: *0.0190)**,** whereas in the cortex (**Figure 35, B**) significant differences were disclosed between the epilepsy condition and the one hour-rescue group (n = 8; p vs epilepsy + 1h NM: *0.0303), the control (n = 8; p vs control: **0.0100), and the control with NM-treatment (n = 8; p vs control + 1h NM: **0.0050). In the collected control slices that incubated in NM-containing aCSF for one hour, a tendency (ns) for enhanced protein expression beyond the level of the control was seen in both hippocampal and cortical tissue. In summary, these findings provide evidence that an administration of NM for one hour can be used to rescue the ubiquilin-1 expression in both cortex and hippocampus.

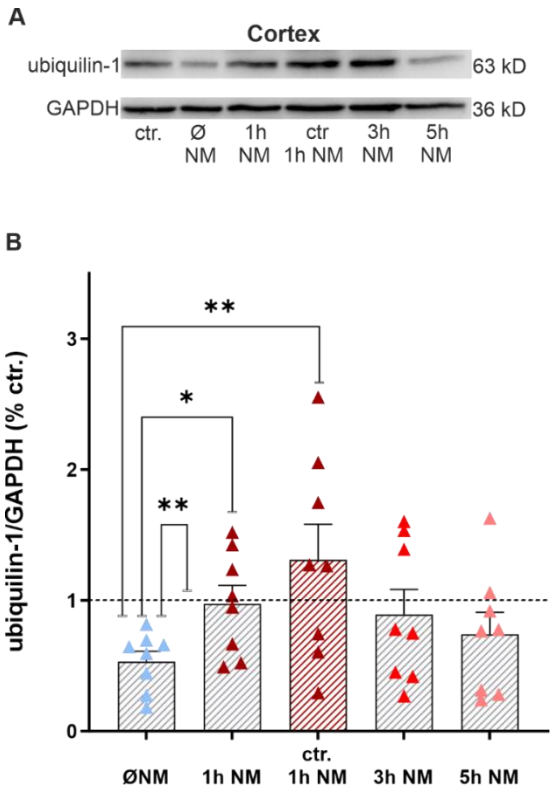

Figure 35. Modified from Kürten et al., 2022 (12).

Western blot quantification of the cortical ubiquilin-1 expression levels following a treatment with nialamide (NM) under epilepsy and control conditions *in vitro*. NM restores the diminished ubiquilin-1 expression caused by PTX and KA.

(A) Representative Western blot weight bands of cortical lysates. The scatter plot depicts the cortical expression of ubiquilin-1 (63 kD) in eight mice each (*n* = 8) at various time points of incubation. The slices incubated in aCSF containing 10 µM NM, either under control conditions from standard aCSF (third group in red in **(B)**) or following *in vitro* epilepsy induction with PTX + KA. The data were normalized to the signal of housekeeping protein GAPDH (36 kD). The dashed line indicates the control group that was kept in standard aCSF and normalized to one, bar plots and error bars represent mean ± SEM. Asterisks represent significantly different values revealed by Kruskal-Wallis tests, they are indicated as *p<0.05, **p<0.01. The first group represented by blue symbols constitutes the epilepsy condition devoid of NM-treatment. **(B)** In the cortex, significantly different values were disclosed between the epilepsy condition and the control group as well as the rescue group and the control plus one hour NM-treatment, respectively. In both hippocampus and cortex, an increased protein expression, almost reaching the initial level, was observed even after one hour. NM-treatment of control groups slightly enhanced the ubiquilin-1 expression level beyond that of the control (ns).

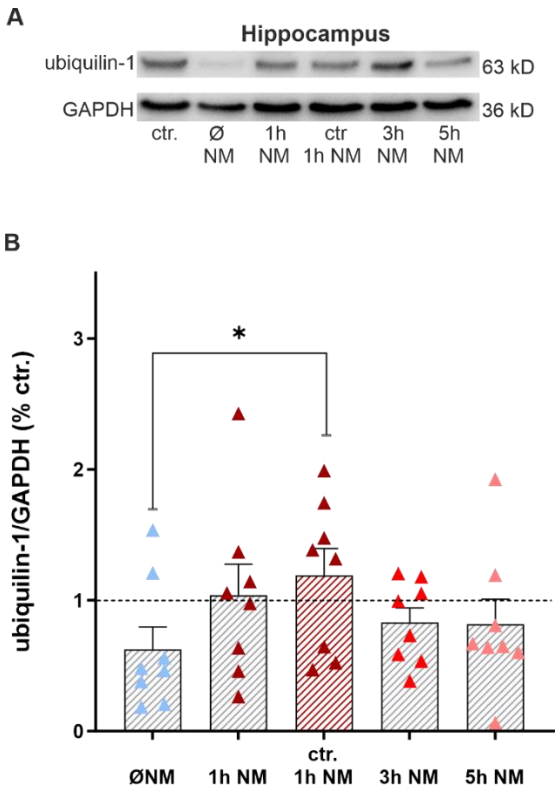

Figure 36. Modified from Kürten et al., 2022 (12).

Western blot quantification of the hippocampal ubiquilin-1 expression levels following a treatment with nialamide (NM) under epilepsy and control conditions *in vitro*. NM restores the diminished ubiquilin-1 expression caused by PTX and KA.

(A) Representative Western blot weight bands of hippocampal lysates. The scatter plot depicts the hippocampal expression of ubiquilin-1 (63 kD) in eight mice each (*n* = 8) at various time points of incubation. The slices incubated in aCSF containing 10 µM NM, either under control conditions from standard aCSF (third group in red in **(B)**) or following *in vitro* epilepsy induction with PTX + KA. The data were normalized to the signal of housekeeping protein GAPDH (36 kD). The dashed line indicates the control group that was kept in standard aCSF and normalized to one, bar plots and error bars represent mean ± SEM. Asterisks represent significantly different values revealed by Kruskal-Wallis tests, they are indicated as *p<0.05, **p<0.01. The first group represented by blue symbols constitutes the epilepsy condition devoid of NM-treatment. **(B)** The recovery of ubiquilin-1 expression in the hippocampus was significantly evident between the epilepsy group and the control that received NM-treatment for one hour.

3.3.4. Immunofluorescence Staining of Ubiquilin-1 Reveals Cell-type Specific Expression in the Cortex but no Regulation of Protein Expression

The expression of ubiquilin-1 was further analyzed in immunohistochemical staining of the somatosensory cortex and quantified in layer 2/3 in coronal brain sections. We further wanted to investigate the cell-type specific ubiquilin-1 expression pattern and ensure that ubiquilin-1 was predominantly co-localized with neurons. For this purpose, we compared three different experimental conditions: 1. Standard aCSF; 2. *In vitro* epilepsy model (one hour incubation in aCSF with 50 µm PTX and 500 nM KA); 3. *In vitro* epilepsy model + NM (rescue incubation for one additional hour with 10 µM NM). The wildtype mice (n = 3) were 26 days old. The distribution of ubiquilin-1 was set in relation to NeuN-expression, a DNA-binding marker for neuronal neuclei in all types of neurons. ImageJ was used to detect cells expressing ubiquilin-1 and GraphPad Prism software for statistical analysis. A Kruskal-Wallis test revealed no significant differences between the ubiquilin-1 expression patterns of the three mentioned experimental conditions. However, it is evident that ubiquilin-1 is widely expressed, co-localized with neurons as well as appearing in cells in the background. **Figure 37** shows the microscopic images and the statistical analysis.

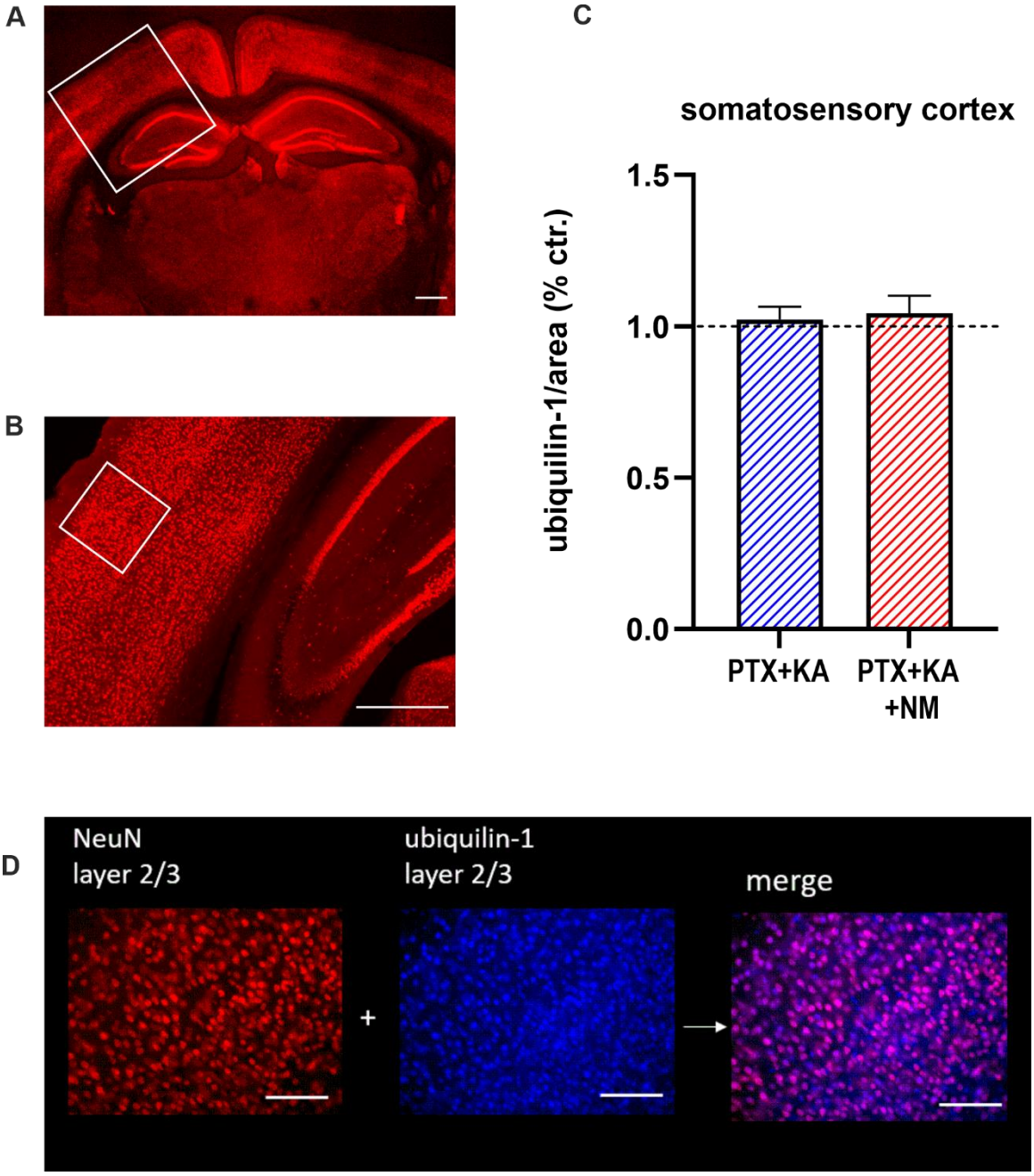

Figure 37. Modified from Kürten et al., 2022 (12).

Immunohistochemistry of the somatosensory cortex in three C57BL/6n-mice (*n* = 3) under three experimental conditions (standard aCSF/ *in vitro* epilepsy model/ *in vitro* epilepsy model + NM). The distribution and expression of ubiquilin-1 in acute sections was analyzed in relation to NeuN.

(A) 1.25x overview of the NeuN staining of a 20 µm thick coronal brain slice. The white square frames the part of the somatosensory cortex, which is shown at higher magnification (4x) in **(B)** Scale bar = 500 µm. The white square in **(B)** indicates the approximate area of interest in cortical layers 2/3. **(C)** Statistical

analysis of ubiquilin-1 expression compared to NeuN using Kruskal-Wallis test revealed no significant differences between the three experimental conditions in layer 2/3 of the somatosensory cortex. **(D)** Merge of the ubiquilin-1 and NeuN expression in layer 2/3 (20x). This resolution was used for the later analysis. Scale bar = 100 µm. Note that ubiquilin-1 is co-localized with neurons and further in cells in the background.

3.3.5. Nialamide Mitigates the Number of Epileptiform Discharges and the Mean Peak Amplitude in Dose-Response Relationships of Increasing Picrotoxin Concentrations in Extracellular Multielectrode Arrays

Next, we were interested in any antiepileptic effects of the MAOI during electrophysiological recordings in the hippocampal CA1 region. Therefore, we investigated dose-response relationships by applying increasing concentrations of the GABA receptor antagonist PTX in aCSF with 500 nM of KA. This allowed an estimation of the minimal concentration needed for the induction of epileptiform events and changes in their properties in the presence of NM. PTX concentrations ranged from 0-100 µM and were washed in for approximately 15 minutes respectively before data acquisition. The induced epileptiform activity was able to reach a saturating plateau during the generation of the dose-response curves. In addition, the same procedure was replicated with the non-selective MAO-inhibitor NM. We compared the dose-response relationships with (*n* = 15 slices/ 5 mice) vs. without NM-treatment (*n* = 9 slices/ 5 mice) regarding the mean event frequency and mean peak amplitude (**Figure 39, A**). Since we disclosed an increase of ubiquilin-1 expression even after one hour in the Western blots (**Figure 36, B**), we also pre-incubated the slices of the NM-group with the MAOI for one hour prior to the recordings. Then, they were transferred to the MEA chamber that was perfused with aCSF containing the same concentration of NM (10 µM) plus KA (500 nM). In the presence of these two substances, increasing concentrations of the GABA receptor blocker were applied again (0-100 µM) before the 10-minute traces were evaluated. The Clampfit analysis was threshold-based, where the settings were adjusted individually per slice and maintained for all applied PTX concentrations. The two-way ANOVA analysis revealed significantly different curve progressions between the two groups with respect to the mean number of events (NM vs no NM: **0.0061) and the mean peak amplitude (NM vs no NM: ***0.0004). Our findings clearly indicate that the epileptic activity was alleviated in the presence of the MAO inhibitor. At a concentration of 10 µM of PTX our data suggest a NM-dependent elevation of the seizure threshold in terms of the minimal PTX concentration needed for seizure-induction (**Figure 39, B**; Mann-Whitney test: NM vs no NM: *****0.0119). However, a direct comparison of the two groups by use of a Mann-Whitney test at a PTX concentration of 50 µM did not reveal significant differences (**Figure 40**), meaning that it is predominantly the course of the concentration curves that differs. In the present study, epileptiform discharges at a PTX

concentration of 50 µM in the presence of 500 nM KA had a mean peak amplitude of 0.19 ± 0.04 mV and comprised 151.11 ± 40.54 mean events in multielectrode array recordings. Additional recordings of the NM-group recorded in aCSF with 50 µM PTX + KA incorporated 95.33 ± 16.36 events with a mean peak amplitude of 0.11 ± 0.02 mV.

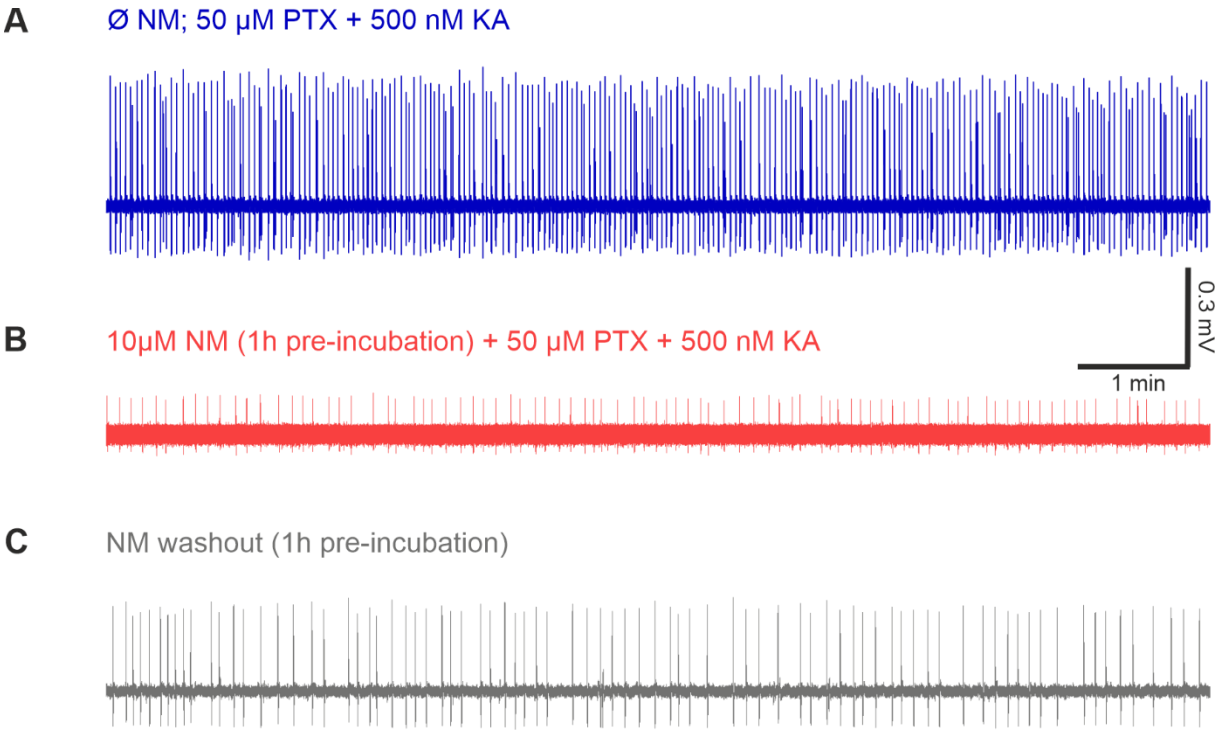

Figure 38. Modified from Kürten et al., 2022 (12).

NM-treatment of brain slices alleviates the number of events and mean peak amplitude under *in vitro* epilepsy conditions in extracellular recordings. Representative voltage traces of extracellular multi-channel recordings, illustrating the effect of NM-treatment on epileptiform activity and PTX-dependent dose-response relationships. Typical properties of pharmacologically evoked epileptiform activity during 10 minutes of multielectrode recording under three different experimental conditions.

(A) The top trace was recorded in the disinhibition model as described (50 µM PTX + 500 nM KA).

(B) For the middle trace slices pre-incubated for one hour in standard aCSF + 10 µM NM, recordings were performed during bath-application of 50 µM PTX + 500 nM + 10 µM NM.

(C) The bottom trace shows a NM-washout experiment after slice pre-incubation for one hour in standard aCSF + 10 µM NM and a subsequent NM-washout in the presence of 50 µM PTX + 500 nM during the recordings.

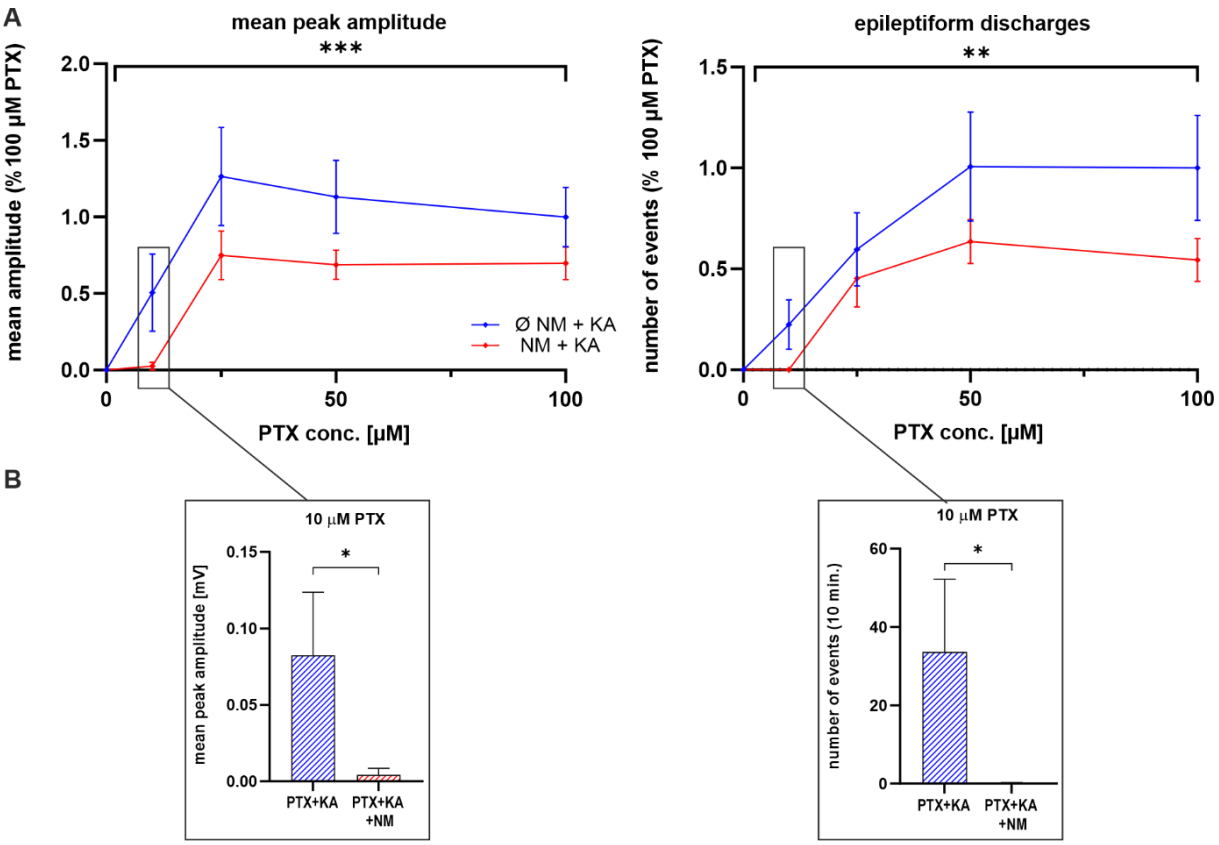

Figure 39. Modified from Kürten et al., 2022 (12)

(A) Dose-response relationships were analyzed with regard to the number of events and mean peak amplitude. Increasing concentrations of PTX (up to 100 µM) were gradually applied in presence of KA (*n* = 9 slices from 5 mice) or KA + NM (*n* = 15 slices from 5 mice). Brain slices that underwent NM-treatment were pre-incubated in aCSF containing 10 µM of NM for at least one hour. All data points are represented as relative values normalized to the mean number of events and mean peak amplitude of recordings in the presence of 100 µM PTX, without NM-application. Bars represent mean ± SEM, the asterisks indicate the level of significance of the detected values as ***p<0.001, **p<0.01. Two-way ANOVA analysis revealed a significantly different curve progression between the two experimental conditions with regard to the number of events (NM vs no NM p = **0.0061) as well as the mean peak amplitude (NM vs no NM p = ***0.0004). **(B)** Mann-Whitney-U test of the two experimental groups (PTX+KA vs. PTX+KA+NM) at a relatively low concentration of 10 µM PTX revealed epileptic events predominantly in the group without NM-treatment (NM vs no NM p = *0.0119 for events and peak amplitude). This indicates that NM might raise the PTX-

dependent threshold for seizure induction and suppress epileptiform activity at low PTX-concentrations.

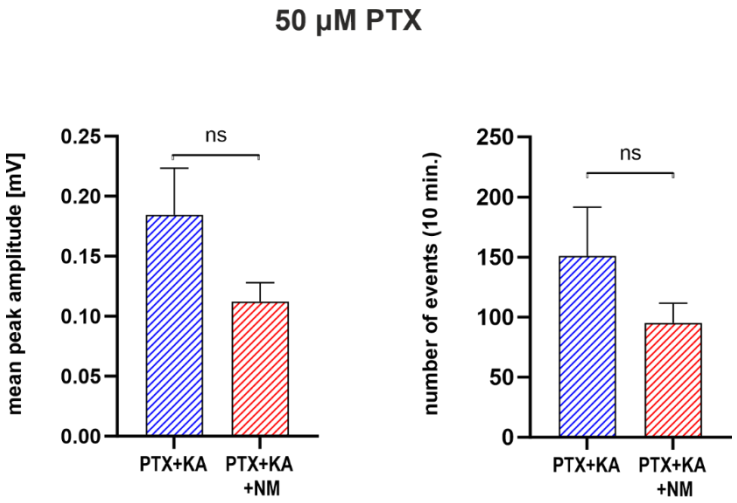

Figure 40.

Mann-Whitney-U test did not reveal significant differences of mean peak amplitude and number of events, when directly comparing the two groups at a PTX concentration of 50 µM.

To conclude, our results from Western blots provide new insights into a NM-dependent enhancement of ubiquilin-1 expression. Our data from electrophysiological MEA recordings in the hippocampal CA1 region strongly suggest an antiepileptic potential of the MAO inhibitor. We hypothesized that this might be related to a $GABA_A$ receptor stabilization through an upregulation of ubiquilin-1 expression.

4.1. Discussion of the Methods

Due to the lack of human specimens from epilepsy patients, studies in humans remain challenging (56). To study the underlying pathophysiology of early epileptogenesis or to have valid amounts and age-matched healthy controls, neural tissue would be required (56), e.g. from many non-epileptic patients that had suffered a head trauma. Rodent models enable us to overcome this issue, to generate significant amounts of comparable data, and to investigate molecular and cellular aspects during the epileptogenic period (56). Furthermore, new techniques, e.g. transgenic mice or optogenetics, offer the valuable opportunity of highly specific and targeted research. Rodents constitute popular animals in research since they are mammals of low breeding costs, small in size and well-established in standardized protocols and outcome values (183). Different key features of human TBI and human epilepsy are replicated by numerous animal models, which make it possible to discuss common and distinct features of the pathophysiologies (56, 183).

These are the main reasons for our research in mice, the use of which enabled us to successfully adopt established models of controlled cortical impact (CCI) and *in vitro* epilepsy in our lab. The models allowed us to gather new information in our fields of research that are closely linked to relevant clinical conditions in humans. However, the failure of neuroprotective drugs in humans that have previously been tested in TBI animal models with success (183), or the lissencephalic structure of the mouse brain, for example, indicate a limited applicability to the human brain, as discussed below in chapter 4.4.

Western blots are used for selective protein analysis by specific antigen-antibody binding and have even been adopted for therapeutic and diagnostic testing for 40 years (174, 177). Here, the reported rate of false positive results is lower than in ELISAs (174, 184). As a well-established and relatively simple method in academic research, it is performed to study the relative abundance, the presence, the post-translational modification, and the interactions of proteins (178). However, the workflow of Western blotting incorporates multiple steps, while each of them represents a source of error or variability (178). They can occur during the process of protein extraction, electrophoretic separation, protein transfer, signal detection, and analysis (178). In order to generate reproducible and precise Western blot data, quality controls during the process are crucial (178). Therefore, normalization to a housekeeping protein, the preliminary implementation of an assay (e.g. BCA) to compute the protein concentration and equal sample loading are necessary to ensure a high standard of semi-quantitative Western blotting.

We used multielectrode array (MEA) recordings in order to detect synchronous activity that is being generated by neural populations. The MEA technique has been widely established to study the electrophysiological properties on the network level (185). The first planar multielectrode arrays were introduced in the 1970s and 1980s (186). Prior to the development of the multisite recording method, the brain was extensively investigated on the single cell level but not on the scale of larger neural populations (185). Not only acute brain slices but also cell cultures and organoids can be investigated by use of MEA (185, 187). It is even possible to grow so-called organotypic cultures directly on the MEA chip to monitor long-term changes at different stages of growth in culture (185). Multi-electrode recordings are conducted to study synaptic plasticity (e.g. long-term potentiation), spontaneous spiking activity, evoked field potentials, single unit activity, rhythmic activity, the effect of drugs, and much more (185, 188, 189). They provide the possibility of extending our knowledge on the complex spatiotemporal dynamics of a functioning network or that of a disease model, e.g. in slices from transgenic mice (186). Furthermore, the technique enables simultaneous stimulation and recording at multiple locations (186).

We performed these extracellular recordings on acute brain slices, which were cut horizontally to obtain good access to the hippocampus. Here, we focused on the histological subfield CA1 and the adjacent Schaffer collaterals that project from CA3 to CA1 as part of the Papez circuit and the hippocampal trisynaptic loop (**Figure 17**), both involved in memory formation and consolidation (190-193). In a kainic-acid model of temporal lobe epilepsy (TLE) in rats, a loss of receptor subunits and loss of $GABA_A$ receptor-containing cells have been described in the areas CA1 and CA3 of the hippocampal formation (194). The postsynaptic $GABA_A$ receptor function, fast ripples and epileptiform activity have been well-studied in the CA1 subfield in further animal studies of epilepsy (193, 195). Moreover, TBI-experiments using the CCI-model monitored recovery of reduced numbers of GABAergic interneurons and altered GABA-mediated inhibitory currents in CA1 (196, 197). Therefore, we considered the CA1 region suitable for our electrophysiological investigations. Nonetheless, it cannot be excluded that one hippocampal subfield might be more afflicted by epileptiform activity and an altered ubiquilin-1 expression than the others.

The combination of electrophysiology and molecular biology in terms of MEA recordings, Western blots, and immunohistochemistry provided a great opportunity to gain a deeper insight into long-used and fundamental methods in basic research.

4.2. Discussion of Previous Studies and Thesis Aims

To date, the question of how brain injury-related alterations occurring on the level of protein expression can initiate the development of neurodegenerative sequelae or posttraumatic epilepsy remains mostly unanswered. Therefore, the central aim of this study was to investigate molecular changes, which appear early after traumatic brain injury and which could play a key role in epileptogenesis and posttraumatic hyperexcitability.

In the Mittmann research group, an early cortical hyperexcitability has been demonstrated and extensively studied in former experiments by use of the CCI-model of TBI in mice. Many of these experiments revealed that the posttraumatic excitability of cortical networks was not spatially limited to the vicinity of the lesion site but mainly observed in the intact contralateral hemisphere. More specifically, Le Prieult et al. performed MEA recordings after unilateral TBI and measured the number of active MEA-channels 1 mm from the lesion border in the right sensorimotor cortex and in the homotopic area of the other brain hemisphere (75). Strikingly, the spontaneous neuronal activity increased exclusively in the contralateral hemisphere one day following TBI (75). The same effect could be measured by whole-cell patch-clamp recordings that revealed an increase in the number of spontaneously active cells contralaterally (75). These remarkable findings correspond with the phenomenon referred to as *transhemispheric diaschisis* (103, 198, 199). It has been discussed as the result of a deafferentiation of transcallosal fibers from the lesion site (199, 200). The impact resulting from a focal unilateral lesion is assumed to cause a disinhibition in remote brain areas, which in turn might represent the primary cause for post-lesional hyperexcitability of uninjured regions (198). The disinhibition is associated with an impaired or altered GABAergic transmission (72, 75, 101, 198). The contralateral and intact hemisphere displays an abnormal hyperexcitability along with a reduced GABA-mediated inhibition (200). As described in the introduction, an injury-related shift from a phasic to a reinforced tonic inhibition has been proven in our lab, reflecting the underlying changes in the subunit composition of postsynaptic $GABA_A$ receptors (75, 201). However, there are multiple factors contributing to this shift, such as the reduced function of GABA transporters GAT-3/GAT-4 (202). Hyperexcitability of the uninjured hemisphere could have a detrimental impact, but it is also being regarded as a potential mechanism of functional recovery that compensates the damage of the lesioned cortex (198).

In our lab, we want to further understand transhemispheric diaschisis and to unravel posttraumatic alterations on the cellular and molecular level. By disclosing these pathomechanisms, it might become possible to distinguish those that are mainly involved in the recovery of the brain from those implicated in neurological sequelae. As an example, Feldmann et al. from our lab discovered that an impairment of proteasome- and autophagy-

mediated protein degradation blocks the induction of long-term potentiation (LTP), which could be responsible for cognitive deficits resulting from TBI (102).

In order to discover more targets that could play a role in the development of hyperexcitability early after TBI, [redacted] conducted an analysis of the proteome changes using FACS, as described in the results section. Proteins were identified that were exclusively regulated in GABAergic and GFP+ interneurons of the contralateral cortex 24 hours following TBI in mice (**Figure 29**)**.** The proteomics dataset uncovered stable biomarkers for TBI and other neurological pathologies, such as neurofilament light chains (NFL) (203-207). As a potential counter-mechanism against this early posttraumatic hyperexcitability in the contralateral hemisphere, Ihbe et al. disclosed a switch in the subunit composition of the L-type voltage-gated calcium channel (VGCC) in SST-interneurons using FACS, with an increase in the expression of CaV1.3 and a decrease of CaV1.2 (182).

Furthermore, the strong downregulation of ubiquilin-1 expression in the dataset from GABAergic interneurons 24 hours after TBI caught our attention. So far, an alteration of ubiquilin-1 expression has been described for several neurological disorders, inter alia, ischemic brain injury and epilepsy (64, 121). One of its main functions is the interaction with the ubiquitin-proteasome system (UPS), where it is known to stabilize $GABA_A$ receptors and indirectly increase their cell surface expression (64, 74, 112, 113). As suggested by recent studies, the decreased expression and binding of ubiquilin-1 to $GABA_A$ receptors is linked to hyperexcitability, an increased duration and severity of seizures as well as a shortened latency to seizure onset in animal studies (64). Studies of ubiquilin-1 expression in tissue from human patients suffering from temporal lobe epilepsy (TLE) revealed decreased levels of protein expression (64). This underlines the high clinical relevance of our target of investigation in this study. Not only could ubiquilin-1 represent a potential aim of future antiepileptogenic therapies but also a biomarker related to brain injury and epilepsy. To assess its potential role as a biomarker, large-scale, international, and multidisciplinary studies would have to be implemented both in animals and, secondly, in patients. With regard to our proteomic dataset and additional Western blots of the whole brain, we hypothesized that the previously observed posttraumatic GABAergic dysfunction and hyperexcitability might be linked to a downregulation of ubiquilin-1. Therefore, we considered it an interesting protein to further investigate in an *in vitro* epilepsy model of cortical disinhibition in the present study.

4.3. Discussion of the Results

First of all, we hypothesized that the hippocampal and cortical ubiquilin-1 expression might be strongly impaired upon $GABA_A$ receptor-blockade. We were able to confirm our assumptions

by performing quantitative Western blots. The Western blot analysis revealed a decline of protein expression in hippocampus and cortex in an acute time window of up to seven hours during epileptiform activity (**Figure 33**, **Figure 34**), which was evoked using the chemoconvulsants PTX and KA. We carefully chose a disinhibition model of *in vitro* epilepsy that would imitate certain aspects of TBI-pathophysiology, such as impaired GABAergic transmission or disinhibition (72, 75, 166, 167).

Next, we conducted an immunohistochemical analysis of ubiquilin-1/ NeuN expression in layer 2/3 of the somatosensory cortex. It did not reveal significant differences in the expression as compared to the control level and the NM-treated group (**Figure 37**). However, we could confirm that ubiquilin-1 was widely distributed not only in cells in the background but mainly co-localized with neurons (NeuN). This goes in line with recent studies that describe a ubiquilin-1 distribution predominantly in the cortex and hippocampus, especially in double-labeled microglia, astrocytes, and neurons (121). It also explains why we discovered a strongly impaired ubiquilin-1 expression not only in GABAergic interneurons in our proteomics dataset but also in the whole cortex and hippocampus. Our Western blots showed an overall decrease of ubiquilin-1 expression in unsorted cortical and hippocampal lysates 24 hours after TBI as well (**Figure 30**). Therefore, the ubiquilin-1 downregulation in CCI-treated mice was clearly not restricted to GABAergic interneurons in particular, which make up a smaller fraction of cells but present in other cell types as well.

Our experiments could prove that TBI leads to a decreased expression of ubiquilin-1, especially in interneurons, which might partly be responsible for the previously detected posttraumatic hyperexcitability and altered GABA transmission (75). We assumed that a downregulation of ubiquilin-1 in our TBI and epilepsy models might result in an enduring susceptibility to epileptiform activity, mediated through a $GABA_A$ receptor subunit-destabilization and loss of their integrity in the neuronal plasma membrane (64, 74, 112). Furthermore, low ubiquilin-1 levels might be connected to earlier ER-related degradation of $GABA_A$ receptors and their subunit isoforms (64, 74). As a consequence of impaired GABAergic control, arising excitatory glutamatergic network activity could compromise the physiological inhibitory synaptic transmission (101). We could not corroborate these assumptions by our experiments, but they would represent a theoretical and logical consequence from a loss of ubiquilin-1 function.

Our aim was to reverse this effect by restoring physiological ubiquilin-1 levels in our *in vitro* epilepsy model. Therefore, we deployed the non-selective MAO inhibitor nialamide (NM), the use of which had the potential to recover the diminished ubiquilin-1 levels according to a study

performed in an I/R-injury model in mice (85). We incubated epileptic and control slices in NM-containing aCSF for different time periods. Next, we examined the ubiquilin-1 expression at different time points from one to five hours again by Western blot quantification. Our Western blot data corroborated our expectation of a NM-mediated rescue. Subsequently, the downregulation of ubiquilin-1 that was induced by *in vitro* epilepsy could be fully reversed as early as one hour after NM-application (**Figure 35**, **Figure 36**). Therefore, we hypothesized that a degradation of the substrate ubiquilin-1 might be decelerated by blocking the different monoamine oxidases, which would indirectly increase its availability.

Our next aim was then to investigate the properties of epileptiform activity in multielectrode array (MEA) recordings during NM-application, which could possibly unfold antiepileptic effects associated with a recovered ubiquilin-1 expression. Since we reported an altered regulation of ubiquilin-1 expression after one hour in our Western blot analyses, we ensured that the baseline conditions for this purpose were similar by pre-incubating the hippocampal slices in NM-containing aCSF for one hour prior to our electrophysiological data acquisition. NM-administration clearly alleviated epileptiform activity in terms of frequency and amplitude of SLEs in our extracellular arrays (**Figure 38**). Our initial hypothesis was that a reduction of epileptiform activity, as observed in our MEA recordings, could be linked to reconstituted $GABA_A$ receptor stabilization, achieved through a NM-mediated upregulation of ubiquilin-1 expression. Since NM did not enact an enduring suppression of SLEs after withdrawal (**Figure 38, C**), it might be more correct to refer to its effect as *epileptostatic*. Significantly different curve progressions in our PTX-dependent dose-response experiments were evident with regard to the mean number of events and the mean peak amplitude in our electrophysiological recordings in the hippocampal CA1 region and Schaffer collaterals (**Figure 39**). Surprisingly, the effect could also be seen at high PTX concentrations of 50-100 µM that would theoretically inhibit nearly all $GABA_A$ receptors. Hence, we must draw the conclusion that the effects of the MAO inhibitor NM on epileptiform activity were not necessarily limited to an upregulation of ubiquilin-1 or a strengthened GABAergic inhibition.

Yet, it seems plausible that the monoamine transmitter systems might play a role in this attenuation of hyperexcitability. Both isoforms of the monoamine oxidases, MAO-A and MAO-B, are being blocked irreversibly by the non-selective inhibitor NM of the hydrazine class (85, 208). By preventing their degradation through monoamine oxidase enzymes, MAO inhibitors indirectly increase the extracellular concentrations of monoamine neurotransmitters and biogenic amines, such as norepinephrine, dopamine, serotonin, or tyramine (209-211). Monoamine oxidases are flavoenzymes that catalyze the oxidative deamination of these monoamines (85, 212). The chemical reaction generates noxious byproducts such as

ammonia (NH_3) or reactive oxygen species like hydrogen peroxide (H_2O_2) (85, 212, 213). This leads to oxidative stress and damaged mitochondria (85, 212, 213), which are both involved in epileptogenesis (84).

Thus, the neuroprotective potential of the drug NM and other MAOIs might be partly attributed to the protection from oxidative stress as a positive side effect (85, 214). MAOIs have been in clinical use for more than 50 years and represent highly effective agents for treating panic disorders and atypical or treatment-resistant depressive disorders (215-217). Like several other non-selective MAOIs, NM was originally introduced to the market for this indication but soon had to be discontinued due to adverse drug effects, such as hypertensive and hepatotoxic effects (85, 210, 217). Moreover, patients taking non-selective MAOIs must adhere to strict dietary tyramine restrictions due to drug-food interactions that can lead to strong adrenergic activity and hypertensive crisis (210, 212). The therapeutic range is narrow, and overdose or drug-drug interactions can cause further serious reactions, e.g. the serotonin syndrome when co-applied with SSRIs (208, 210, 217). With the invention of newer and safer antidepressants, the prescription rate of MAOIs, particularly concerning the non-selective type, has declined over the last decades (210, 217). However, patients do not always respond to other available antidepressants, which have side effects of their own (208, 218). Few non-selective MAOIs such as phenelzine or tranylcypromine are still in clinical use and are commonly being prescribed after the failure of first-or second line therapies for treatment-resistant, bipolar, or atypical depression (208). Since the drugs have been proven to be highly effective, randomized double-blind clinical trials and long-term research data promote the need for integrating their safe application more into clinical expertise and education (218).

Although MAOIs and monoamine transmitters have been discussed controversially as possible treatments of epileptic disorders, studies evince anticonvulsive effects upon $5HT_{1A}$-serotonine and D_2-dopamine receptor activation (219-221). In rat models, an intrahippocampal application of dopamine (D) and serotonin (5-HT) within moderate concentration ranges could prevent epileptogenesis in pilocarpine-induced epilepsy models (220). The anticonvulsant properties of dopamine can be ascribed to a D2 receptor activation, whereas a D1 receptor agonism, on the contrary, turns out to act proconvulsively (222, 223). Serotonin, on the other hand, is known to reduce neuronal network excitability through $5HT_{1A}$-mediated hyperpolarization of glutamatergic neurons and $5HT_{2C}$-mediated depolarization of GABAergic interneurons (221). Low serotonin activity is considered a major risk factor for the pathogenesis of epilepsy (224). By the end of 2020, the drug Fenfluramin (Fintepla®) that increases the release of serotonin (5-HT) and works as a selective agonist on 5-HT receptor subtypes (225, 226), was authorized for use by the European Medicines Agency (EMA) for treating Dravet syndrome. Dravet

syndrome is a severe epilepsy syndrome characterized by drug-resistance, infantile onset, multiple seizure types, and developmental epileptic encephalopathy (30, 225, 227). In the majority of patients with Dravet syndrome, a pathological variant of the subunit sodium channel gene SCN1A can be identified (30, 62). Multiple randomized controlled trials demonstrated an impressive median efficacy of ≥75% in reducing convulsive seizure frequency in Dravet syndrome patients (225, 228). This successful therapy result emphasizes the promising potential of medication interacting with the monoamine transmitter systems for treating epileptic disorders. In future, there might be new treatment options making use of the potential of monoamines for other forms of drug-resistant- or posttraumatic epilepsies, which remain particularly challenging to treat.

4.4. Discussion of the Limitations of the Present Study Design

The experiments performed for this work were realized as part of an *ex vivo-in vitro* study. Epileptiform activity was evoked pharmacologically according to an established *in vitro* epilepsy-model (170). In spite of its reproducibility and efficiency in MEA recordings, the applicability of an *in vitro* epilepsy mouse model to epilepsy in humans is limited. In this context, it is important to consider disruptive factors, such as the lissencephalic structure of the mouse brain or the age of the respective mouse. The slice preparation itself, the exact location, and tissue contact of the electrodes, or the level of noise cause an inevitable natural variability during the extracellular recordings.

Furthermore, the etiology of PTE must be considered multifactorial, as head trauma and brain injury elicit damages and mechanisms that are individually distinct and multiplex. In addition to that, the proneness and risk of PTE differs between individuals. A neuropathological example for predisposed epileptogenicity is focal cortical dysplasia, a clinical condition which is associated with a higher risk of developing PTE (229, 230). The pathomechanisms described in the introduction give an overview of the common observations in studies of TBI and epileptogenesis. However, the descriptions provided by this work do not cover them in their full scope.

Since NM is an obsolete medication, further studies in mice using selective or different non-selective MAO inhibitors or other serotonin and dopamine-interacting drugs would be useful. This would help us to understand the role of the distinct monoamine transmitters in epileptogenesis and its prevention.

To corroborate our findings, it would be of great interest to address our target ubiquilin-1 more specifically by the use of knockout mice, transgenic mice or synthetic ubiquilin-1 inhibitors.

Moreover, it would be interesting to reproduce the conducted experiments in distinct *in vitro* epilepsy models. A non-disinhibition model, for example, would enable a differentiation between a common effect of epileptiform activity on ubiquilin-1 expression and a disinhibition exclusively mediated by PTX.

In order to monitor long-term changes in ubiquilin-1 expression or to study its potential as a biomarker for epileptogenesis, *in vivo* animal models of chronic posttraumatic epilepsy would be a valuable option. In our lab, this could be achieved, for instance, by combining CCI-induced TBI and a kindling model of epileptogenesis.

4.5. Conclusions and Outlook

Concluding, without any antiepileptogenic treatment available at the current state of research, it is of great importance to extend our knowledge on endogenous targets. In the future, specific proteins, transmitters, and molecules could be identified that protect from neuronal network excitability. Or they might represent suitable biomarkers that would one day enable us to define the state of epileptogenesis after head trauma. In order to devise effective prophylactic treatments that prevent late-seizure onset, it is highly relevant to decipher the underlying adaptive mechanisms following traumatic brain injury. The present study provides new insights into the role of ubiquilin-1 and its regulation in models of traumatic brain injury and *in vitro* epilepsy. The $GABA_A$ receptor stabilizing protein possesses neuroprotective qualities, while its regulation on the level of protein expression might play a detrimental role in epileptogenesis. By including the MAO inhibitor nialamide in our study, we were able to regain physiological ubiquilin-1 expression in acute brain slices. In addition, our electrophysiological findings in hippocampal slices strongly suggest anti-epileptiform or epileptostatic effects of nialamide. The monoamine transmitter systems might become more important in the future, since they have a great therapeutic potential for forms of epilepsy that continue to be eminently difficult to treat to this day.

5. Summary

For more than ten years following a traumatic brain injury (TBI), the risk of being diagnosed with posttraumatic epilepsy (PTE) is substantially increased (104). PTEs constitute an increasing socioeconomic and global public health concern and thus, a large proportion of acquired epilepsies (97, 99). To this day, no effective and antiepileptogenic treatment strategy has been implemented in clinical practice and therefore remains a challenging subject of research (98). With the advent of newer techniques in epilepsy research, the deciphering of the pathophysiology underlying posttraumatic epileptogenesis is steadily improving. The use of animal models of epilepsy and TBI is of great significance for the discovery of biomarkers or potential therapeutic interventions (56). For this purpose, specific molecular targets with an altered expression during TBI-inflicted epileptogenesis prove promising for devising antiepileptogenic treatment strategies (98). By using our established animal models of TBI and *in vitro* epilepsy, we gained new insights into the regulation of the $GABA_A$ receptor-interacting protein ubiquilin-1. Recent studies have demonstrated that ubiquilin-1 is strongly regulated in epilepsy (64), ischemic brain injuries (121) as well as in neurodegenerative diseases, e.g. Alzheimer's and Huntington's disease (118, 120). In the preliminary work for this study, a quantitative approach of proteomic analysis on isolated GFP+ interneurons from the contralateral hemisphere after unilateral TBI-induction was implemented to identify target proteins implicated in posttraumatic brain injury mechanisms. The label-free quantification in cortical GABAergic interneurons from CCI-treated GAD67-GFP mice revealed a significant downregulation of ubiquilin-1 24 hours post-lesion. To investigate the common features between this regulation post-TBI and epilepsy, we implemented an epilepsy model to study the ubiquilin-1 expression in slices from the cortex and hippocampus. In the present study, epileptiform activity was induced *in vitro* by application of the combination of kainic acid (KA, 500 nM) and the $GABA_A$ receptor antagonist picrotoxin (PTX, 50 µM). These chemoconvulsives have already been established as a highly reliable *in vitro* model of epilepsy by Ridler et al. (170). We monitored the highly repetitive occurrence of seizure-like events (SLEs) with extracellular multielectrode array (MEA) recordings in the hippocampal CA1 region of acute brain slices. Following the induction of epileptiform events, we quantified the expression of our target ubiquilin-1 in hippocampal and cortical slices in a time window of up to seven hours after seizure induction with Western blots. Here, we disclosed a reduction of ubiquilin-1 expression at all time points of incubation in both the hippocampus and the cortex. Next, we successfully performed a pharmacological rescue in order to recover the previously diminished ubiquilin-1 levels by use of the non-selective monoamine oxidase inhibitor nialamide (NM,10 µM). Our Western blot data raised the question of whether an upregulation of ubiquilin-1 expression would alter the properties of *in vitro* epileptiform activity. Therefore, we recorded dose-response relationships by applying increasing concentrations of PTX (0-100

µM). Interestingly, the application of NM during MEA recordings substantially alleviated epileptiform activity with regard to the number of SLEs and the mean peak amplitudes. Our observation indicates that aside from a restored ubiquilin-1 expression, the different monoamine transmitter systems might contribute to this epileptostatic effect and have a great potential for future investigations.

5.1. Zusammenfassung

Für einen Zeitraum von mehr als zehn Jahren nach einer traumatischen Hirnverletzung (TBI) ist das Risiko, die Diagnose Posttraumatische Epilepsie (PTE) zu erhalten, deutlich erhöht (104). Posttraumatische Epilepsien stellen ein wachsendes sozioökonomisches Problem der öffentlichen Gesundheit weltweit dar und machen einen großen Anteil der erworbenen Epilepsien aus (97, 99). Bis heute wurde keine effektive und anti-epileptogene Therapie in die klinische Praxis umgesetzt und bleibt daher weiterhin ein herausfordernder Gegenstand der aktuellen Forschung (98). Mit der Entwicklung neuer Technologien im Forschungsbereich der Epilepsien hat sich die Entschlüsselung zugrundeliegender Pathomechanismen der Epileptogenese kontinuierlich verbessert. Der Einsatz von Tiermodellen der Epilepsie und der traumatischen Hirnverletzung ist von großer Bedeutung für die Entdeckung von Biomarkern und potenziellen therapeutischen Interventionsmöglichkeiten (56). Für diesen Zweck stellen sich spezielle molekulare Zielproteine- und Strukturen mit einer veränderten Expression während einer TBI-induzierten Epileptogenese als aussichtsreich für die Entwicklung anti-epileptogener Behandlungsstrategien heraus (98). Durch die Verwendung unserer etablierten Tiermodelle der traumatischen Hirnverletzung und *in vitro* Epilepsie konnten wir neue Einblicke in die Regulation des mit $GABA_A$ Rezeptoren-interagierenden Proteins Ubiquilin-1 gewinnen. Neuere Studien haben eine ausgeprägte Regulation der Expression von Ubiquilin-1 in Epilepsien (64), ischämischen Hirnschädigungen (121), sowie in neurodegenerativen Erkrankungen wie Morbus Alzheimer und Morbus Huntington belegt (118, 120). In einem früheren Projekt wurde ein quantitativer Ansatz der Proteom-analyse von isolierten GFP-positiven Interneuronen der kontralateralen Hemisphäre nach unilateraler Induktion einer traumatischen Hirnverletzung umgesetzt, um mögliche Zielproteine zu identifizieren, die an posttraumatischen Mechanismen beteiligt sind. Die markierungsfreie Quantifizierung in kortikalen GABAergen Interneuronen von CCI-behandelten GAD67-GFP Mäusen zeigte eine signifikante Herunterregulierung der Ubiquilin-1 Expression 24 Stunden nach Läsionsinduktion. Um gemeinsame Merkmale zwischen der Regulation nach traumatischer Hirnverletzung und Epilepsien zu ermitteln, haben wir ein Epilepsiemodell umgesetzt, um die Ubiquilin-1 Expression in Hirnschnitten des Kortex und Hippocampus zu messen. In der vorliegenden Studie wurde epileptiforme Aktivität *in vitro* durch das Applizieren einer Kombination aus Kainat (KA, 500 nM) und dem $GABA_A$ Rezeptor Antagonisten Picrotoxin

(PTX, 50 µM) ausgelöst. Diese Chemokonvulsiva wurden bereits zuvor als ein bewährtes *in vitro* Epilepsiemodell von Ridler et al. etabliert (170). Das repetitive Auftreten der epileptiformen Ereignisse in der hippokampalen CA1 Region von akuten Hirnschnitten haben wir mithilfe von Multielektrodenarrays (MEA) aufgezeichnet. Nach der Induktion epileptiformer Aktivität haben wir die Expression unseres Zielproteins Ubiquilin-1 in einem Zeitfenster von bis zu sieben Stunden nach Anfallsinduktion in kortikalen und hippokampalen Hirnschnitten mithilfe von Western Blots quantifiziert. Hier konnten wir eine signifikante Reduktion der Ubiquilin-1 Expression zu allen Inkubationszeitpunkten feststellen, sowohl im Kortex als auch im Hippocampus. Als nächstes konnten wir die zuvor verminderten Ubiquilin-1 Levels erfolgreich wiederherstellen unter Zuhilfenahme des nicht-selektiven Monoaminooxidase-Hemmers Nialamide (NM,10 µM). Unsere Western Blot Daten ließen die Frage aufkommen, ob solch eine Hochregulation der Ubiquilin-1 Expression auch die Eigenschaften der epileptiformen Aktivität *in vitro* verändern würde. Daher haben wir Dosis-Wirkungsbeziehungen gemessen, indem wir steigende PTX-Konzentrationen (0-100 µM) appliziert haben. Bemerkenswerterweise hat die Anwendung von NM während der MEA-Aufzeichnungen die epileptiforme Aktivität substanziell abgeschwächt im Hinblick auf die Anzahl der epileptiformen Events und der mittleren Maximalamplitude. Unsere Beobachtungen deuten darauf hin, dass neben einer wiederhergestellten Ubiquilin-1 Expression auch die verschiedenen Systeme der Monoaminen Neurotransmitter zu dem antiepileptischen Effekt beitragen und ein großes Potenzial für zukünftige Studien besitzen.

6. Bibliography

6.1. Figure References

1. Global, regional, and national burden of epilepsy, 1990-2016: a systematic analysis for the Global Burden of Disease Study 2016. The Lancet Neurology. 2019;18(4):357-75.

2. Scheffer IE, Berkovic S, Capovilla G, Connolly MB, French J, Guilhoto L, et al. ILAE classification of the epilepsies: Position paper of the ILAE Commission for Classification and Terminology. Epilepsia. 2017;58(4):512-21.

3. Lévesque M, Salami P, Shiri Z, Avoli M. Interictal oscillations and focal epileptic disorders. The European journal of neuroscience. 2018;48(8):2915-27.

4. Pitkänen A, Lukasiuk K, Dudek FE, Staley KJ. Epileptogenesis. Cold Spring Harb Perspect Med. 2015;5(10):a022822.

5. Bak LK, Schousboe A, Waagepetersen HS. The glutamate/GABA-glutamine cycle: aspects of transport, neurotransmitter homeostasis and ammonia transfer. J Neurochem. 2006;98(3):641-53.

6. Gong P, Hong H, Perkins EJ. Ionotropic GABA receptor antagonism-induced adverse outcome pathways for potential neurotoxicity biomarkers. Biomarkers in medicine. 2015;9(11):1225-39.

7. Le Prieult F, Thal SC, Engelhard K, Imbrosci B, Mittmann T. Acute Cortical Transhemispheric Diaschisis after Unilateral Traumatic Brain Injury. Journal of neurotrauma. 2017;34(5):1097-110.

8. Mattson MP. Excitotoxic and excitoprotective mechanisms: abundant targets for the prevention and treatment of neurodegenerative disorders. Neuromolecular medicine. 2003;3(2):65-94.

9. Sharma S, Tiarks G, Haight J, Bassuk AG. Neuropathophysiological Mechanisms and Treatment Strategies for Post-traumatic Epilepsy. Front Mol Neurosci. 2021;14:612073.

10. Timofeev I, Sejnowski TJ, Bazhenov M, Chauvette S, Grand LB. Age dependency of trauma-induced neocortical epileptogenesis. Front Cell Neurosci. 2013 Sep 18;7:154.

11. Jansen AH, Reits EA, Hol EM. The ubiquitin proteasome system in glia and its role in neurodegenerative diseases. Front Mol Neurosci. 2014;7:73.

12. Kürten T, Ihbe N, Ueberbach T, Distler U, Sielaff M, Tenzer S, et al. GABA(A) Receptor-Stabilizing Protein Ubqln1 Affects Hyperexcitability and Epileptogenesis after Traumatic Brain Injury and in a Model of In Vitro Epilepsy in Mice. International journal of molecular sciences. 2022;23(7).

13. Löscher W. Animal Models of Seizures and Epilepsy: Past, Present, and Future Role for the Discovery of Antiseizure Drugs. Neurochemical research. 2017;42(7):1873-88.

14. Olsen RW. Picrotoxin-like channel blockers of GABAA receptors. Proceedings of the National Academy of Sciences of the United States of America. 2006;103(16):6081-2.

15. Tian Z, Clark BLM, Menard F. Kainic Acid-Based Agonists of Glutamate Receptors: SAR Analysis and Guidelines for Analog Design. ACS chemical neuroscience. 2019;10(10):4190-8.

16. Goldberg EM, Coulter DA. Mechanisms of epileptogenesis: a convergence on neural circuit dysfunction. Nature reviews Neuroscience. 2013;14(5):337-49.

17. Oh K. Technical Considerations for Contemporary Western Blot Techniques. Methods in molecular biology (Clifton, NJ). 2021;2261:457-79.

18. Allen Institute. Allen Brain Atlas ”Mouse, P56, Coronal” (online). 2011. [Available from: Interactive Atlas Viewer :: Atlas Viewer (brain-map.org), accessed: 14.03.2022, 10:30]

6.2. Literature References

1. Desai J, Sadrieh K. It's Time to Remember Hippocrates. Journal of child neurology. 2018;33(8):501-2.

2. Magiorkinis E, Sidiropoulou K, Diamantis A. Hallmarks in the history of epilepsy: epilepsy in antiquity. Epilepsy & behavior : E&B. 2010;17(1):103-8.

3. Ali R, Connolly ID, Feroze AH, Awad AJ, Choudhri OA, Grant GA. Epilepsy: A Disruptive Force in History. World neurosurgery. 2016;90:685-90.

4. Orrego-GonzÁlez E, Peralta-GarcÍa A, Palacios-SÁnchez L. Heracles and epilepsy: the sacred disease. Arquivos de neuro-psiquiatria. 2020;78(10):660-2.

5. de Boer HM, Mula M, Sander JW. The global burden and stigma of epilepsy. Epilepsy & behavior : E&B. 2008;12(4):540-6.

6. Breitenfeld T, Jurasic MJ, Breitenfeld D. Hippocrates: the forefather of neurology. Neurological sciences : official journal of the Italian Neurological Society and of the Italian Society of Clinical Neurophysiology. 2014;35(9):1349-52.

7. Beghi E. The Epidemiology of Epilepsy. Neuroepidemiology. 2020;54(2):185-91.

8. Sadr SS, Javanbakht J, Javidan AN, Ghaffarpour M, Khamse S, Naghshband Z. Descriptive epidemiology: prevalence, incidence, sociodemographic factors, socioeconomic domains, and quality of life of epilepsy: an update and systematic review. Archives of medical science : AMS. 2018;14(4):717-24.

9. Yang RR, Wang WZ, Snape D, Chen G, Zhang L, Wu JZ, et al. Stigma of people with epilepsy in China: views of health professionals, teachers, employers, and community leaders. Epilepsy & behavior : E&B. 2011;21(3):261-6.

10. Holtkamp M, May TW, Berkenfeld R, Bien CG, Coban I, Knake S, et al. Erster epileptischer Anfall und Epilepsien im Erwachsenenalter, S2k-Leitlinie, 2023; in: Deutsche Gesellschaft für Neurologie (Hrsg.), Leitlinien für Diagnostik und Therapie in der Neurologie 2023 [Available from: www.dgn.org/leitlinien, accessed: 26.05.2024, 8:30]

11. World Health Organization. "Epilepsy" (online). June 2019. [Available from: https://www.who.int/news-room/fact-sheets/detail/epilepsy, accessed: 04.04.2021, 9:15]

12. Fisher RS, Acevedo C, Arzimanoglou A, Bogacz A, Cross JH, Elger CE, et al. ILAE official report: a practical clinical definition of epilepsy. Epilepsia. 2014;55(4):475-82.

13. Meyer AC, Dua T, Ma J, Saxena S, Birbeck G. Global disparities in the epilepsy treatment gap: a systematic review. Bulletin of the World Health Organization. 2010;88(4):260-6.

14. Scheffer IE, Berkovic S, Capovilla G, Connolly MB, French J, Guilhoto L, et al. ILAE classification of the epilepsies: Position paper of the ILAE Commission for Classification and Terminology. Epilepsia. 2017;58(4):512-21.

15. Sands TT, Gelinas JN. Epilepsy and Encephalopathy. Pediatric neurology. 2024;150:24-31.

16. Scheffer IE, Liao J. Deciphering the concepts behind "Epileptic encephalopathy" and "Developmental and epileptic encephalopathy". European journal of paediatric neurology : EJPN : official journal of the European Paediatric Neurology Society. 2020;24:11-4.

17. Stafstrom CE, Carmant L. Seizures and epilepsy: an overview for neuroscientists. Cold Spring Harb Perspect Med. 2015;5(6).

18. Fiest KM, Sauro KM, Wiebe S, Patten SB, Kwon CS, Dykeman J, et al. Prevalence and incidence of epilepsy: A systematic review and meta-analysis of international studies. Neurology. 2017;88(3):296-303.

19. Murray CJ, Vos T, Lozano R, Naghavi M, Flaxman AD, Michaud C, et al. Disability-adjusted life years (DALYs) for 291 diseases and injuries in 21 regions, 1990-2010: a systematic analysis for the Global Burden of Disease Study 2010. Lancet (London, England). 2012;380(9859):2197-223.

20. Ding D, Hong Z, Wang WZ, Wu JZ, de Boer HM, Prilipko L, et al. Assessing the disease burden due to epilepsy by disability adjusted life year in rural China. Epilepsia. 2006;47(12):2032-7.

21. Global, regional, and national burden of epilepsy, 1990-2016: a systematic analysis for the Global Burden of Disease Study 2016. The Lancet Neurology. 2019;18(4):357-75.

22. Pitkänen A, Löscher W, Vezzani A, Becker AJ, Simonato M, Lukasiuk K, et al. Advances in the development of biomarkers for epilepsy. The Lancet Neurology. 2016;15(8):843-56.

23. Levira F, Thurman DJ, Sander JW, Hauser WA, Hesdorffer DC, Masanja H, et al. Premature mortality of epilepsy in low- and middle-income countries: A systematic review from the Mortality Task Force of the International League Against Epilepsy. Epilepsia. 2017;58(1):6-16.

24. Sander JW. The epidemiology of epilepsy revisited. Current opinion in neurology. 2003;16(2):165-70.

25. Beghi E, Giussani G. Aging and the Epidemiology of Epilepsy. Neuroepidemiology. 2018;51(3-4):216-23.

26. Preux PM, Druet-Cabanac M. Epidemiology and aetiology of epilepsy in sub-Saharan Africa. The Lancet Neurology. 2005;4(1):21-31.

27. Banerjee PN, Filippi D, Allen Hauser W. The descriptive epidemiology of epilepsy-a review. Epilepsy research. 2009;85(1):31-45.

28. Falco-Walter J. Epilepsy-Definition, Classification, Pathophysiology, and Epidemiology. Seminars in neurology. 2020;40(6):617-23.

29. Adelow C, Andell E, Amark P, Andersson T, Hellebro E, Ahlbom A, et al. Newly diagnosed single unprovoked seizures and epilepsy in Stockholm, Sweden: First report from the Stockholm Incidence Registry of Epilepsy (SIRE). Epilepsia. 2009;50(5):1094-101.

30. Zuberi SM, Wirrell E, Yozawitz E, Wilmshurst JM, Specchio N, Riney K, et al. ILAE classification and definition of epilepsy syndromes with onset in neonates and infants: Position statement by the ILAE Task Force on Nosology and Definitions. Epilepsia. 2022;63(6):1349-97.

31. Faul M, Coronado V. Epidemiology of traumatic brain injury. Handbook of clinical neurology. 2015;127:3-13.

32. Avanzini G, Beghi E, de Boer H, Engel Jr. J, Sander JW, Wolf P. "Epilepsy". In: Neurological disorders: public health challenges: World Health Organization; 2006. p. 56-69.

33. Shackleton DP, Westendorp RG, Kasteleijn-Nolst Trenité DG, de Craen AJ, Vandenbroucke JP. Survival of patients with epilepsy: an estimate of the mortality risk. Epilepsia. 2002;43(4):445-50.

34. Morgan CL, Kerr MP. Epilepsy and mortality: a record linkage study in a U.K. population. Epilepsia. 2002;43(10):1251-5.

35. Thurman DJ, Logroscino G, Beghi E, Hauser WA, Hesdorffer DC, Newton CR, et al. The burden of premature mortality of epilepsy in high-income countries: A systematic review from the Mortality Task Force of the International League Against Epilepsy. Epilepsia. 2017;58(1):17-26.

36. Harden C, Tomson T, Gloss D, Buchhalter J, Cross JH, Donner E, et al. Practice guideline summary: Sudden unexpected death in epilepsy incidence rates and risk factors: Report of the Guideline Development, Dissemination, and Implementation Subcommittee of the American Academy of Neurology and the American Epilepsy Society. Neurology. 2017;88(17):1674-80.

37. Mesraoua B, Tomson T, Brodie M, Asadi-Pooya AA. Sudden unexpected death in epilepsy (SUDEP): Definition, epidemiology, and significance of education. Epilepsy & behavior : E&B. 2022;132:108742.

38. Velasquez M, De Marinis A, Benavides E. [Sudden death in epilepsy]. Revista medica de Chile. 2018;146(8):902-8.

39. DeGiorgio CM, Curtis A, Hertling D, Moseley BD. Sudden unexpected death in epilepsy: Risk factors, biomarkers, and prevention. Acta neurologica Scandinavica. 2019;139(3):220-30.

40. Trinka E, Cock H, Hesdorffer D, Rossetti AO, Scheffer IE, Shinnar S, et al. A definition and classification of status epilepticus--Report of the ILAE Task Force on Classification of Status Epilepticus. Epilepsia. 2015;56(10):1515-23.

41. Rao VR, Lowenstein DH. Epilepsy. Current biology : CB. 2015;25(17):R742-6.

42. Süße M, Hamann L, Flöel A, von Podewils F. Nonlesional late-onset epilepsy: Semiology, EEG, cerebrospinal fluid, and seizure outcome characteristics. Epilepsy & behavior : E&B. 2019;91:75-80.

43. Fordington S, Manford M. A review of seizures and epilepsy following traumatic brain injury. Journal of neurology. 2020;267(10):3105–11.

44. Fisher RS, van Emde Boas W, Blume W, Elger C, Genton P, Lee P, et al. Epileptic seizures and epilepsy: definitions proposed by the International League Against Epilepsy (ILAE) and the International Bureau for Epilepsy (IBE). Epilepsia. 2005;46(4):470-2.

45. Pottkämper JCM, Hofmeijer J, van Waarde JA, van Putten M. The postictal state - What do we know? Epilepsia. 2020;61(6):1045-61.

46. Rémi J, Noachtar S. Clinical features of the postictal state: correlation with seizure variables. Epilepsy & behavior : E&B. 2010;19(2):114-7.

47. Xu SY, Li ZX, Wu XW, Li L, Li CX. Frequency and Pathophysiology of Post-Seizure Todd's Paralysis. Medical science monitor : international medical journal of experimental and clinical research. 2020;26:e920751.

48. Trimble M, Kanner A, Schmitz B. Postictal psychosis. Epilepsy & behavior : E&B. 2010;19(2):159-61.

49. Jiruska P, de Curtis M, Jefferys JG, Schevon CA, Schiff SJ, Schindler K. Synchronization and desynchronization in epilepsy: controversies and hypotheses. J Physiol. 2013;591(4):787-97.

50. Liou JY, Ma H, Wenzel M, Zhao M, Baird-Daniel E, Smith EH, et al. Role of inhibitory control in modulating focal seizure spread. Brain : a journal of neurology. 2018;141(7):2083-97.

51. Engel J, Jr., Bragin A, Staba R, Mody I. High-frequency oscillations: what is normal and what is not? Epilepsia. 2009;50(4):598-604.

52. Lévesque M, Salami P, Shiri Z, Avoli M. Interictal oscillations and focal epileptic disorders. The European journal of neuroscience. 2018;48(8):2915-27.

53. Fisher RS, Scharfman HE, deCurtis M. How can we identify ictal and interictal abnormal activity? Advances in experimental medicine and biology. 2014;813:3-23.

54. Ortiz F, Zapfe WPK, Draguhn A, Gutiérrez R. Early Appearance and Spread of Fast Ripples in the Hippocampus in a Model of Cortical Traumatic Brain Injury. The Journal of neuroscience : the official journal of the Society for Neuroscience. 2018;38(42):9034-46.

55. Pitkänen A, Lukasiuk K, Dudek FE, Staley KJ. Epileptogenesis. Cold Spring Harb Perspect Med. 2015;5(10):a022822.

56. Becker AJ. Review: Animal models of acquired epilepsy: insights into mechanisms of human epileptogenesis. Neuropathology and applied neurobiology. 2018;44(1):112-29.

57. Chandel S, Gupta SK, Medhi B. Epileptogenesis following experimentally induced traumatic brain injury - a systematic review. Reviews in the neurosciences. 2016;27(3):329-46.

58. Mann EO, Mody I. The multifaceted role of inhibition in epilepsy: seizure-genesis through excessive GABAergic inhibition in autosomal dominant nocturnal frontal lobe epilepsy. Current opinion in neurology. 2008;21(2):155-60.

59. Briggs SW, Galanopoulou AS. Altered GABA signaling in early life epilepsies. Neural plasticity. 2011;2011:527605.

60. Frei MG, Zaveri HP, Arthurs S, Bergey GK, Jouny CC, Lehnertz K, et al. Controversies in epilepsy: debates held during the Fourth International Workshop on Seizure Prediction. Epilepsy & behavior : E&B. 2010;19(1):4-16.

61. Sayin U, Osting S, Hagen J, Rutecki P, Sutula T. Spontaneous seizures and loss of axo-axonic and axo-somatic inhibition induced by repeated brief seizures in kindled rats. The Journal of neuroscience : the official journal of the Society for Neuroscience. 2003;23(7):2759-68.

62. Borowicz-Reutt K, Czernia J, Krawczyk M. Genetic Background of Epilepsy and Antiepileptic Treatments. International journal of molecular sciences. 2023;24(22).

63. Zhang MW, Liang XY, Wang J, Gao LD, Liao HJ, He YH, et al. Epilepsy-associated genes: an update. Seizure. 2024;116:4-13.

64. Zhang Y, Li Z, Gu J, Zhang Y, Wang W, Shen H, et al. Plic-1, a new target in repressing epileptic seizure by regulation of GABAAR function in patients and a rat model of epilepsy. Clin Sci (Lond). 2015;129(12):1207-23.

65. Poduri A, Lowenstein D. Epilepsy genetics--past, present, and future. Current opinion in genetics & development. 2011;21(3):325-32.

66. Devinsky O, Vezzani A, O'Brien TJ, Jette N, Scheffer IE, de Curtis M, et al. Epilepsy. Nat Rev Dis Primers. 2018;4:18024.

67. Ben-Ari Y. Excitatory actions of gaba during development: the nature of the nurture. Nature reviews Neuroscience. 2002;3(9):728-39.

68. Swann JW, Smith KL, Lee CL. Neuronal activity and the establishment of normal and epileptic circuits during brain development. International review of neurobiology. 2001;45:89-118.

69. Smith KL, Swann JW. Long-term depression of perforant path excitatory postsynaptic potentials following synchronous network bursting in area CA3 of immature hippocampus. Neuroscience. 1999;89(3):625-30.

70. Yang C, Liu Z, Wang Q, Luan G, Zhai F. Epileptic seizures in a heterogeneous excitatory network with short-term plasticity. Cognitive neurodynamics. 2021;15(1):43-51.

71. Swanson OK, Maffei A. From Hiring to Firing: Activation of Inhibitory Neurons and Their Recruitment in Behavior. Front Mol Neurosci. 2019;12:168.

72. Guerriero RM, Giza CC, Rotenberg A. Glutamate and GABA imbalance following traumatic brain injury. Current neurology and neuroscience reports. 2015;15(5):27.

73. Walls AB, Waagepetersen HS, Bak LK, Schousboe A, Sonnewald U. The glutamine-glutamate/GABA cycle: function, regional differences in glutamate and GABA production and effects of interference with GABA metabolism. Neurochemical research. 2015;40(2):402-9.

74. Bedford FK, Kittler JT, Muller E, Thomas P, Uren JM, Merlo D, et al. GABA(A) receptor cell surface number and subunit stability are regulated by the ubiquitin-like protein Plic-1. Nat Neurosci. 2001;4(9):908-16.

75. Le Prieult F, Thal SC, Engelhard K, Imbrosci B, Mittmann T. Acute Cortical Transhemispheric Diaschisis after Unilateral Traumatic Brain Injury. Journal of neurotrauma. 2017;34(5):1097-110.

76. Dudek FE, Sutula TP. Epileptogenesis in the dentate gyrus: a critical perspective. Progress in brain research. 2007;163:755-73.

77. Raible DJ, Frey LC, Cruz Del Angel Y, Russek SJ, Brooks-Kayal AR. GABA(A) receptor regulation after experimental traumatic brain injury. Journal of neurotrauma. 2012;29(16):2548-54.

78. Naylor DE, Liu H, Wasterlain CG. Trafficking of GABA(A) receptors, loss of inhibition, and a mechanism for pharmacoresistance in status epilepticus. The Journal of neuroscience : the official journal of the Society for Neuroscience. 2005;25(34):7724-33.

79. Cobb SR, Buhl EH, Halasy K, Paulsen O, Somogyi P. Synchronization of neuronal activity in hippocampus by individual GABAergic interneurons. Nature. 1995;378(6552):75-8.

80. Boehme R, Uebele VN, Renger JJ, Pedroarena C. Rebound excitation triggered by synaptic inhibition in cerebellar nuclear neurons is suppressed by selective T-type calcium channel block. Journal of neurophysiology. 2011;106(5):2653-61.

81. Goldberg EM, Coulter DA. Mechanisms of epileptogenesis: a convergence on neural circuit dysfunction. Nature reviews Neuroscience. 2013;14(5):337-49.

82. de Lanerolle NC, Kim JH, Robbins RJ, Spencer DD. Hippocampal interneuron loss and plasticity in human temporal lobe epilepsy. Brain research. 1989;495(2):387-95.

83. Cossart R, Dinocourt C, Hirsch JC, Merchan-Perez A, De Felipe J, Ben-Ari Y, et al. Dendritic but not somatic GABAergic inhibition is decreased in experimental epilepsy. Nat Neurosci. 2001;4(1):52-62.

84. Aguiar CC, Almeida AB, Araújo PV, de Abreu RN, Chaves EM, do Vale OC, et al. Oxidative stress and epilepsy: literature review. Oxidative medicine and cellular longevity. 2012;2012:795259.

85. Liu Y, Feng S, Subedi K, Wang H. Attenuation of Ischemic Stroke-Caused Brain Injury by a Monoamine Oxidase Inhibitor Involves Improved Proteostasis and Reduced Neuroinflammation. Molecular neurobiology. 2020;57(2):937-48.

86. Ladak AA, Enam SA, Ibrahim MT. A Review of the Molecular Mechanisms of Traumatic Brain Injury. World neurosurgery. 2019;131:126-32.

87. Wang K, Cui D, Gao L. Traumatic brain injury: a review of characteristics, molecular basis and management. Frontiers in bioscience (Landmark edition). 2016;21:890-9.

88. Mattson MP. Excitotoxic and excitoprotective mechanisms: abundant targets for the prevention and treatment of neurodegenerative disorders. Neuromolecular medicine. 2003;3(2):65-94.

89. Decollogne S, Tomas A, Lecerf C, Adamowicz E, Seman M. NMDA receptor complex blockade by oral administration of magnesium: comparison with MK-801. Pharmacology, biochemistry, and behavior. 1997;58(1):261-8.

90. de Lores Arnaiz GR, Ordieres MG. Brain Na(+), K(+)-ATPase Activity In Aging and Disease. International journal of biomedical science : IJBS. 2014;10(2):85-102.

91. Mani R, Pollard J, Dichter MA. Human clinical trails in antiepileptogenesis. Neuroscience letters. 2011;497(3):251-6.

92. Dewan MC, Rattani A, Gupta S, Baticulon RE, Hung YC, Punchak M, et al. Estimating the global incidence of traumatic brain injury. Journal of neurosurgery. 2018:1-18.

93. Maas AIR, Menon DK, Adelson PD, Andelic N, Bell MJ, Belli A, et al. Traumatic brain injury: integrated approaches to improve prevention, clinical care, and research. The Lancet Neurology. 2017;16(12):987-1048.

94. Tagliaferri F, Compagnone C, Korsic M, Servadei F, Kraus J. A systematic review of brain injury epidemiology in Europe. Acta neurochirurgica. 2006;148(3):255-68; discussion 68.

95. Langlois JA, Rutland-Brown W, Wald MM. The epidemiology and impact of traumatic brain injury: a brief overview. The Journal of head trauma rehabilitation. 2006;21(5):375-8.

96. Bruns J, Jr., Hauser WA. The epidemiology of traumatic brain injury: a review. Epilepsia. 2003;44(s10):2-10.

97. Lowenstein DH. Epilepsy after head injury: an overview. Epilepsia. 2009;50 Suppl 2:4-9.

98. Lucke-Wold BP, Nguyen L, Turner RC, Logsdon AF, Chen YW, Smith KE, et al. Traumatic brain injury and epilepsy: Underlying mechanisms leading to seizure. Seizure. 2015;33:13-23.

99. Pitkänen A, Immonen R. Epilepsy related to traumatic brain injury. Neurotherapeutics. 2014;11(2):286-96.

100. Orr TJ, Lesha E, Kramer AH, Cecia A, Dugan JE, Schwartz B, et al. Traumatic Brain Injury: A Comprehensive Review of Biomechanics and Molecular Pathophysiology. World neurosurgery. 2024;185:74-88.

101. Cantu D, Walker K, Andresen L, Taylor-Weiner A, Hampton D, Tesco G, et al. Traumatic Brain Injury Increases Cortical Glutamate Network Activity by Compromising GABAergic Control. Cereb Cortex. 2015;25(8):2306-20.

102. Feldmann LK, Le Prieult F, Felzen V, Thal SC, Engelhard K, Behl C, et al. Proteasome and Autophagy-Mediated Impairment of Late Long-Term Potentiation (l-LTP) after Traumatic Brain Injury in the Somatosensory Cortex of Mice. International journal of molecular sciences. 2019;20(12).

103. Meyer JS, Obara K, Muramatsu K. Diaschisis. Neurological research. 1993;15(6):362-6.

104. Christensen J, Pedersen MG, Pedersen CB, Sidenius P, Olsen J, Vestergaard M. Long-term risk of epilepsy after traumatic brain injury in children and young adults: a population-based cohort study. Lancet (London, England). 2009;373(9669):1105-10.

105. Bockaert J, Marin P. mTOR in Brain Physiology and Pathologies. Physiological reviews. 2015;95(4):1157-87.

106. Huang X, Zhang H, Yang J, Wu J, McMahon J, Lin Y, et al. Pharmacological inhibition of the mammalian target of rapamycin pathway suppresses acquired epilepsy. Neurobiology of disease. 2010;40(1):193-9.

107. Berdichevsky Y, Dryer AM, Saponjian Y, Mahoney MM, Pimentel CA, Lucini CA, et al. PI3K-Akt signaling activates mTOR-mediated epileptogenesis in organotypic hippocampal culture model of post-traumatic epilepsy. The Journal of neuroscience : the official journal of the Society for Neuroscience. 2013;33(21):9056-67.

108. Buckmaster PS, Wen X. Rapamycin suppresses axon sprouting by somatostatin interneurons in a mouse model of temporal lobe epilepsy. Epilepsia. 2011;52(11):2057-64.

109. Guo D, Zeng L, Brody DL, Wong M. Rapamycin attenuates the development of posttraumatic epilepsy in a mouse model of traumatic brain injury. PloS one. 2013;8(5):e64078.

110. Chong SA, Balosso S, Vandenplas C, Szczesny G, Hanon E, Claes K, et al. Intrinsic Inflammation Is a Potential Anti-Epileptogenic Target in the Organotypic Hippocampal Slice Model. Neurotherapeutics. 2018;15(2):470-88.

111. Pitkänen A, Lukasiuk K. Mechanisms of epileptogenesis and potential treatment targets. The Lancet Neurology. 2011;10(2):173-86.

112. Saliba RS, Pangalos M, Moss SJ. The ubiquitin-like protein Plic-1 enhances the membrane insertion of GABAA receptors by increasing their stability within the endoplasmic reticulum. J Biol Chem. 2008;283(27):18538-44.

113. Luscher B, Fuchs T, Kilpatrick CL. GABAA receptor trafficking-mediated plasticity of inhibitory synapses. Neuron. 2011;70(3):385-409.

114. Kleijnen MF, Shih AH, Zhou P, Kumar S, Soccio RE, Kedersha NL, et al. The hPLIC proteins may provide a link between the ubiquitination machinery and the proteasome. Mol Cell. 2000;6(2):409-19.

115. Ko HS, Uehara T, Tsuruma K, Nomura Y. Ubiquilin interacts with ubiquitylated proteins and proteasome through its ubiquitin-associated and ubiquitin-like domains. FEBS Lett. 2004;566(1-3):110-4.

116. Upadhya SC, Hegde AN. A potential proteasome-interacting motif within the ubiquitin-like domain of parkin and other proteins. Trends Biochem Sci. 2003;28(6):280-3.

117. Jansen AH, Reits EA, Hol EM. The ubiquitin proteasome system in glia and its role in neurodegenerative diseases. Front Mol Neurosci. 2014;7:73.

118. Natunen T, Takalo M, Kemppainen S, Leskelä S, Marttinen M, Kurkinen KMA, et al. Relationship between ubiquilin-1 and BACE1 in human Alzheimer's disease and APdE9 transgenic mouse brain and cell-based models. Neurobiology of disease. 2016;85:187-205.

119. Zhang C, Saunders AJ. An emerging role for Ubiquilin 1 in regulating protein quality control system and in disease pathogenesis. Discov Med. 2009;8(40):18-22.

120. Safren N, Chang L, Dziki KM, Monteiro MJ. Signature changes in ubiquilin expression in the R6/2 mouse model of Huntington's disease. Brain research. 2015;1597:37-46.

121. Luo L, Liu Y, Tu X, Ren X, Zhao W, Liu J, et al. Decreased expression of ubiquilin-1 following neonatal hypoxia-ischemic brain injury in mice. Mol Med Rep. 2019;19(6):4597-602.

122. Benke D, Fritschy JM, Trzeciak A, Bannwarth W, Mohler H. Distribution, prevalence, and drug binding profile of gamma-aminobutyric acid type A receptor subtypes differing in the beta-subunit variant. J Biol Chem. 1994;269(43):27100-7.

123. Wang Y, Le WD. Autophagy and Ubiquitin-Proteasome System. Advances in experimental medicine and biology. 2019;1206:527-50.

124. Lemberg MK, Strisovsky K. Maintenance of organellar protein homeostasis by ER-associated degradation and related mechanisms. Mol Cell. 2021;81(12):2507-19.

125. Thompson SJ, Loftus LT, Ashley MD, Meller R. Ubiquitin-proteasome system as a modulator of cell fate. Current opinion in pharmacology. 2008;8(1):90-5.

126. Lilienbaum A. Relationship between the proteasomal system and autophagy. International journal of biochemistry and molecular biology. 2013;4(1):1-26.

127. Sommer T, Wolf DH. The ubiquitin-proteasome-system. Biochim Biophys Acta. 2014;1843(1):1.

128. Liu Y, Lü L, Hettinger CL, Dong G, Zhang D, Rezvani K, et al. Ubiquilin-1 protects cells from oxidative stress and ischemic stroke caused tissue injury in mice. The Journal of neuroscience : the official journal of the Society for Neuroscience. 2014;34(8):2813-21.

129. Liu Y, Qiao F, Wang H. Enhanced Proteostasis in Post-ischemic Stroke Mouse Brains by Ubiquilin-1 Promotes Functional Recovery. Cell Mol Neurobiol. 2017;37(7):1325-9.

130. Kürten T, Ihbe N, Ueberbach T, Distler U, Sielaff M, Tenzer S, et al. GABA(A) Receptor-Stabilizing Protein Ubqln1 Affects Hyperexcitability and Epileptogenesis after Traumatic Brain Injury and in a Model of In Vitro Epilepsy in Mice. International journal of molecular sciences. 2022;23(7).

131. Meierkord H, Boon P, Engelsen B, Göcke K, Shorvon S, Tinuper P, et al. EFNS guideline on the management of status epilepticus in adults. European journal of neurology. 2010;17(3):348-55.

132. Beerhorst K, van der Kruijs SJ, Verschuure P, Tan IY, Aldenkamp AP. Bone disease during chronic antiepileptic drug therapy: general versus specific risk factors. Journal of the neurological sciences. 2013;331(1-2):19-25.

133. Perucca P, Gilliam FG. Adverse effects of antiepileptic drugs. The Lancet Neurology. 2012;11(9):792-802.

134. Rao VR, Parko KL. Clinical approach to posttraumatic epilepsy. Seminars in neurology. 2015;35(1):57-63.

135. Kwan P, Arzimanoglou A, Berg AT, Brodie MJ, Allen Hauser W, Mathern G, et al. Definition of drug resistant epilepsy: consensus proposal by the ad hoc Task Force of the ILAE Commission on Therapeutic Strategies. Epilepsia. 2010;51(6):1069-77.

136. Gouveia FV, Warsi NM, Suresh H, Matin R, Ibrahim GM. Neurostimulation treatments for epilepsy: Deep brain stimulation, responsive neurostimulation and vagus nerve stimulation. Neurotherapeutics. 2024;21(3):e00308.

137. Rizvi S, Ladino LD, Hernandez-Ronquillo L, Tellez-Zenteno JF. Epidemiology of early stages of epilepsy: Risk of seizure recurrence after a first seizure. Seizure. 2017;49:46-53.

138. Hauser WA, Anderson VE, Loewenson RB, McRoberts SM. Seizure recurrence after a first unprovoked seizure. The New England journal of medicine. 1982;307(9):522-8.

139. Bergey GK. Management of a First Seizure. Continuum (Minneapolis, Minn). 2016;22(1 Epilepsy):38-50.

140. Xue-Ping W, Hai-Jiao W, Li-Na Z, Xu D, Ling L. Risk factors for drug-resistant epilepsy: A systematic review and meta-analysis. Medicine. 2019;98(30):e16402.

141. Cockerell OC, Johnson AL, Sander JW, Hart YM, Shorvon SD. Remission of epilepsy: results from the National General Practice Study of Epilepsy. Lancet (London, England). 1995;346(8968):140-4.

142. Berg AT, Rychlik K, Levy SR, Testa FM. Complete remission of childhood-onset epilepsy: stability and prediction over two decades. Brain : a journal of neurology. 2014;137(Pt 12):3213-22.

143. Thurman DJ, Begley CE, Carpio A, Helmers S, Hesdorffer DC, Mu J, et al. The primary prevention of epilepsy: A report of the Prevention Task Force of the International League Against Epilepsy. Epilepsia. 2018;59(5):905-14.

144. Staton C, Vissoci J, Gong E, Toomey N, Wafula R, Abdelgadir J, et al. Road Traffic Injury Prevention Initiatives: A Systematic Review and Metasummary of Effectiveness in Low and Middle Income Countries. PloS one. 2016;11(1):e0144971.

145. Wagenaar JB, Worrell GA, Ives Z, Dümpelmann M, Litt B, Schulze-Bonhage A. Collaborating and sharing data in epilepsy research. J Clin Neurophysiol. 2015;32(3):235-9.

146. Osier ND, Dixon CE. The Controlled Cortical Impact Model: Applications, Considerations for Researchers, and Future Directions. Frontiers in neurology. 2016;7:134.

147. Lighthall JW. Controlled cortical impact: a new experimental brain injury model. Journal of neurotrauma. 1988;5(1):1-15.

148. Anderson TE. A controlled pneumatic technique for experimental spinal cord contusion. Journal of neuroscience methods. 1982;6(4):327-33.

149. Ma X, Aravind A, Pfister BJ, Chandra N, Haorah J. Animal Models of Traumatic Brain Injury and Assessment of Injury Severity. Molecular neurobiology. 2019;56(8):5332-45.

150. Dixon CE, Clifton GL, Lighthall JW, Yaghmai AA, Hayes RL. A controlled cortical impact model of traumatic brain injury in the rat. Journal of neuroscience methods. 1991;39(3):253-62.

151. Cernak I. Animal models of head trauma. NeuroRx : the journal of the American Society for Experimental NeuroTherapeutics. 2005;2(3):410-22.

152. Dinallo S, Waseem M. Cushing Reflex. StatPearls. Treasure Island (FL): StatPearls Publishing
Copyright © 2022, StatPearls Publishing LLC.; 2022.

153. Tamamaki N, Yanagawa Y, Tomioka R, Miyazaki J, Obata K, Kaneko T. Green fluorescent protein expression and colocalization with calretinin, parvalbumin, and somatostatin in the GAD67-GFP knock-in mouse. The Journal of comparative neurology. 2003;467(1):60-79.

154. Goddard GV. Development of epileptic seizures through brain stimulation at low intensity. Nature. 1967;214(5092):1020-1.

155. Goddard GV, McIntyre DC, Leech CK. A permanent change in brain function resulting from daily electrical stimulation. Experimental neurology. 1969;25(3):295-330.

156. Brandt C, Glien M, Potschka H, Volk H, Löscher W. Epileptogenesis and neuropathology after different types of status epilepticus induced by prolonged electrical stimulation of the basolateral amygdala in rats. Epilepsy research. 2003;55(1-2):83-103.

157. Leite JP, Garcia-Cairasco N, Cavalheiro EA. New insights from the use of pilocarpine and kainate models. Epilepsy research. 2002;50(1-2):93-103.

158. Ben-Ari Y, Lagowska J. [Epileptogenic action of intra-amygdaloid injection of kainic acid]. Comptes rendus hebdomadaires des seances de l'Academie des sciences Serie D: Sciences naturelles. 1978;287(8):813-6.

159. Ben-Ari Y. Limbic seizure and brain damage produced by kainic acid: mechanisms and relevance to human temporal lobe epilepsy. Neuroscience. 1985;14(2):375-403.

160. Nadler JV, Perry BW, Cotman CW. Intraventricular kainic acid preferentially destroys hippocampal pyramidal cells. Nature. 1978;271(5646):676-7.

161. Cavalheiro EA, Leite JP, Bortolotto ZA, Turski WA, Ikonomidou C, Turski L. Long-term effects of pilocarpine in rats: structural damage of the brain triggers kindling and spontaneous recurrent seizures. Epilepsia. 1991;32(6):778-82.

162. Gonzalez-Sulser A, Wang J, Motamedi GK, Avoli M, Vicini S, Dzakpasu R. The 4-aminopyridine in vitro epilepsy model analyzed with a perforated multi-electrode array. Neuropharmacology. 2011;60(7-8):1142-53.

163. Yoon KW, Covey DF, Rothman SM. Multiple mechanisms of picrotoxin block of GABA-induced currents in rat hippocampal neurons. J Physiol. 1993;464:423-39.

164. Löscher W. Animal Models of Seizures and Epilepsy: Past, Present, and Future Role for the Discovery of Antiseizure Drugs. Neurochemical research. 2017;42(7):1873-88.

165. Newland CF, Cull-Candy SG. On the mechanism of action of picrotoxin on GABA receptor channels in dissociated sympathetic neurones of the rat. J Physiol. 1992;447:191-213.

166. Huusko N, Romer C, Ndode-Ekane XE, Lukasiuk K, Pitkanen A. Loss of hippocampal interneurons and epileptogenesis: a comparison of two animal models of acquired epilepsy. Brain structure & function. 2015;220(1):153-91.

167. Carron SF, Yan EB, Allitt BJ, Rajan R. Immediate and Medium-term Changes in Cortical and Hippocampal Inhibitory Neuronal Populations after Diffuse TBI. Neuroscience. 2018;388:152-70.

168. Olsen RW. Picrotoxin-like channel blockers of GABAA receptors. Proceedings of the National Academy of Sciences of the United States of America. 2006;103(16):6081-2.

169. Olsen RW. Allosteric ligands and their binding sites define γ-aminobutyric acid (GABA) type A receptor subtypes. Advances in pharmacology (San Diego, Calif). 2015;73:167-202.

170. Ridler T, Matthews P, Phillips KG, Randall AD, Brown JT. Initiation and slow propagation of epileptiform activity from ventral to dorsal medial entorhinal cortex is constrained by an inhibitory gradient. J Physiol. 2018;596(11):2251-66.

171. Tian Z, Clark BLM, Menard F. Kainic Acid-Based Agonists of Glutamate Receptors: SAR Analysis and Guidelines for Analog Design. ACS chemical neuroscience. 2019;10(10):4190-8.

172. Pinheiro P, Mulle C. Kainate receptors. Cell and tissue research. 2006;326(2):457-82.

173. Butler JL, Paulsen O. Hippocampal network oscillations - recent insights from in vitro experiments. Current opinion in neurobiology. 2015;31:40-4.

174. Gavini K, Parameshwaran K. Western Blot. StatPearls. Treasure Island (FL): StatPearls Publishing

175. Towbin H, Staehelin T, Gordon J. Electrophoretic transfer of proteins from polyacrylamide gels to nitrocellulose sheets: procedure and some applications. Proceedings of the National Academy of Sciences of the United States of America. 1979;76(9):4350-4.

176. Burnette WN. "Western blotting": electrophoretic transfer of proteins from sodium dodecyl sulfate--polyacrylamide gels to unmodified nitrocellulose and radiographic detection with antibody and radioiodinated protein A. Analytical biochemistry. 1981;112(2):195-203.

177. Oh K. Technical Considerations for Contemporary Western Blot Techniques. Methods in molecular biology (Clifton, NJ). 2021;2261:457-79.

178. Pillai-Kastoori L, Schutz-Geschwender AR, Harford JA. A systematic approach to quantitative Western blot analysis. Analytical biochemistry. 2020;593:113608.

179. Mahmood T, Yang PC. Western blot: technique, theory, and trouble shooting. North American journal of medical sciences. 2012;4(9):429-34.

180. Kim B. Western Blot Techniques. Methods in molecular biology (Clifton, NJ). 2017;1606:133-9.

181. Nie X, Li C, Hu S, Xue F, Kang YJ, Zhang W. An appropriate loading control for western blot analysis in animal models of myocardial ischemic infarction. Biochemistry and biophysics reports. 2017;12:108-13.

182. Ihbe N, Le Prieult F, Wang Q, Distler U, Sielaff M, Tenzer S, et al. Adaptive Mechanisms of Somatostatin-Positive Interneurons after Traumatic Brain Injury through a Switch of α Subunits in L-Type Voltage-Gated Calcium Channels. Cereb Cortex. 2022;32(5):1093-109.

183. Xiong Y, Mahmood A, Chopp M. Animal models of traumatic brain injury. Nature reviews Neuroscience. 2013;14(2):128-42.

184. Alexander TS. Human Immunodeficiency Virus Diagnostic Testing: 30 Years of Evolution. Clinical and vaccine immunology : CVI. 2016;23(4):249-53.

185. Liu MG, Chen XF, He T, Li Z, Chen J. Use of multi-electrode array recordings in studies of network synaptic plasticity in both time and space. Neuroscience bulletin. 2012;28(4):409-22.

186. Burley R, Harvey JRM. Multielectrode Arrays. Methods in molecular biology (Clifton, NJ). 2021;2188:109-32.

187. Yokoi R, Shibata M, Odawara A, Ishibashi Y, Nagafuku N, Matsuda N, et al. Analysis of signal components < 500 Hz in brain organoids coupled to microelectrode arrays: A reliable test-bed for preclinical seizure liability assessment of drugs and screening of antiepileptic drugs. Biochemistry and biophysics reports. 2021;28:101148.

188. Fan J, Thalody G, Kwagh J, Burnett E, Shi H, Lewen G, et al. Assessing seizure liability using multi-electrode arrays (MEA). Toxicol In Vitro. 2019;55:93-100.

189. Manz KM, Siemann JK, McMahon DG, Grueter BA. Patch-clamp and multi-electrode array electrophysiological analysis in acute mouse brain slices. STAR protocols. 2021;2(2):100442.

190. Lin X, Amalraj M, Blanton C, Avila B, Holmes TC, Nitz DA, et al. Noncanonical projections to the hippocampal CA3 regulate spatial learning and memory by modulating the feedforward hippocampal trisynaptic pathway. PLoS biology. 2021;19(12):e3001127.

191. Cochran SM, Harvey AL, Pratt JA. Regionally selective alterations in local cerebral glucose utilization evoked by charybdotoxin, a blocker of central voltage-activated K+-channels. The European journal of neuroscience. 2001;14(9):1455-63.

192. Stepan J, Dine J, Eder M. Functional optical probing of the hippocampal trisynaptic circuit in vitro: network dynamics, filter properties, and polysynaptic induction of CA1 LTP. Frontiers in neuroscience. 2015;9:160.

193. Núñez-Ochoa MA, Chiprés-Tinajero GA, González-Domínguez NP, Medina-Ceja L. Causal relationship of CA3 back-projection to the dentate gyrus and its role in CA1 fast ripple generation. BMC neuroscience. 2021;22(1):37.

194. Schwarzer C, Tsunashima K, Wanzenböck C, Fuchs K, Sieghart W, Sperk G. GABA(A) receptor subunits in the rat hippocampus II: altered distribution in kainic acid-induced temporal lobe epilepsy. Neuroscience. 1997;80(4):1001-17.

195. Gibbs JW, 3rd, Shumate MD, Coulter DA. Differential epilepsy-associated alterations in postsynaptic GABA(A) receptor function in dentate granule and CA1 neurons. Journal of neurophysiology. 1997;77(4):1924-38.

196. Figueiredo T, Harbert CL, Pidoplichko V, Almeida-Suhett CP, Rossetti K, Braga MFM, et al. The Recovery of GABAergic Function in the Hippocampus CA1 Region After mTBI. Molecular neurobiology. 2020;57(1):23-31.

197. Almeida-Suhett CP, Prager EM, Pidoplichko V, Figueiredo TH, Marini AM, Li Z, et al. GABAergic interneuronal loss and reduced inhibitory synaptic transmission in the hippocampal CA1 region after mild traumatic brain injury. Experimental neurology. 2015;273:11-23.

198. Imbrosci B, Wang Y, Arckens L, Mittmann T. Neuronal mechanisms underlying transhemispheric diaschisis following focal cortical injuries. Brain structure & function. 2015;220(3):1649-64.

199. Andrews RJ. Transhemispheric diaschisis. A review and comment. Stroke. 1991;22(7):943-9.

200. Imbrosci B, Mittmann T. Functional consequences of the disturbances in the GABA-mediated inhibition induced by injuries in the cerebral cortex. Neural plasticity. 2011;2011:614329.

201. Imbrosci B, Neubacher U, White R, Eysel UT, Mittmann T. Shift from phasic to tonic GABAergic transmission following laser-lesions in the rat visual cortex. Pflugers Archiv : European journal of physiology. 2013;465(6):879-93.

202. Clarkson AN, Huang BS, Macisaac SE, Mody I, Carmichael ST. Reducing excessive GABA-mediated tonic inhibition promotes functional recovery after stroke. Nature. 2010;468(7321):305-9.

203. Gaiottino J, Norgren N, Dobson R, Topping J, Nissim A, Malaspina A, et al. Increased neurofilament light chain blood levels in neurodegenerative neurological diseases. PloS one. 2013;8(9):e75091.

204. Khalil M, Teunissen CE, Otto M, Piehl F, Sormani MP, Gattringer T, et al. Neurofilaments as biomarkers in neurological disorders. Nature reviews Neurology. 2018;14(10):577-89.

205. Gao W, Zhang Z, Lv X, Wu Q, Yan J, Mao G, et al. Neurofilament light chain level in traumatic brain injury: A system review and meta-analysis. Medicine. 2020;99(38):e22363.

206. Shahim P, Politis A, van der Merwe A, Moore B, Chou YY, Pham DL, et al. Neurofilament light as a biomarker in traumatic brain injury. Neurology. 2020;95(6):e610-e22.

207. Garland P, Morton M, Zolnourian A, Durnford A, Gaastra B, Toombs J, et al. Neurofilament light predicts neurological outcome after subarachnoid haemorrhage. Brain : a journal of neurology. 2021;144(3):761-8.

208. Shulman KI, Herrmann N, Walker SE. Current place of monoamine oxidase inhibitors in the treatment of depression. CNS drugs. 2013;27(10):789-97.

209. Berton O, Nestler EJ. New approaches to antidepressant drug discovery: beyond monoamines. Nature reviews Neuroscience. 2006;7(2):137-51.

210. Garcia E, Santos C. Monoamine Oxidase Inhibitor Toxicity. StatPearls. Treasure Island (FL): StatPearls Publishing
Copyright © 2021, StatPearls Publishing LLC.; 2021.

211. Kitaichi Y, Inoue T, Nakagawa S, Boku S, Izumi T, Koyama T. Combined treatment with MAO-A inhibitor and MAO-B inhibitor increases extracellular noradrenaline levels more than MAO-A inhibitor alone through increases in beta-phenylethylamine. European journal of pharmacology. 2010;637(1-3):77-82.

212. Kaludercic N, Carpi A, Menabò R, Di Lisa F, Paolocci N. Monoamine oxidases (MAO) in the pathogenesis of heart failure and ischemia/reperfusion injury. Biochim Biophys Acta. 2011;1813(7):1323-32.

213. Baker G, Matveychuk D, MacKenzie EM, Holt A, Wang Y, Kar S. Attenuation of the effects of oxidative stress by the MAO-inhibiting antidepressant and carbonyl scavenger phenelzine. Chem Biol Interact. 2019;304:139-47.

214. Cebak JE, Singh IN, Hill RL, Wang JA, Hall ED. Phenelzine Protects Brain Mitochondrial Function In Vitro and In Vivo following Traumatic Brain Injury by Scavenging the Reactive Carbonyls 4-Hydroxynonenal and Acrolein Leading to Cortical Histological Neuroprotection. Journal of neurotrauma. 2017;34(7):1302-17.

215. Norman TR, Burrows GD. Monoamine oxidase, monoamine oxidase inhibitors, and panic disorder. Journal of neural transmission Supplementum. 1989;28:53-63.

216. Al-Nuaimi SK, Mackenzie EM, Baker GB. Monoamine oxidase inhibitors and neuroprotection: a review. American journal of therapeutics. 2012;19(6):436-48.

217. Culpepper L. The use of monoamine oxidase inhibitors in primary care. J Clin Psychiatry. 2012;73 Suppl 1:37-41.

218. Gillman PK, Feinberg SS, Fochtmann LJ. Revitalizing monoamine oxidase inhibitors: a call for action. CNS spectrums. 2020;25(4):452-4.

219. Alam AM, Starr MS. Dopaminergic modulation of pilocarpine-induced motor seizures in the rat: the role of hippocampal D2 receptors. Neuroscience. 1993;53(2):425-31.

220. Clinckers R, Smolders I, Meurs A, Ebinger G, Michotte Y. Anticonvulsant action of hippocampal dopamine and serotonin is independently mediated by D and 5-HT receptors. J Neurochem. 2004;89(4):834-43.

221. Bagdy G, Kecskemeti V, Riba P, Jakus R. Serotonin and epilepsy. J Neurochem. 2007;100(4):857-73.

222. Costa C, Parnetti L, D'Amelio M, Tozzi A, Tantucci M, Romigi A, et al. Epilepsy, amyloid-β, and D1 dopamine receptors: a possible pathogenetic link? Neurobiol Aging. 2016;48:161-71.

223. Starr MS. The role of dopamine in epilepsy. Synapse. 1996;22(2):159-94.

224. Maia GH, Brazete CS, Soares JI, Luz LL, Lukoyanov NV. Serotonin depletion increases seizure susceptibility and worsens neuropathological outcomes in kainate model of epilepsy. Brain research bulletin. 2017;134:109-20.

225. Specchio N, Pietrafusa N, Doccini V, Trivisano M, Darra F, Ragona F, et al. Efficacy and safety of Fenfluramine hydrochloride for the treatment of seizures in Dravet syndrome: A real-world study. Epilepsia. 2020;61(11):2405-14.

226. Sourbron J, Partoens M, Scheldeman C, Zhang Y, Lagae L, de Witte P. Drug repurposing for Dravet syndrome in scn1Lab(-/-) mutant zebrafish. Epilepsia. 2019;60(2):e8-e13.

227. Zhang L, Li W, Wang C. Efficacy and safety of fenfluramine in patients with Dravet syndrome: A meta-analysis. Acta neurologica Scandinavica. 2021;143(4):339-48.

228. Lagae L, Sullivan J, Knupp K, Laux L, Polster T, Nikanorova M, et al. Fenfluramine hydrochloride for the treatment of seizures in Dravet syndrome: a randomised, double-blind, placebo-controlled trial. Lancet (London, England). 2019;394(10216):2243-54.

229. Nemes A, Najm IM, Gale JT, Ying Z, Johnson M, Gonzalez-Martinez J. Underlying Cortical Dysplasia as Risk Factor for Traumatic Epilepsy: An Animal Study. Journal of neurotrauma. 2016;33(20):1883-91.

230. Sakakura K, Fujimoto A, Arai Y, Ichikawa N, Sato K, Baba S, et al. Posttraumatic epilepsy may be a state in which underlying epileptogenicity involves focal cortical dysplasia. Epilepsy & behavior : E&B. 2021;114(Pt A):107352.

7. Acknowledgements

First of all, I would like to express my very special thanks to my supervisor [redacted] who gave me the unique opportunity to gain insight into basic research and the world of electrophysiology. I am grateful for the dedicated mentoring and guidance throughout my project as well as for the outstanding personal support at any time during and after my research year in the [redacted] lab. It was an honor for me to work in his group.

Thousand thanks go to [redacted] who gave me skilled introductions to all the methods in the lab and supported me with her friendly expertise. Furthermore, she contributed the proteomics data to our publication of which we share the first author title.

Here, I would also like to thank [redacted] I will always remember his positive character and his great ability to make everyone laugh around him as well as his huge commitment to emergency medicine and his passion for science. [redacted] kindly contributed the Western blot data 24 hours post-TBI to our publication.

[redacted] provided excellent technical assistance throughout my experiments. I could always rely on practical support and would like to thank her specially for the thorough introduction to Western blotting. With her patient and friendly manner, it was great fun to work beside her.

I also want to thank the director of the Institute of Pathophysiology in Mainz, [redacted] for his kind guidance as my second supervisor, for supporting my application for the FTN stipend and for reviewing this thesis from the perspective of a scientist and neurologist.

I also would like to express my gratitude to [redacted] for very valuable and professional advice on my career. The weekly progress reports and inter-institute meetings were a great inspiration and chance to gain deeper insight into the fascinating field of neuroscience. I was given the opportunity to present my results in the progress reports and received very constructive feedback.

Furthermore, I want to thank all the members of the institute for the always pleasant working atmosphere, the interesting talks and kind support. Although my research year was accompanied by a pandemic and took place during a time of social distancing and home office, I have never felt alone.

Another special credit goes to [redacted] for helpful comments on the thesis from an English reader's perspective, they were very useful to make the manuscript more readable.

I would also like to express my sincere gratitude to the focus program translational medicine (FTN) for the financial support during my year in research. The stipend enabled me to focus on the project for a whole and intense year. I gathered experiences that will stay with me for a long time and that will be of great value in my future career as a medical doctor.
Many thanks also go to the MAInz-DOC Basic graduate school that provides useful courses for medical students during doctoral graduation.

Most importantly, I thank my friends and my family for giving me endless support. I am very grateful to be surrounded by people that enrich my life day by day.

8. CV

Personal details

Name	Tabea Kürten
Date of birth	21st April 1998 in Bremen, Germany

Education

May 2024	**Third part of the state examination in medicine (M3)** Grade: 1.0
Apr. 2023	**Second part of the state examination in medicine (M2)** Grade: 2.0 (88.5%)
Mar. 2019	**First part of the state examination in medicine (M1)** Grade: 1.0
Apr. 2017 – May 2024	**Study of medicine (state examination)** Johannes Gutenberg University Mainz
Jul. 2008 – May 2016	**Gymnasium am Markt Achim, Niedersachsen** Abitur, Graduation Grade: 1.2

Work and internships

Since Sept. 2024	**Residency** Department of neurology of the University Hospital Schleswig-Holstein (UKSH) Lübeck
May 2023 – Apr. 2024	**Practical Year** • Jan.-Apr. 2024: Neurology University Medical Center Hamburg-Eppendorf (UKE) • Sept.-Dec. 2023: Internal Medicine Hannover Medical School (MHH) • May-Sept. 2023: Surgery University Medicine Göttingen-Hospital St. Joseph-Stift Bremen
Nov. 2023	**96th Conference of the German Neurological Society (DGN)** CityCube Berlin
Sept. 2022 – Apr. 2023	**University Medical Center of the Johannes Gutenberg-University** Night duty for video EEG-monitoring in the department of neurology
Sept. 2022 – Oct. 2022	**Ambulatory Neurology and Psychiatry in Achim, Niedersachsen** Medical internship

Mar. 2022	**International Journal of Molecular Sciences – first authorship (shared):** Kürten, T.; Ihbe, N.; Ueberbach, T.; Distler, U.; Sielaff, M.; Tenzer, S.; Mittmann, T. "$GABA_A$ Receptor-Stabilizing Protein Ubqln1 Affects Hyperexcitability and Epileptogenesis after Traumatic Brain Injury and in a Model of In Vitro Epilepsy in Mice." *Int. J. Mol. Sci.* **2022**, *23*, 3902. https://doi.org/10.3390/ijms23073902
Nov. 2021	**94th Conference of the German Neurological Society (DGN)** Digital meeting
Oct. 2021	**Diako Mannheim** "Tag der Neurologie"
Oct. 2021	**100th meeting of the German Physiological Society (DPG) in Frankfurt** Poster Presentation "Altered expression of $GABA_A$ -receptor stabilizing protein ubiquilin-1 contributes to hyperexcitability in mouse models of *in vitro* epilepsy and traumatic brain injury"
Sept. 2021 – Oct. 2021	**General practitioner in Mainz** Medical internship
Since June 2021	**German Neurological Society (DGN)** Membership
Since May 2021	**German Neuroscience Society (NWG)** Membership
Feb. 2021 – Mar. 2021	**University Medical Center of the Johannes Gutenberg-University Mainz / Neurology and Stroke Unit** Medical internship
Feb. 2020 – Feb. 2021	**Promotion program "MAInz DOC-Basic" of the Mainz Research School of Translational Biomedicine (TransMed) with participation in several study courses:** • Good clinical practice • Statistical evaluation with SPSS • Literature administration with EndNote • Literature research with PubMed • Introduction to clinical trials
Mar. 2020 – Apr. 2020	**Klinikum Bremen-Ost / Radiology** Medical internship
Feb. 2020 – Dec. 2020	**MD-Fellowship of the Focus Program Translational Neurosciences (FTN)** **Institute of Physiology in Mainz - research group of Prof. Mittmann** Experimental research project for doctoral degree (MD) **"**Investigating the role of molecular target ubiquilin-1 under *in vitro* epilepsy conditions in mice." • Electrophysiological and molecular biological methods:

	Multi-electrode Arrays, Western blots, Immunohistochemistry • Weekly lab meetings with scientific talks
Sept. 2019 – Oct. 2019	**Hospital St. Joseph-Stift Bremen / Internal medicine** Medical internship
May 2019 – May 2023	**Student initiative "Aufklärung Organspende" in Mainz** • Neutral educational work (through school visits, information booths, university group fairs and internet articles) • Encouraging personal decision-making and documentation on the organ donor card
Oct. 2018 – Jul. 2019	**Johannes Gutenberg University Mainz** Student assistant in the biology course for medical students • Help with substantive or organisational matters, with handling of microscopes and histological specimens • Weekly preparation and implementation of colloquia
Oct. 2017 – Mar. 2019	**Johannes Gutenberg University Mainz** Member of the medical student council
Feb. 2017 - Mar. 2017	**Klinikum Bremen-Ost / Pneumology** Six-week internship in nursing
Nov. 2016 – Dec. 2016	**Medical training at the Arbeiter-Samariter-Bund Bremen-Ost** Four-week course
Aug. 2016 – Oct. 2016	**Klinikum Bremen-Ost / Neurology** Six-week internship in nursing

Languages

German	native
English	fluent Federal Foreign Language Competition English, 3rd Lower Saxony State Prize Pearson LCCI Certificate: London Chamber of Commerce: English for Business, Level 3 Advanced level in the Abitur
French	good command Advanced level in the Abitur

Hobbies and interests

Running, biking, literature, guitar, surfing